Introduction to the use of microstrip and pixel based devices and the corresponding main challenges to be confronted by their associated Front-End Electronics

Cinzia Da Vià
The University of Manchester, UK

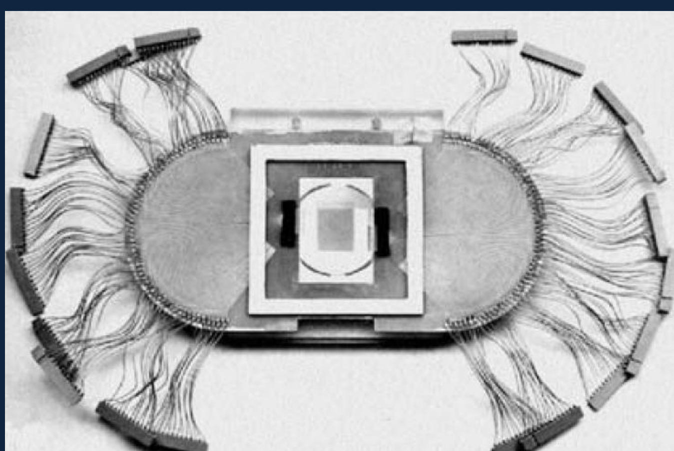

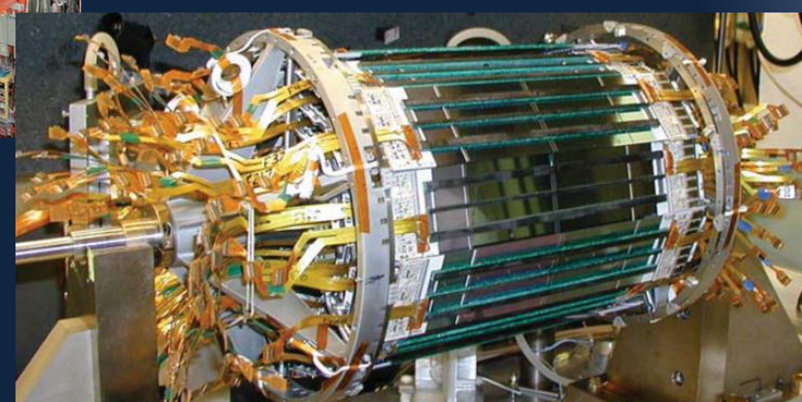

INFIERI Oxford School 12 July 2013

Introduction

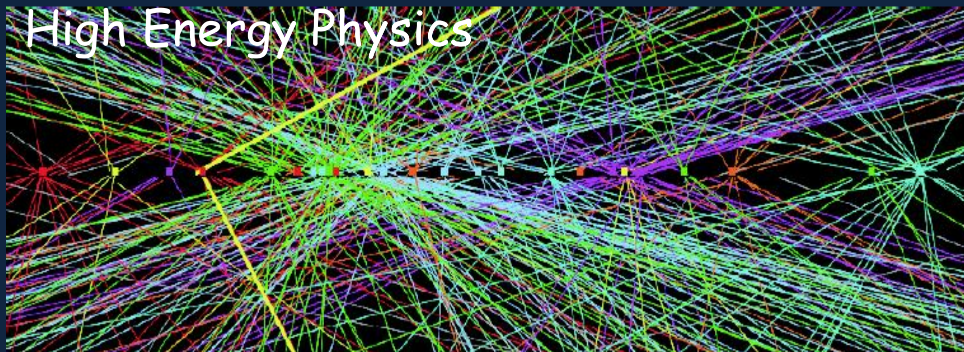

Z -> μμ event from 15 April 2012,
L = 4 · 1033 cm–2 s–1, 25 vertices (ATLAS at the CERN LHC)

Microstrips and pixel detectors are widely used as 'radiation imager' and are mainly made of semiconductors (Silicon in particular) but not only!

They basically convert radiation into an electronic signal

Space applications, Medicine , Biology

Every day life

X. Llopart, Medipix collaboration

Why Silicon?

- ❖ Low ionization energy (good signal).
  The band gap is 1.12 eV, but it takes 3.6 eV to ionize an atom. The remaining energy goes to phonon excitations (heat)
- ❖ High purity (long carrier lifetime)
- ❖ High mobility (fast charge collection)
- ❖ Low Z (Z=14 low multiple scattering but low x-ray detection efficiency)
- ❖ Oxide (SiO_2) has excellent electrical properties
- ➢ Good mechanical properties:
  - Easily patterned to small dimensions
- ➢ Can be operated in air and at room temperature (before irradiation –afterwards requires cooling)
- ➢ Industrial experience and commercial applications
- ➢ Silicon is abundant!

Over 90% of the Earth's crust is composed of silicate minerals, making silicon the second most abundant element in the Earth's crust (about 28% by mass) after oxygen

Parameter	cBN	hBN	Diamond	AlN	GaN	3C-SiC	GaAs	Si
Energy Bandgap (eV)	6.4	5.2	5.45	6.2	3.39	3.00	1.43	1.12
Electron Mobility (cm^2/Vs)	280	-	2200	300	440	400	8500	1500
Hole Mobility (cm^2/Vs)	-	-	1600	30	~20	50	400	600
Thermal Conductivity (W/cm K)	13	a = 6.0 c = 0.3	20	2.9	1.3	5	0.46	1.5
Breakdown ($\times 10^5$ Vcm^{-1})	~80	~80	100	~80	~80	40	60	3
Lattice Constant (Å)	3.615	a = 2.504 c = 6.661	3.567	4.982	a = 3.189 c = 5.185	4.358	5.65	5.43
Thermal Expansion Coefficient ($\times 10^{-6}$ $°C^{-1}$)	3.5	a = -2.7 c = 38	1.1	4.0	4.5	4.7	5.9	2.6
Density (gm/cm^3)	3.487	2.28	3.515	3.26	6.15	3.216	5.316	2.328
Melting Point (℃)	2973	3000	3800	2200	>2500	2540	1238	1420
Dielectric Constant	7.1	5.1	5.5	-	9.5	9.7	12.5	11.8
Resistivity (Ω cm)	10^{16}	10^{10}	10^{13}	10^{14}	10^{12}	150	10^8	10^3
Absorption Edge (μm)	0.205	0.212	0.20	-	0.35	0.40	-	1.40
Refractive Index	2.17	1.80	2.42	2.00	2.33	2.65	3.4	3.5
Hardness (kg/mm^2), T = 300 K Kg/mm^2	5000	100	10,000	2500	1100	3000	600	1000

Silicon detectors' wafers are made with very pure quartzite sand

a) The sand is cleaned and further purified by chemical processes. It is then melted a tiny concentration of phosphorus (boron) dopant is added to make n(p) type poly-crystalline ingots

b) Single-crystal silicon is obtained by melting the vertically oriented poly-silicon cylinder onto a single crystal "seed"

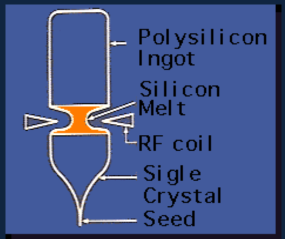

c) Wafers of thickness 200- 500μm are cut with diamond encrusted wire or disc saws.

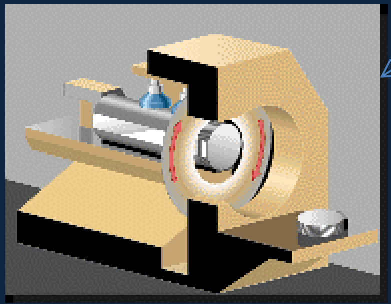

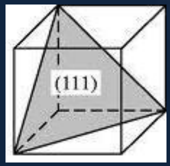

Note: the crystal orientation matters!
<111> and <100> crystals can influence
The detector properties eg. capacitance

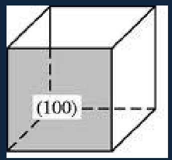

From Wafers to Sensors

1) 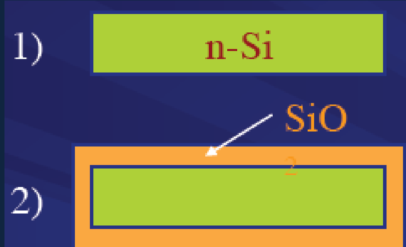

Start with n-doped silicon wafer, $\rho \approx$ 1-10 kΩcm. Silicon can be turned into n-type by neutron doping (^{30}Si+n $\rightarrow$ ^{31}Si, ^{31}Si $\rightarrow$^{31}P+β^{-}+ν)

Oxidation at 800 - 1200°C

3) Photolithography (= mask align + photo-resist layer + developing) followed by etching to make windows in oxide

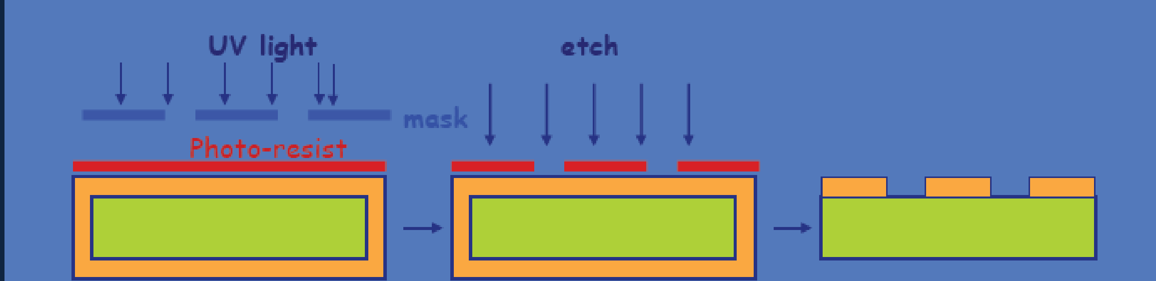

D. Bortoletto Lecture 4 50

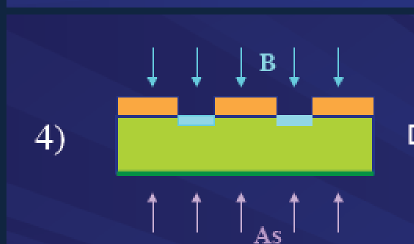

Doping (ion implantation or diffusion)

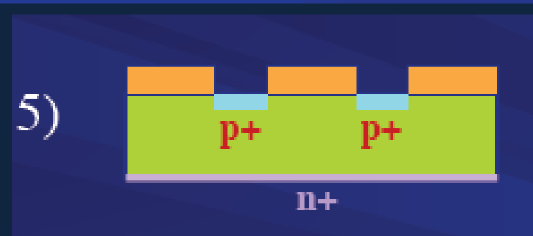

Crystal lattice annealing at 600C

Note:

This process is used for single and double side processing

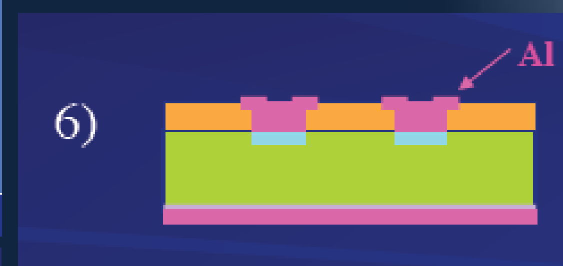

Photo-lithography
Followed by Aluminum
Deposition in the contact
Regions (front and back)

Silicon detector basic working principle

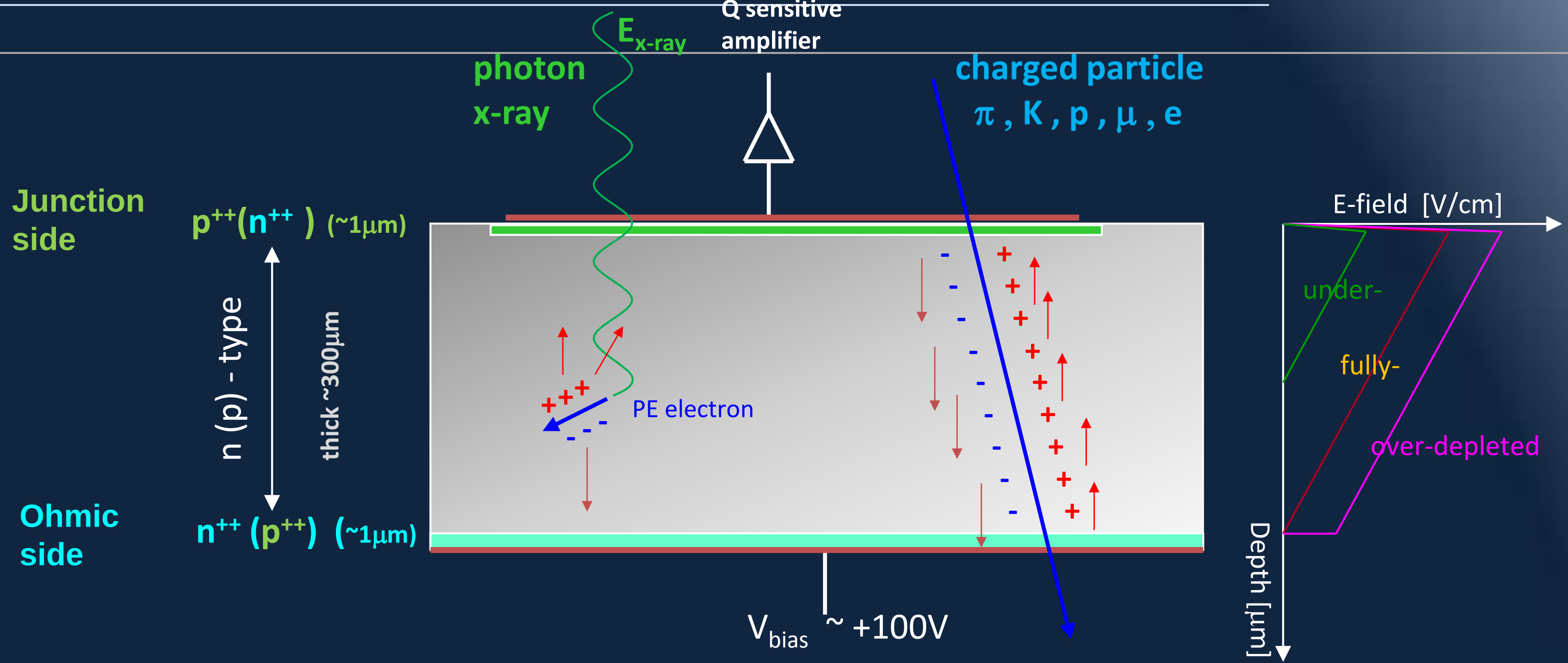

- n+ and p+ electrodes are implanted on the wafer's surfaces to form a p-i-n junction
- V_{bias} is the applied reverse bias voltage, W is the depletion region and Neff the space charge (also called effective doping concentration)
- e-h pairs are created by the energy released by the impinging particle (different interaction mechanism for photons/x-rays and charged particles)
- e-h drift towards the positive and negative electrode "inducing " a current pulse
- Charge collection time depends on the carrier mobility, bias voltage and carrier polarity

$$V_{bias} = \frac{(W)^2 \times e \times |N_{eff}|}{2\varepsilon_0 \varepsilon_{Si}}$$

Segmented Silicon Sensors for Position Sensitivity: Microstrips

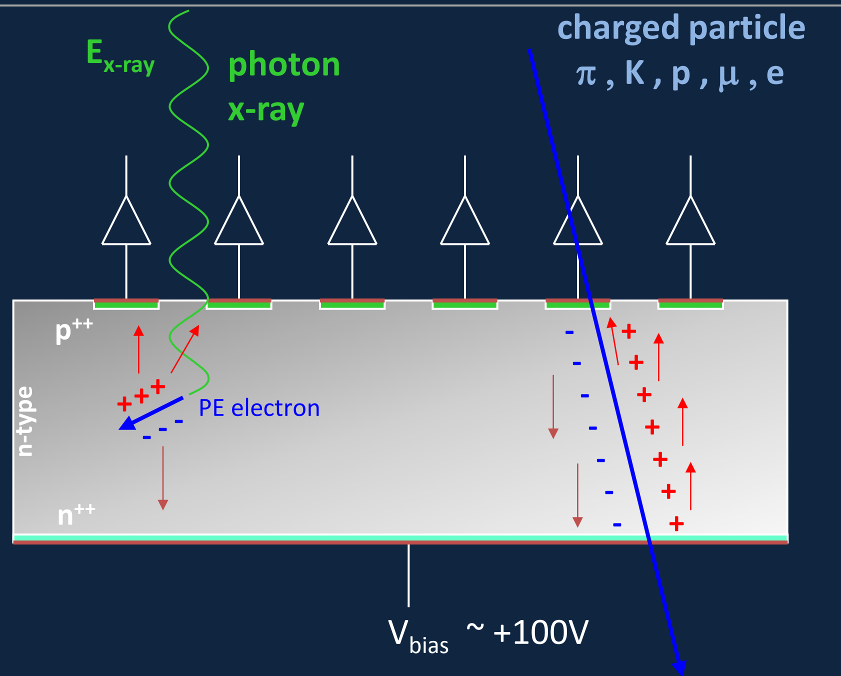

By segmenting one implant we can reconstruct the position of the traversing particle in one dimension.

Standard micro-strip configuration:

– Strips implants separated by 50 um (pitch)
– Substrate resistivity ~2-10 kΩcm
-Substrate thickness ~300μm thick
– V dep< ~200 V

Several layers (with tilted angles) for 2 dimensional information without ambiguity

Two tracks resolution depends on:

- segmentation pitch (strips, pixels)
- charge sharing (angle, B-field, diffusion)
- S/N performance of readout electronics
- d-rays

Charge sharing in segmented electrodes due to:

- Diffusion during drift time
- Lorentz angle due to presence of B-field
- Tilted tracks

Individual readout of charge signal on electrodes allows position interpolation that is better than the pitch of segmentation.

Example: CMS micro-strip module

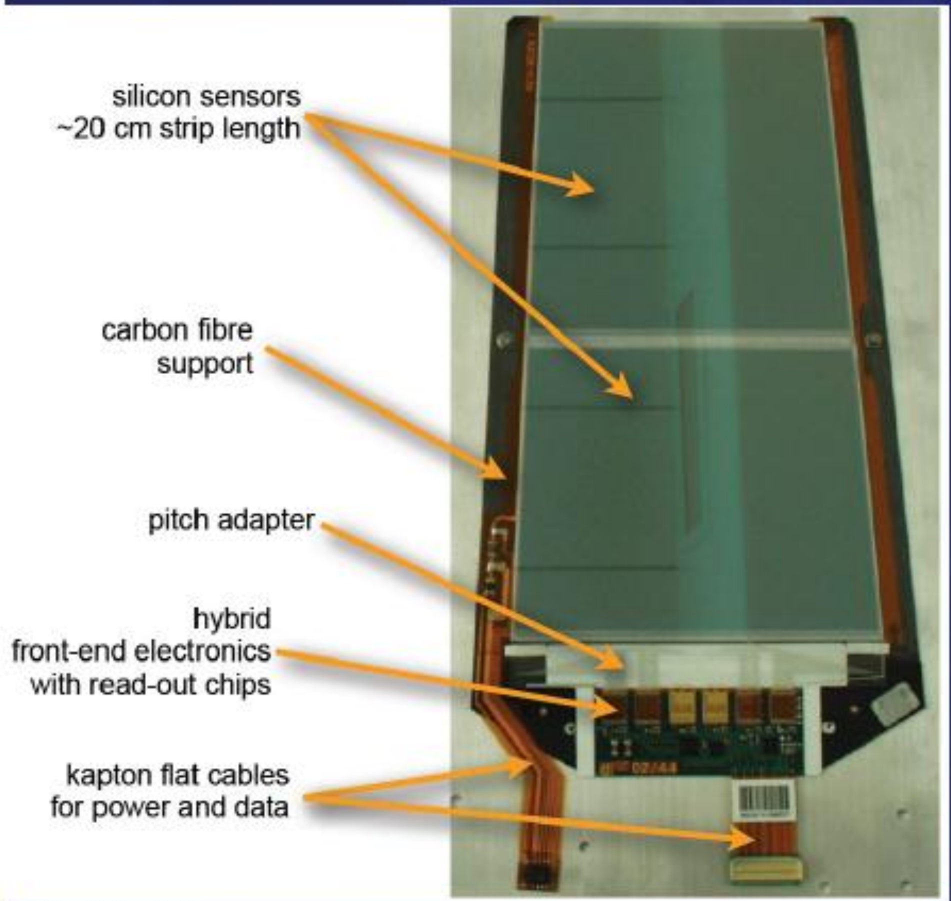

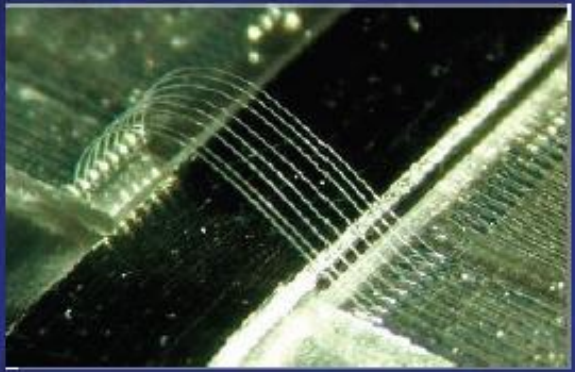

Wire-bonding

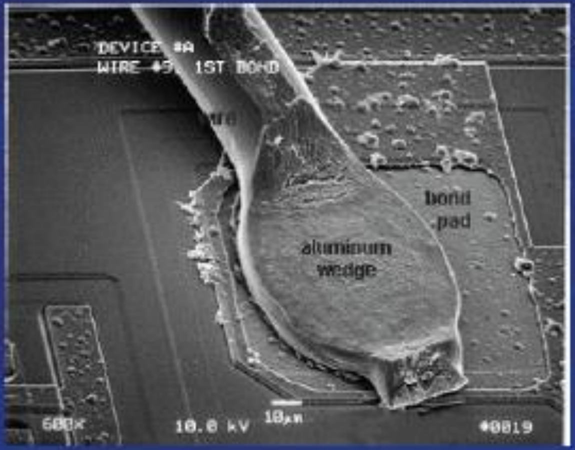

CMS strip module

31

Slide from D. Bortoletto

Double Sided Silicon Strip Detectors

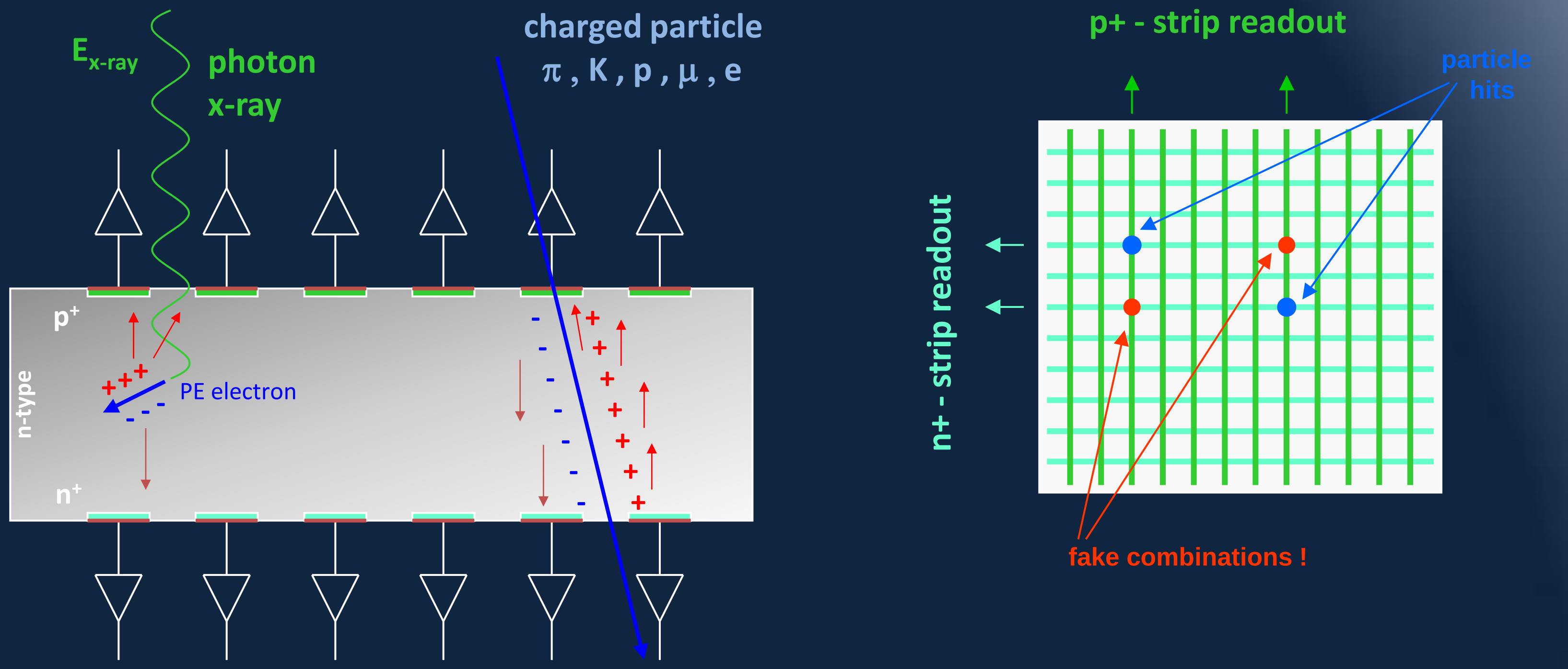

Crossed p-strip and n-strips allows readout of x & y coordinate of particle !

→ But still ambiguity problem for many hits !

→ Problem solved by using pixel segmentation

Pixel Detectors "Hybrid"

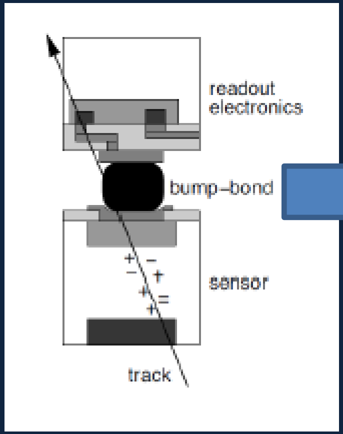

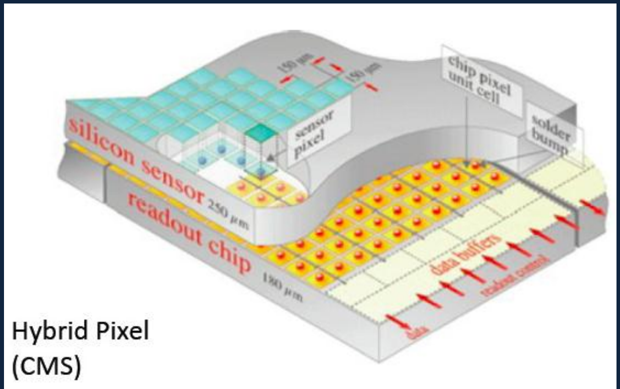

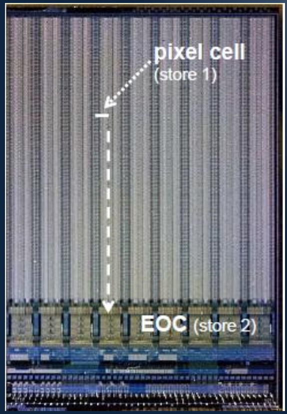

FE-I3 ATLAS:

18 x 160
=2880 pixels
50 x 400 um2

~1cm^2

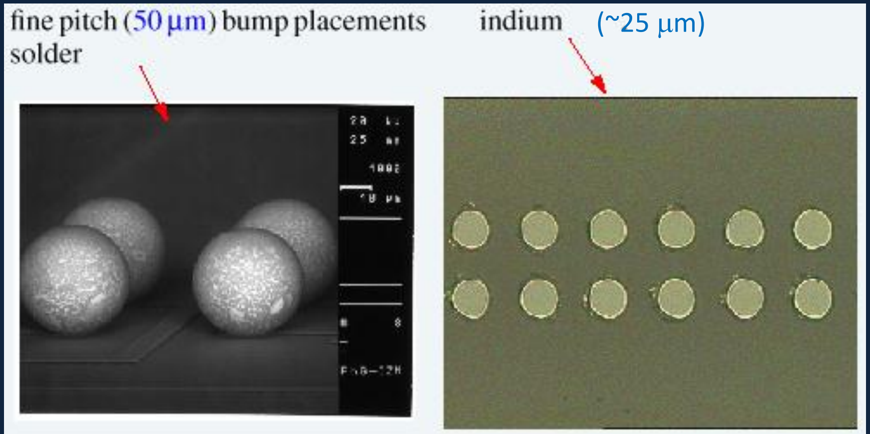

- Sensor and electronics are developed separately then 'bump-bonded
- Segmentation in "true" two dimensions
- Small pixel dimension (low leakage current
- and high spatial resolution)
- Large signal to noise ratio
- Large number of connections and channels
- Large power consumption!!

Example the ATLAS Pixel "FE-I" Family

	FEI4B	FEI3
Year	2011	2003
Technology	130nm	250nm
Chip size	20x19mm²	7.6x10.8mm²
Active area	89%	74%
Array	80x336 (26'880)	18x160 (2'880)
Pixel size	50x250µm²	50x400µm²
Number of transistors	87M	3.5M
Data rate	320 Mb/s	40Mb/s
Wafer yield	60%	80%

!!

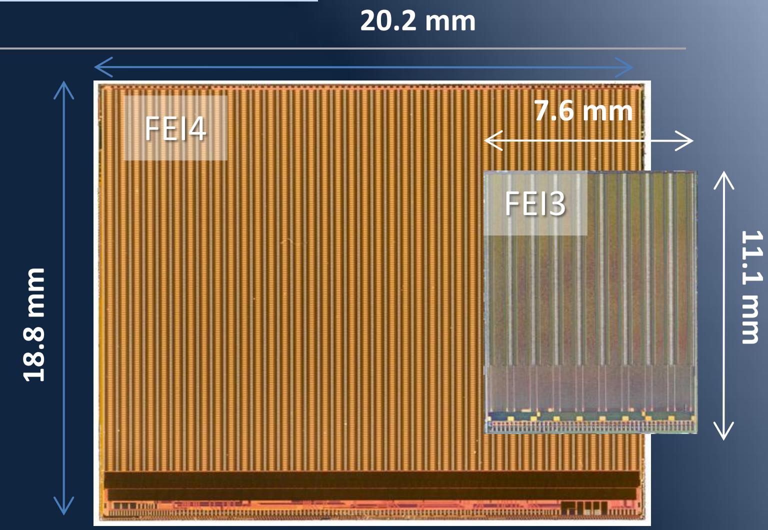

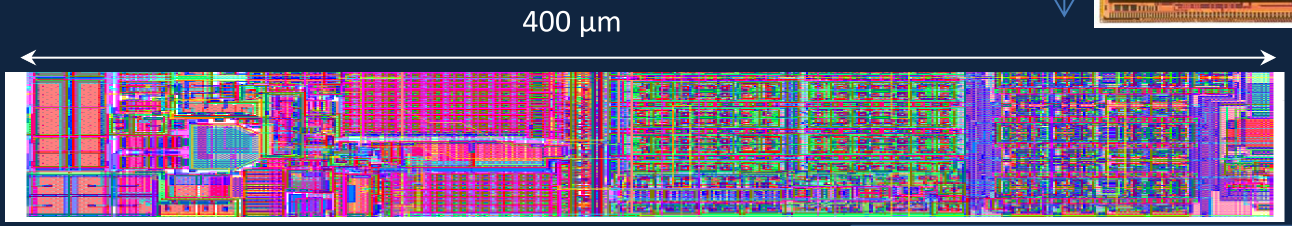

FE-I3 CMOS 250 nm

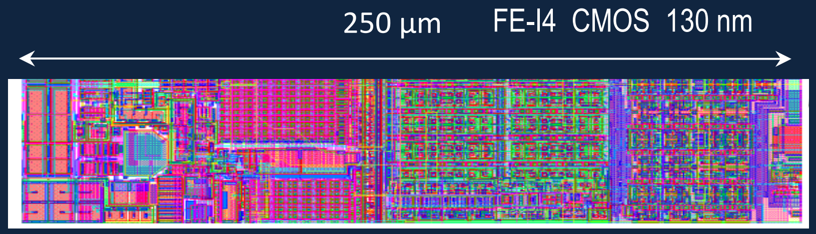

FE-I4 CMOS 130 nm

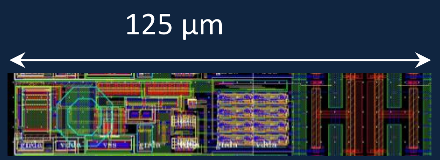

FE-I5 CMOS 65 nm

Half pitch definition

Depends on IC designs

250nm-130nm-65nm Technology nodes

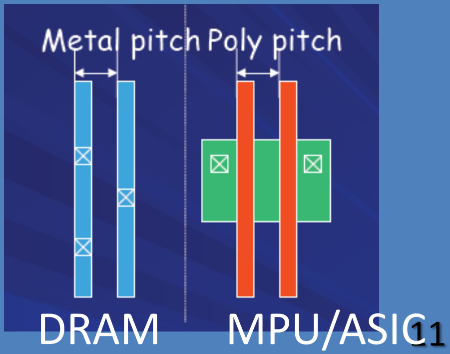

MANCHESTER 1824

Diamond

Current status:

270 mm collection distance diamond attained in pCVD (polycrystalline Chemical Vapor Deposition)

MP signal about 8000 e-

Noise is zero

Single crystal exists but expensive

Applications:

Beam Position Monitors in various experiments (ATLAS, CMS) and beamlines

Bump-bonded to various readout chips

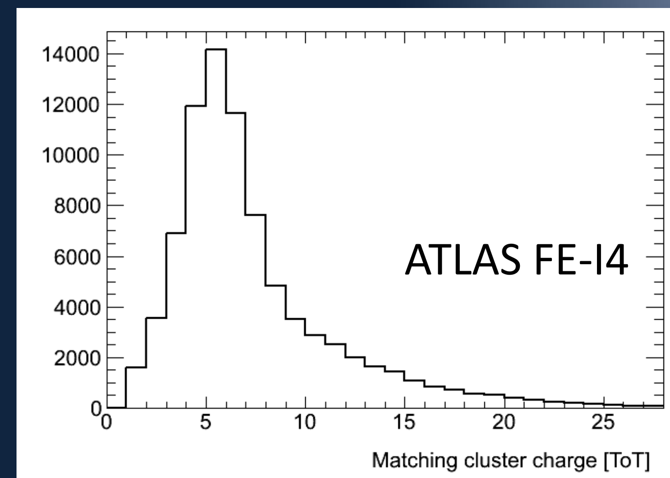

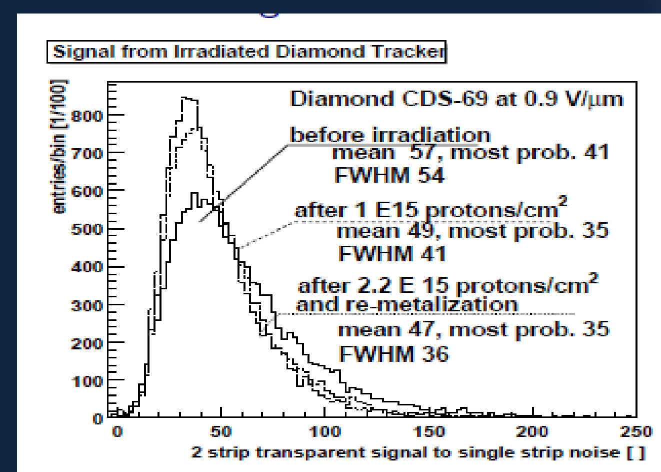

But there are also Gaseous Pixel Detectors!

H. van der Graaf (Nikhef) TIPP2011

Gaseous Pixel detector (GridPix) is a MEMS made Micromegas like structure on a CMOS readout chip

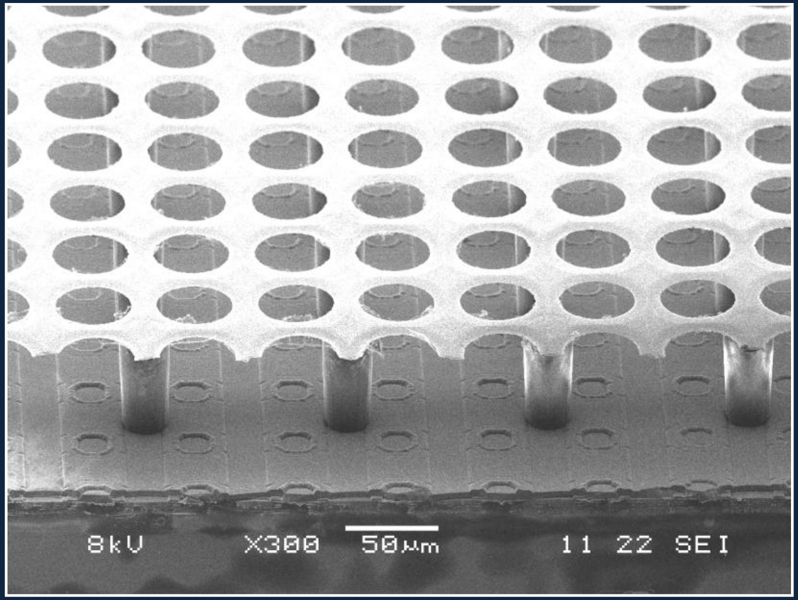

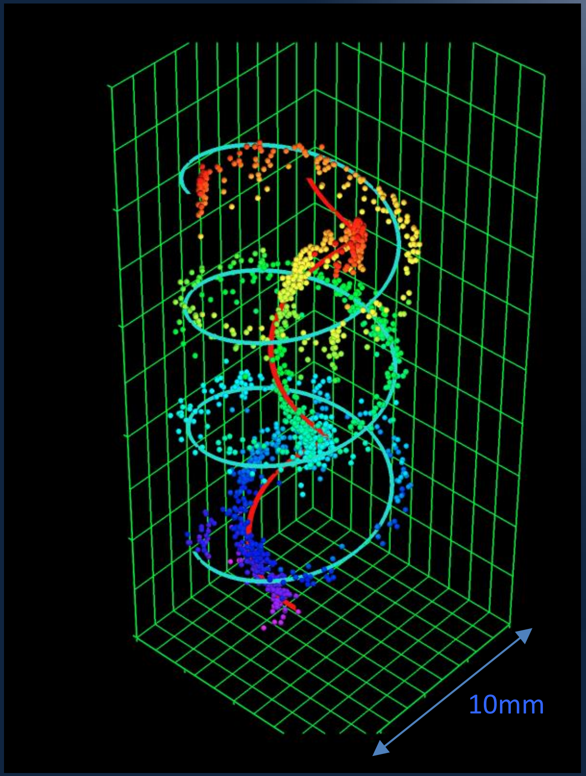

^{90}Sr electrons in 0.2 T B-field

Performance :

- position resolution:15 µm
-single electron efficiency: > 90 %
- track detection efficiency: 99.6 %;

µ-TPC operation with TimePix chip

Pixel detectors "Monolithic"

Integrates the readout circuitry together with the detector in 'one piece ' of silicon

The charge generated by a particle is collected on a defined collection electrode either by diffusion or by the application of an E-field

Small pixel size and thin effective detection thickness

Radiation soft, optimal for high granularity applications

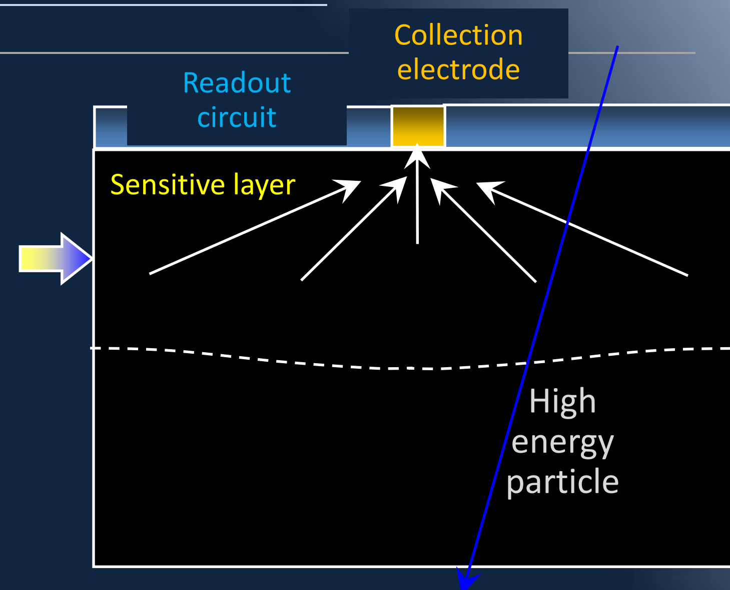

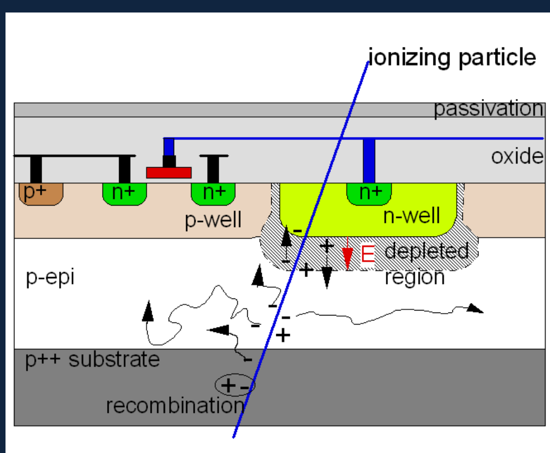

IEEE TNS Vol: 56, Issue: 3, 2009

MAPS

Pixel size :
20 x 20 micron
Thickness
20-50 um

Used in the
EUDET telescope
And at STAR
At RICH

CCD
Charge
coupled
Device
Various
dimensions

Many uses in
Different
fields

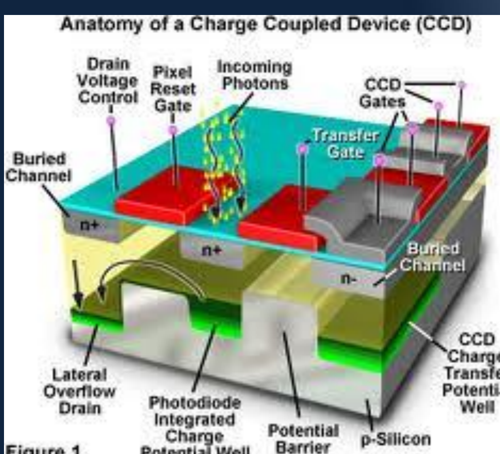

Leakage Current

- Generation Current:

From “thermal” generation in the depleted region

$$j_{gen} \propto T^{3/2} \exp\left(\frac{1}{2kT}\right)$$

Doubles every ~8°C !

It’s minimal if the bulk is high resistivity and with low impurities

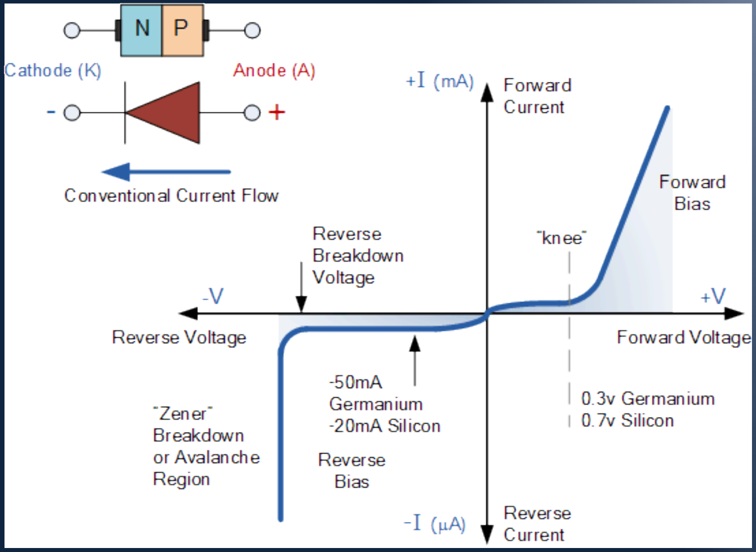

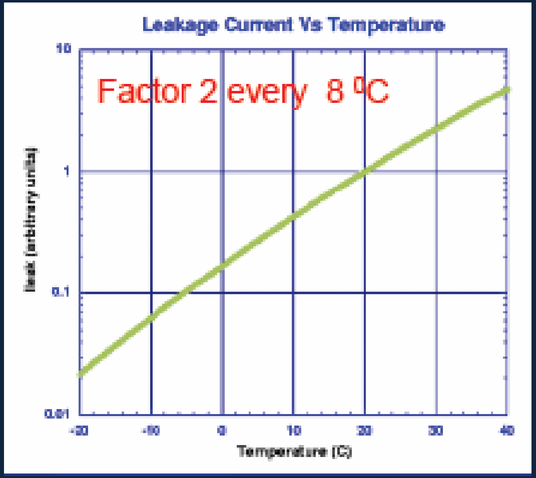

$$I \sim I_0\, e^{\frac{qV}{kT}}$$

- Diffusion Current

Carriers from the ‘un-depleted’ region
Diffusing into the depleted region

Essentials for a good detector: Signal/Noise. Example MIP

❖SIGNAL if there is PARTICLE

→ Signal formed no matter what

→ Detection efficiency

❖NO SIGNAL if NO PARTICLE

→Noise under control

→Discrimination

Charge signal for Minimum Ionizing P article (MIP):

➢ Landau distribution with a low energy tail which broadens because of noise and high energy tail due to secondary "delta" electrons

Mean $(dE/dx)Si = 3.88$ MeV/cm
$\Rightarrow$116 keV for 300 μm thick Si (~80e/μm)

Most probable loss = 81 keV for 300μm Si
Since 3.6eV needed to make e-h pair
$\Rightarrow$ charge in 300 μm= 22500 e- (=3.6 fC) (75e/μm)

Mean charge = Most probable charge ≈ 0.7× mean

Width depends on Substrate thickness

High energy tail From delta rays

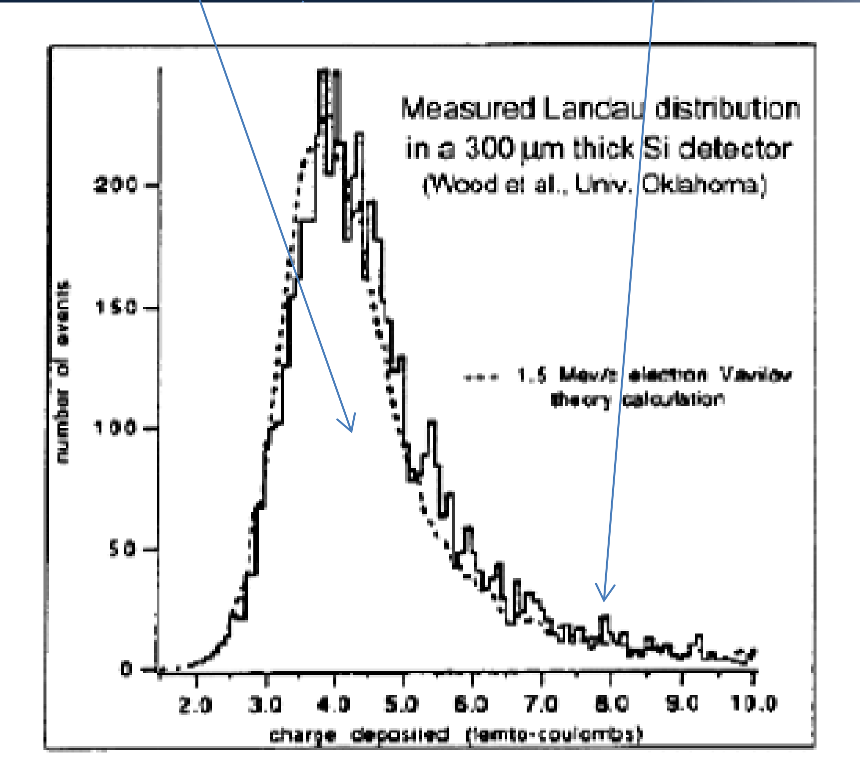

Noise

- **Noise depends on**:
  detector geometry,
  biasing scheme,
  readout electronics..

- Noise is typically given as "equivalent noise charge" ENC.
  This is the noise at the input of the amplifier in elementary charges.

- The most important noise contributions are:
  - Leakage current
  - Detector capacitance
  - Detector parallel resistor
  - Detector series resistor

- The overall noise is the quadratic sum of all contributions:

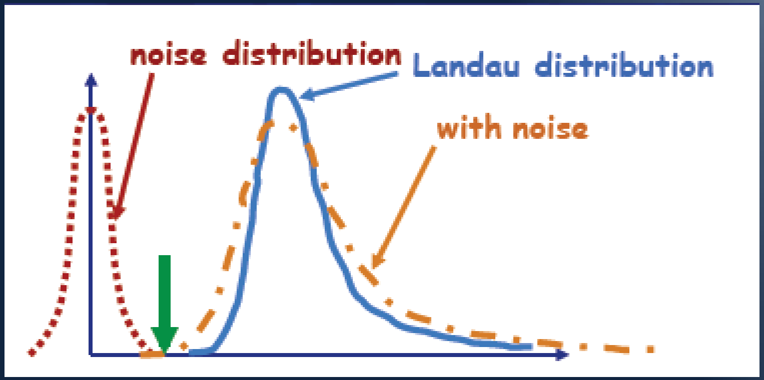

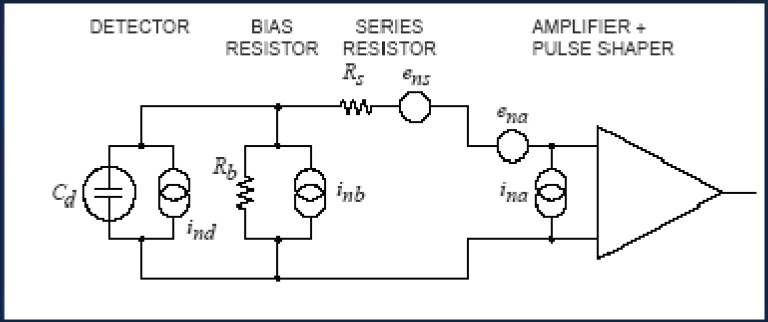

$$ENC = \sqrt{ENC_C^2 + ENC_I^2 + ENC_{Rp}^2 + ENC_{Rs}^2}$$

Capacitance

C_{ac} = coupling capacitance
~10pf/cm dependent on thickness and composition of dielectric.
Thin oxide - larger coupling capacitance, large signal, lower Vb, more fragile structure

C_b = backplane capacitance
~0.1 pf/cm - due to parallel plate front-back coupling, dependent on depletion

C_i = interstrip capacitance
~ 1 pf/cm - usually dominant preamplifier load. Dependent on detector layout, surface and oxide charges, irradiation. Is larger for n-side due to p-stop coupling. Also larger for double metal devices

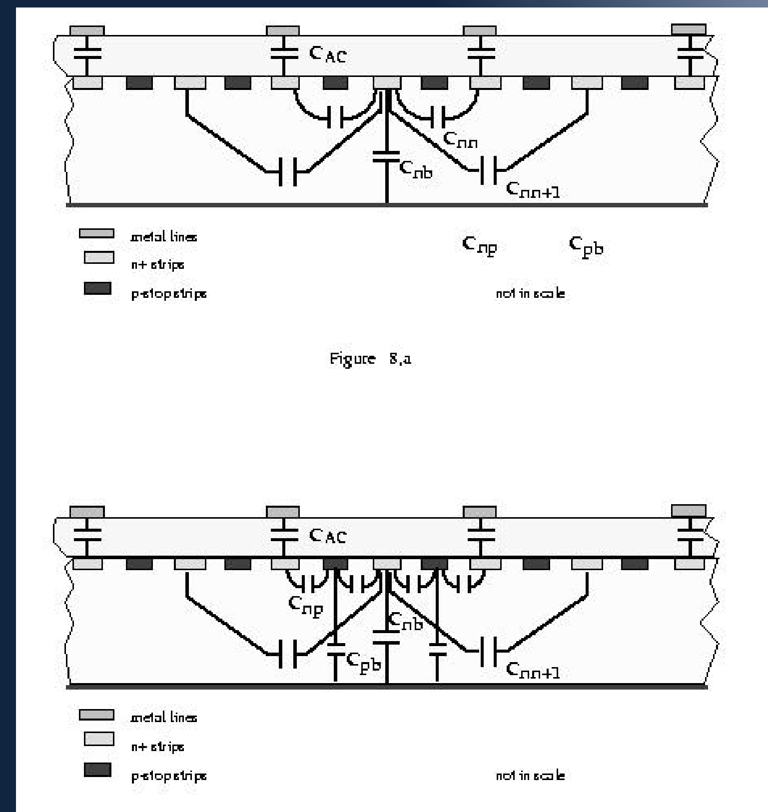

Signal formation: Ramo's theorem

from A. Castoldi

Current induced on electrode k by the motion of charge q:

$$Q_k = -q_P \tilde{V}_w \longrightarrow i_k(t) = \frac{dQ_k}{dt} = -\frac{d\left(q_P \tilde{V}_w\right)}{dt} = -q_P \frac{d\tilde{V}_w}{dt} \cdot \frac{d\vec{l}}{d\vec{l}} = -q_P \frac{d\tilde{V}_w}{d\vec{l}} \cdot \frac{d\vec{l}}{dt}$$

potential at P due to electrode *k* at 1 V

$$Q_k^A = -q_P \frac{V_P^B}{V_k^B} = -q_P \tilde{V}_w$$

charge induced by q_P on electrode *k*

$$i_k(t) = q_P \tilde{E}_w \cdot v(x(t), y(t), z(t))$$

weighting field:

$$\tilde{E}_w = -grad\, \tilde{V}_w$$

true carrier velocity:

$$v = \mu E(x(t), y(t), z(t))$$

(here charge transport by drift is assumed)

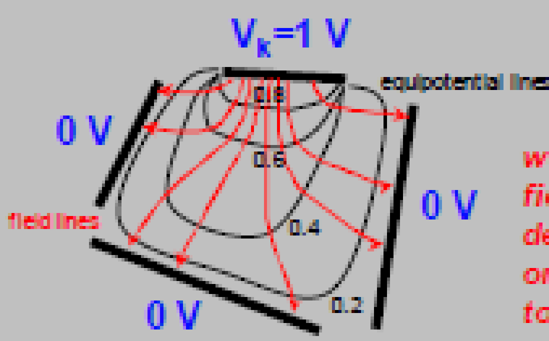

weighting field/potential depends only on device topology (Laplace eq.)

(V_k=1 V, all others grounded)

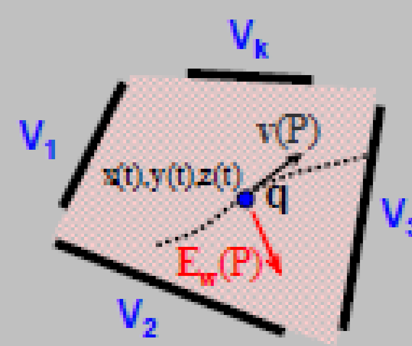

carrier trajectory computed in the true electric field (i.e. with bias voltages, fixed space charge, etc.)

Signal and weighting potential

*the **induced charge** can be computed directly on the **weighting potential map** (depends only on moving charge and topology of device)*

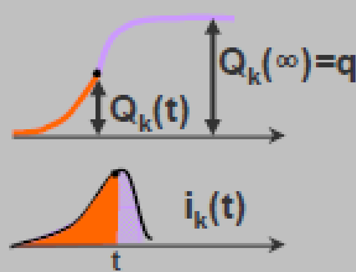

$$Q(t)=\int_0^t i(\tau)d\tau =$$

$$\boxed{q\int_{\vec{r}_0}^{\vec{r}} \vec{E}_w \cdot d\vec{l} = -q\left[V_w(\vec{r})-V_w(\vec{r}_0)\right]}$$

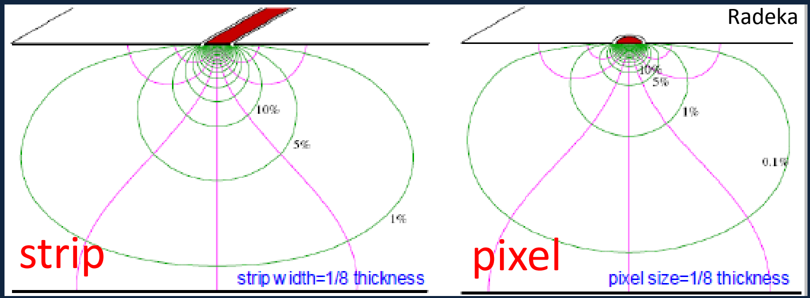

- In segmented devices V_W strength depends on $\frac{d}{pitch}$ where d = p-n electrodes distance and "pitch "is the strips or pixel mutual distance

- Signal charge for MIPs independent of Position for most of the sensor volume except near the collecting electrode ('small pixel effect')

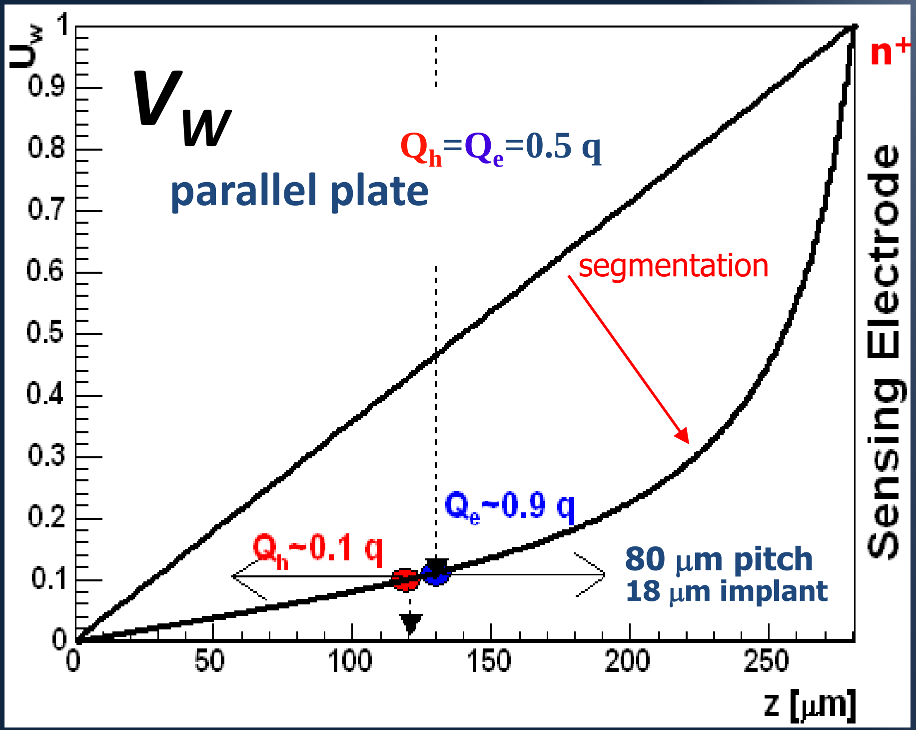

Front-end Readout electronics chain

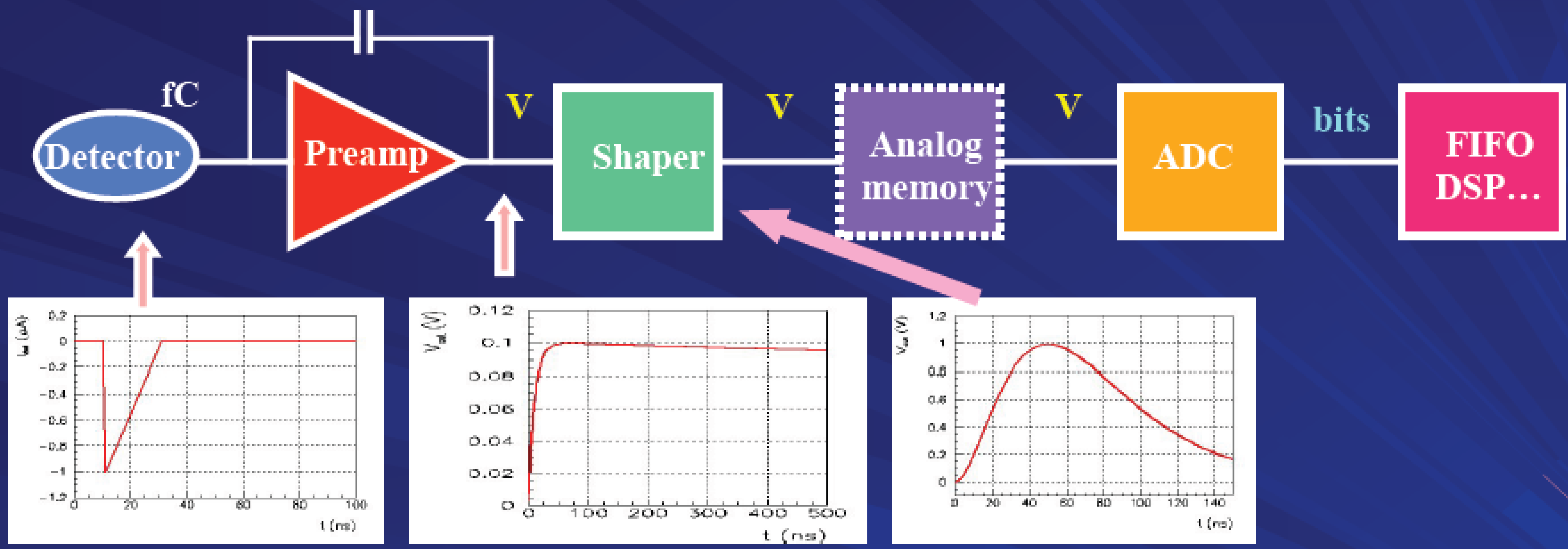

- Very small signals (fC) -> need amplification
- Measurement of amplitude and/or time
  - (ADCs, discris, TDCs) (Example Time over Threshold)
- Several thousands to millions of channels

Example: Charge sensitive Amplifier

- Uses and Feedback amplifier with gain –A
- Assumes infinite input impedance (and no current in the amplifier)
- $V_o = -A\ V_i$
- The output charge Q depends only on C_f where Q=CV

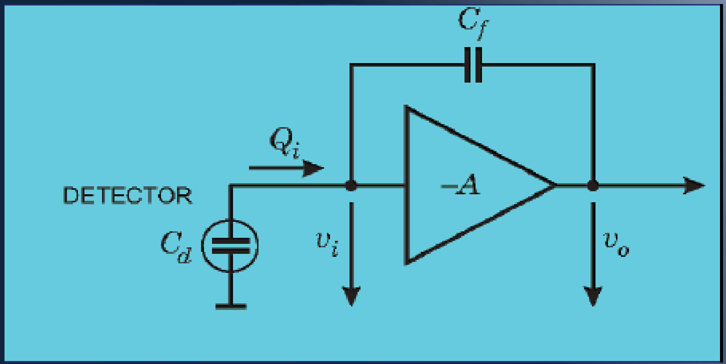

NOTE:

- The bandwidth (BW) of an amplifier is the frequency range for which the output is at least half of the nominal amplification
- The rise-time t_r of a signal is the time a signal takes to go from 10% to 90% of its peak-value
- For a simple 1 stage RC network (amplifier) with time constant τ ~ RC
  t_r~2.2τ and BW * $t_r \approx 0.35$
- For fast rising signals (t_r small) one needs a high bandwidth

Cinzia Da Via, Uni. Manchester INFIERI 2013 , Oxford July 2013

Example: Time Over Threshold

- 1 TDC (Time to Digital Converter) channel measuring both leading edge and pulse width

- Single threshold timing: as soon as the signal Is above threshold a digital signal is generated

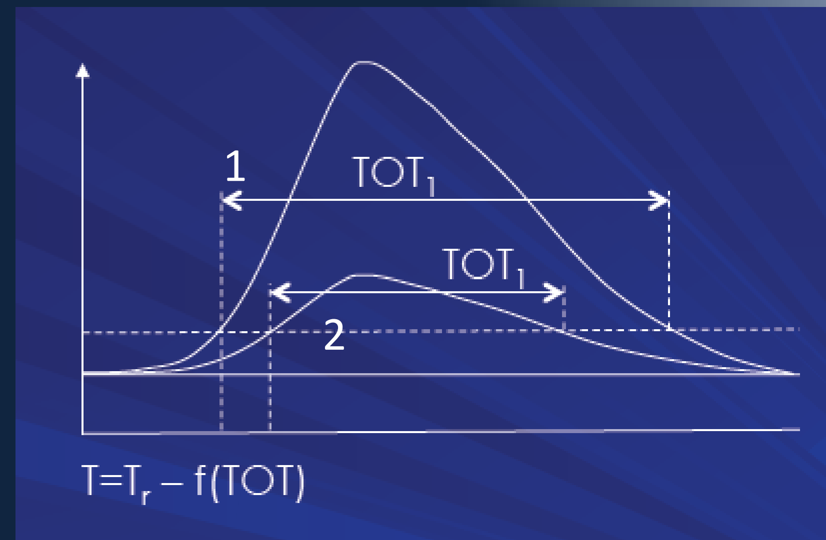

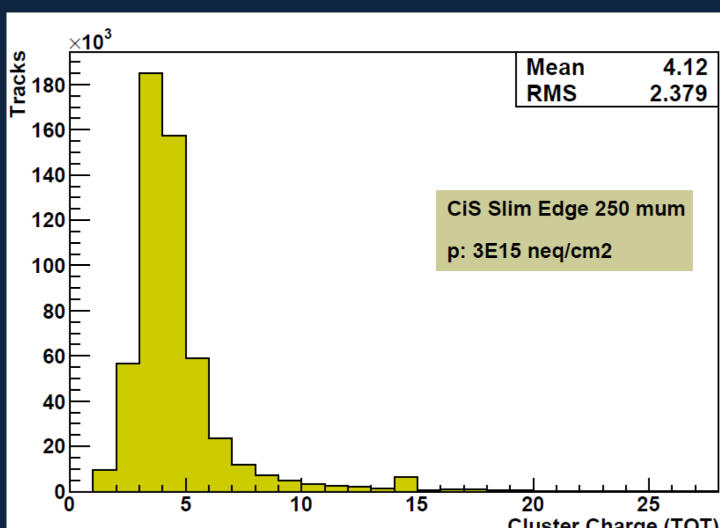

- There is a dependence of the signal rise-time (1 and2) and amplitude ("time walk") which depends on the sensor capacitance C
  - can even be used as an ADC (Analog to Digital Converter)

– E.g. ATLAS Pixel

Total Required signal =
= (threshold + overdrive) * 2

Application1:Tracking Detectors in HEP

- Separate tracks by charge and momentum

- Position measurement layer by layer:

  Inner layers: silicon pixel and strips → presence of hit determines position

  Outer layers: strips or "straw" drift chambers → need time of hit to determine position

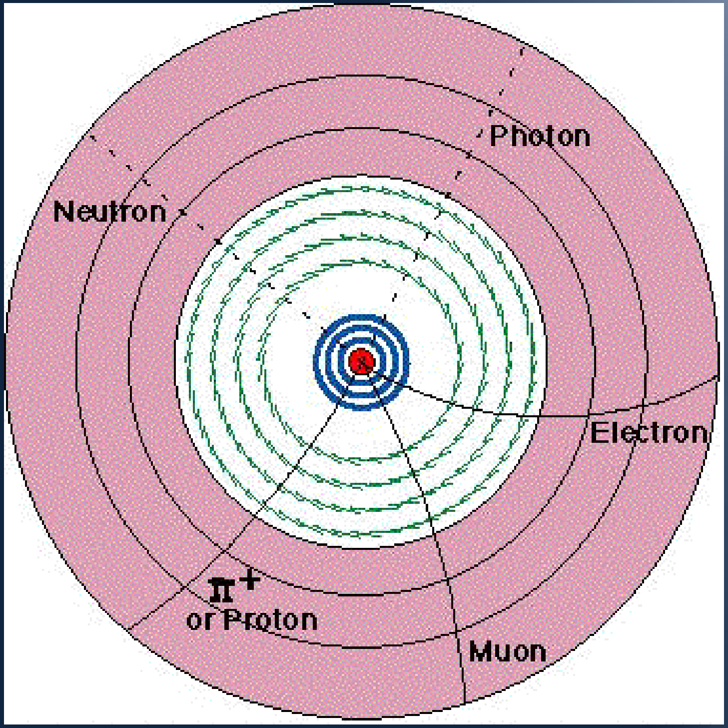

Example: Identification of Event Vertices

- primary event vertex reconstruction crucial in multiple collision events
- secondary vertices for live time tagging
- b- jet tagging
- Identification of exclusive B-meson decays

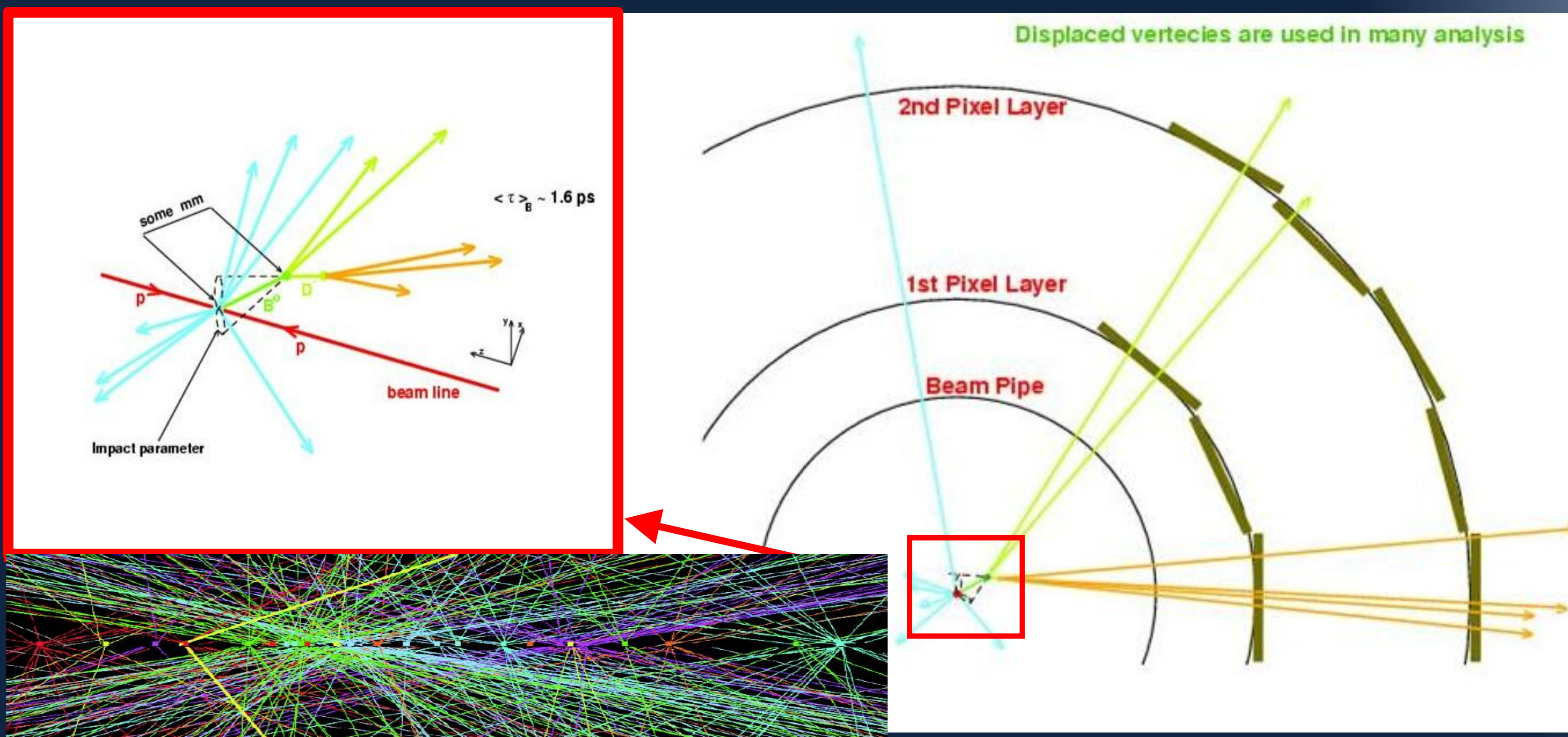

A brief history of strips and pixels

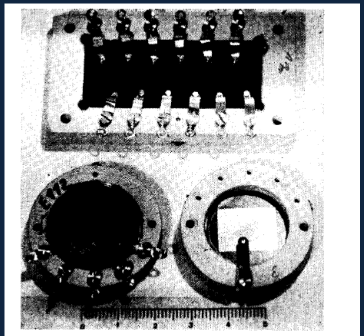
Fig. 1. Ion-implanted semiconductor detectors with subdivided front-contact and common back-contact.

Segmented diodes 1967

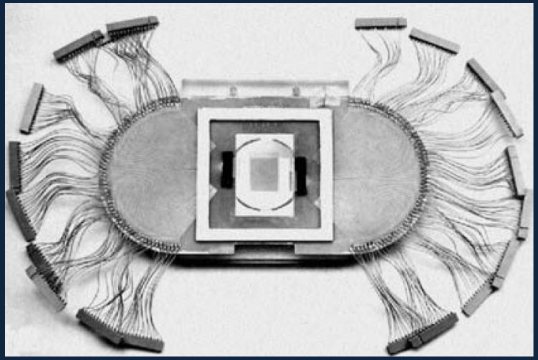

Strips in Na11 in 1980

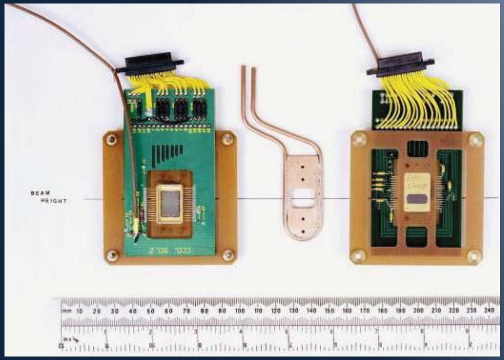

CCDs in Na32 in 1984

1943 Semiconductor detectors developed (Utrecht) –
1955 (Bell Labs, Oak Ridge)
1955 Surface barrier diodes on Si and on Ge in **1949**
~**1958-1960** Diffused Si junctions and p-i-n/n-i-p introduced
~ **1960** Ion-implanted diodes by J. Mayer and others (e.g.at Philips Amsterdam)
Several diodes on same slice was done 'right away' at AERE, LBL and CEA Saclay
1967 Patent on double-sided Si 'checker board' detector by Philips (NL)
1970 Invention of CCD by Boyle and Smith, Bell Syst Tech J, 49 (1970) 49
1971 1st strip sensor: NIM 97 (**1971**) 465-469, *Striped Semiconductor Detectors for Digital Position Encoding*, E.L. Haase, M.A. Fawzi, D.P. Saylor and E. Velten, Karlsruhe, Ge.
1980 Kemmer publishes Fabrication of low noise silicon radiation detectors by the planar process NIMA(1980)499-502
1980 Surface barrier microstrip sensors for experiments NA11, 100-200μm strip pitch
1984 CERN NA32 installs 0.5M Pixels CCDs 2cm beyond the target

Thanks to E. Heijne, S. Parker, C. Damerell

1984 NA32 experiment at CERN

C. Damerell

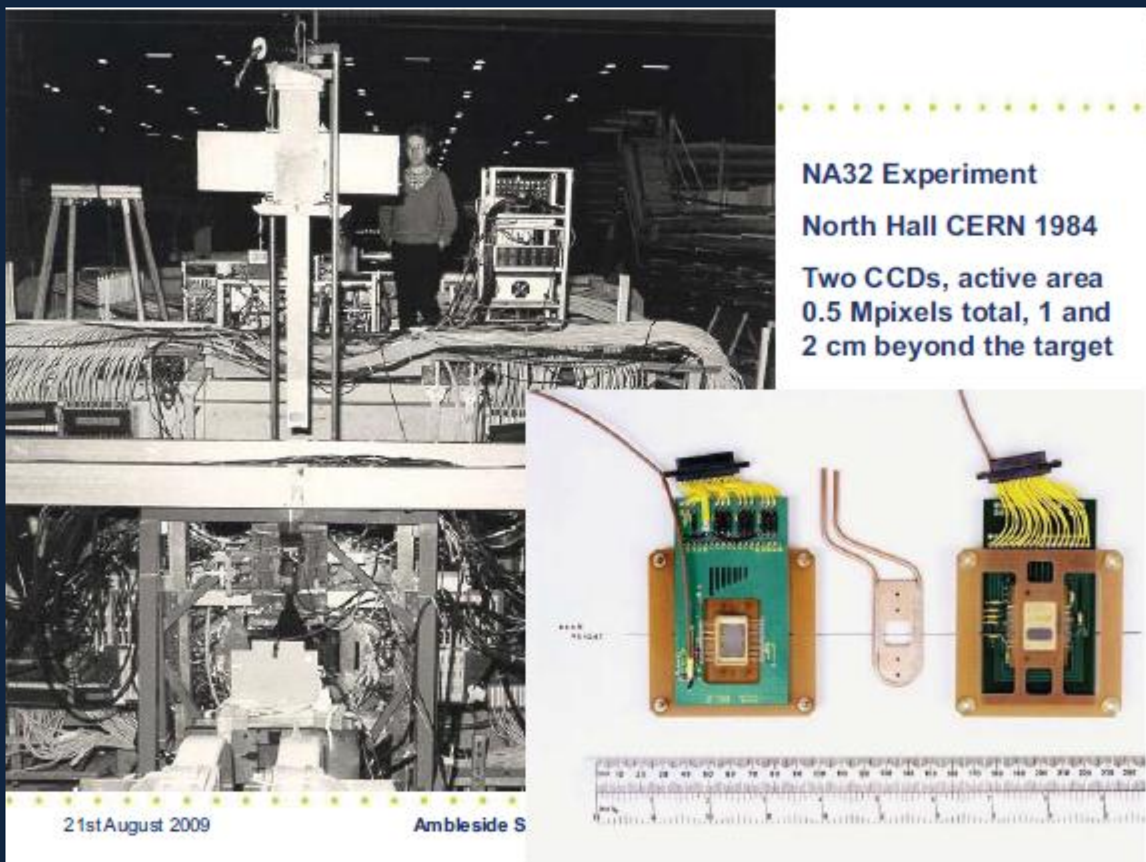

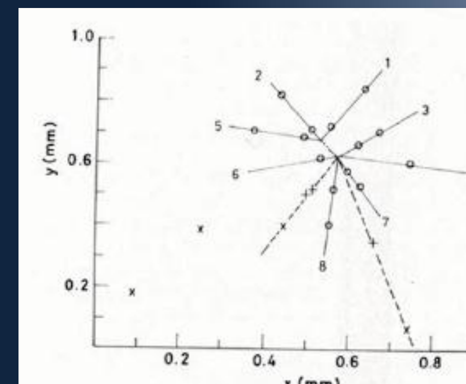

2 CCD pixel layers identified Charm decay without "Ghosts" And proved the power of pixel vertex detectors

1991 SLAC SLD

C. Damerell

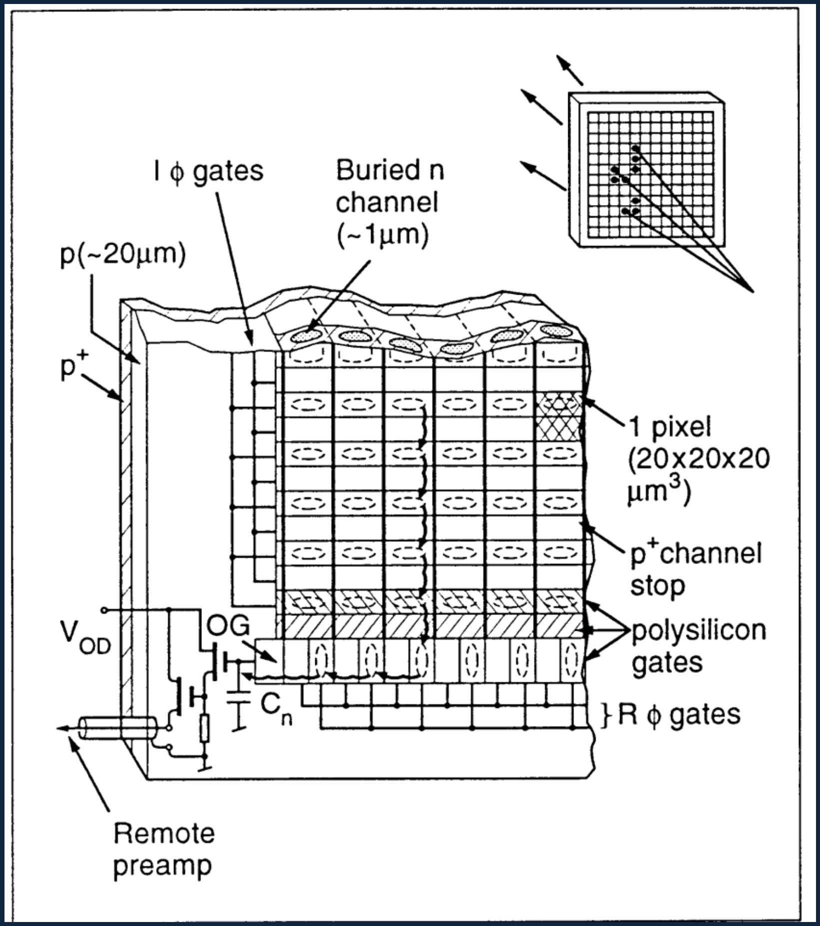

What was installed in 1995:
307 Mpixel CCD system, with
Layer thickness 0.4% Xo

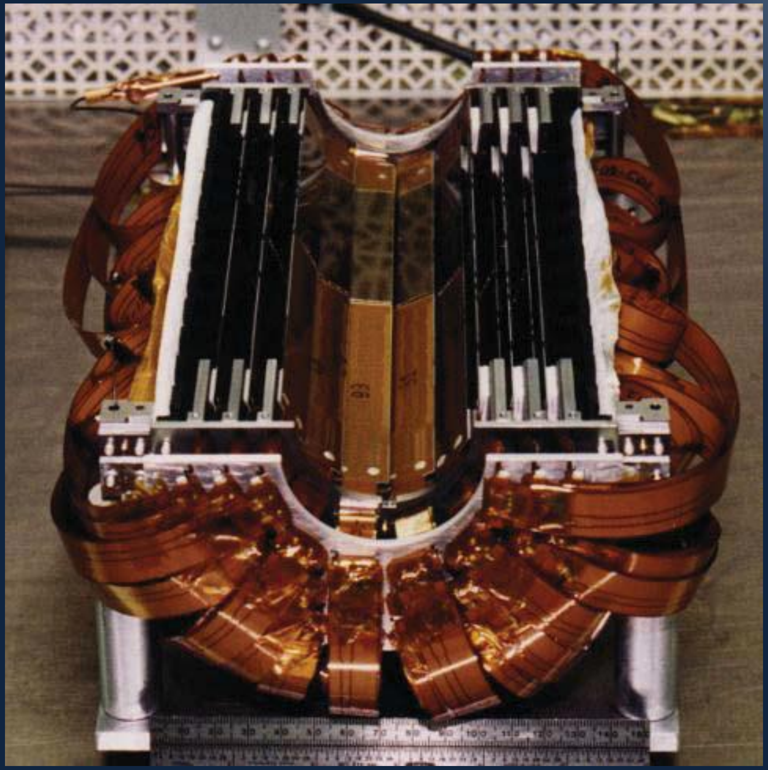

SLD

The CERN - LEP experiments

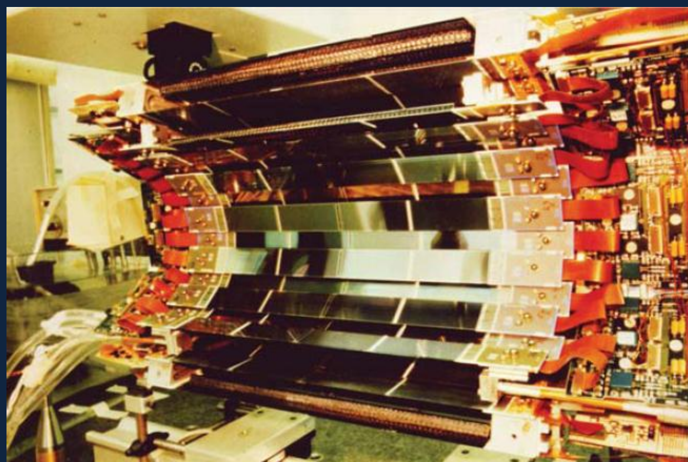

1994

DELPHI

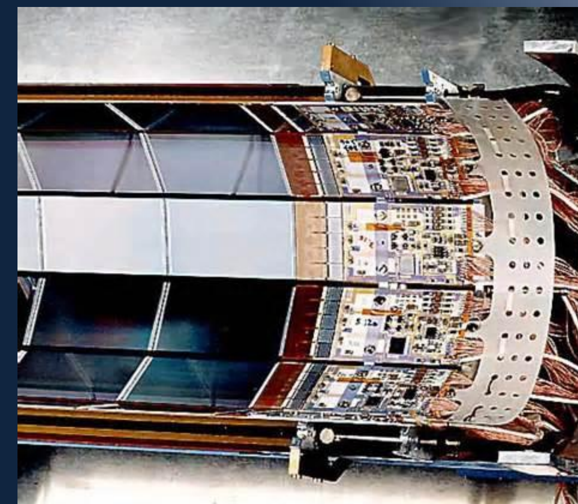

OPAL

ALEPH

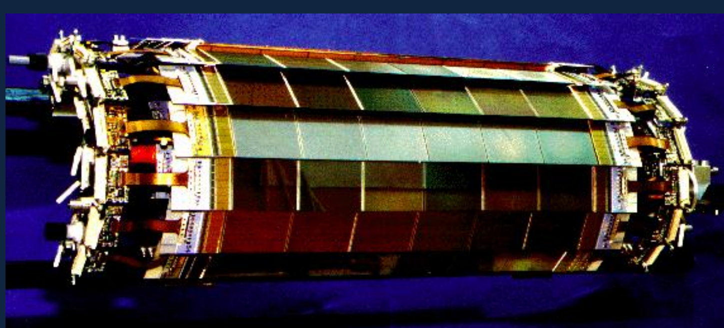

	Closer	Inner	Outer	Ministrip	Pixel
Radius (cm)	6.6	9.2	10.6		
Number of modules	24	20	24	48	152
Detectors/module	4 ds	4 ds + 4 ss	$R\phi$:8, z:8	2ss	1ss
Sensitive area (cm^2)	292	208	103	324	378
Channels/module	1536	2560	2560	512	8064
Coverage $\pm\Theta$	25	21	23	10	12.2
Support	Kevlar + carbon	Kevlar + carbon	Kevlar + carbon	Al	Al
Angle to z-axis	0	0	0	49	12 and 32
Length	6.07; 7.91	5.75; 6	6	5.3	6.9
Width	2.08	3.35	3.35	5.3	1.7–2.2
Readout pitch (μm)	$R\phi$ 50	$R\phi$ 50	$R\phi$ 50	200	330
	z 49.5, 99, 150	z 42, 84	z 44, 88, 176		
Intermediate strips	$R\phi$ 1 z 0	$R\phi$ 1 z 0	$R\phi$ 1 z 0,1	1	0
Biasing	R_{poly}	FOXFET/R_{poly}	FOXFET/R_{poly}	FOXFET	
n-side isolation	field plate	$p+$	–	–	–
Operating voltage	60	60	60–95	50–60	60
Readout chip	MX6	MX6	Triplex	MX6	SP8
RO channels/module	2 × 384	2 × 640	2 × 640	8064	300
Power/chip (W)	0.2	0.2	0.2	0.2	0.017

ds: double sided; ss: single sided. More detailed tables exist in [146]

The Fermilab Central Trackers

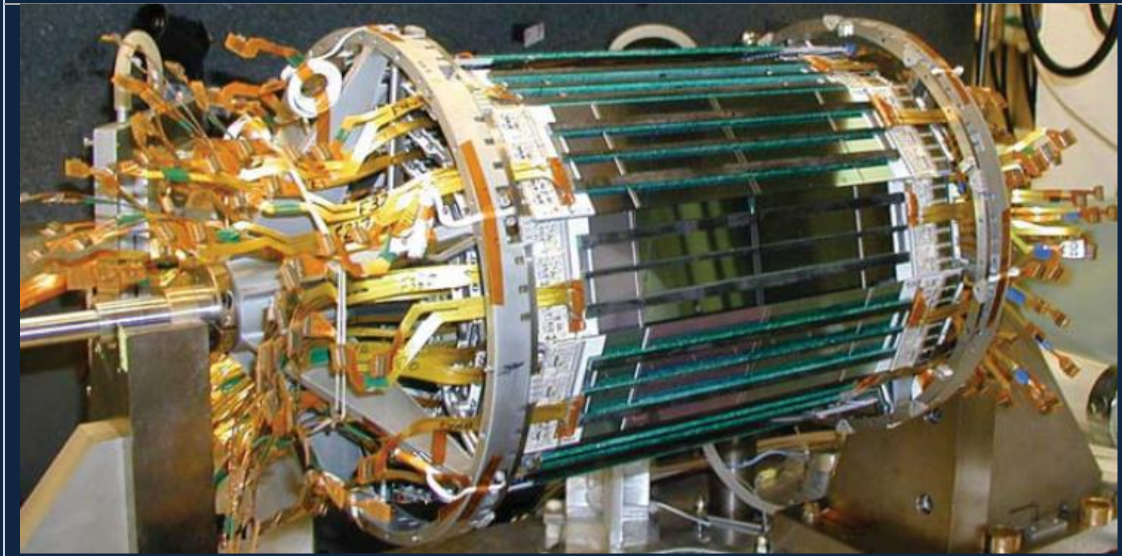

CDF
720000 readout channels
- about 6m^2 of Si

DØ
800 000 readout channels
-about 3m^2 of Si

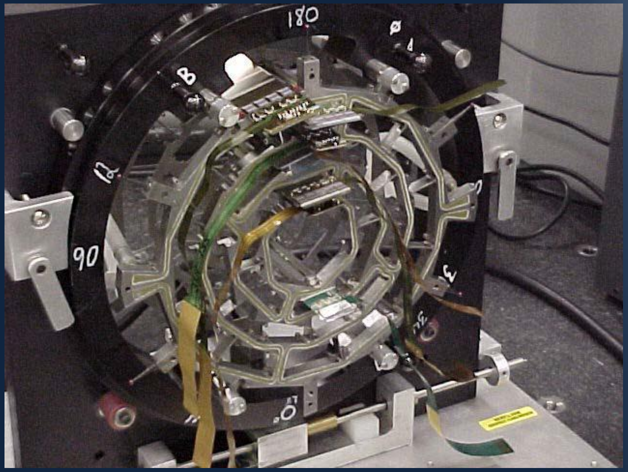

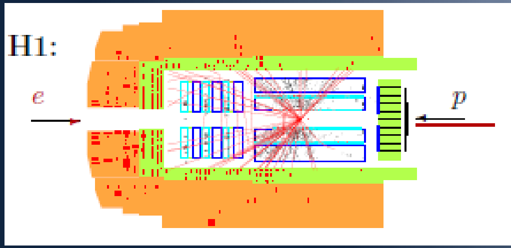

Zeus and H1 at HERA

(study of the proton structure and more at e-p collider)

H1 Backward Si Tracker (BST)

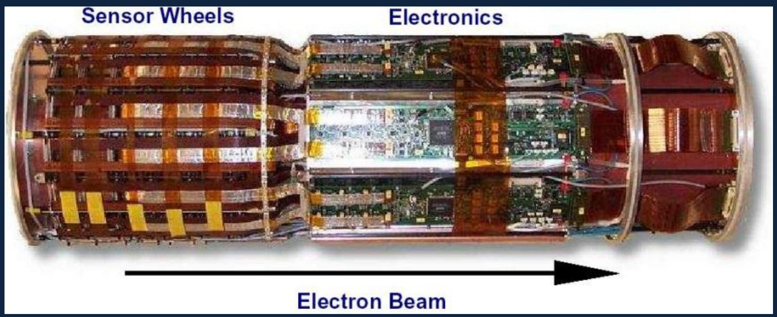

Central ST

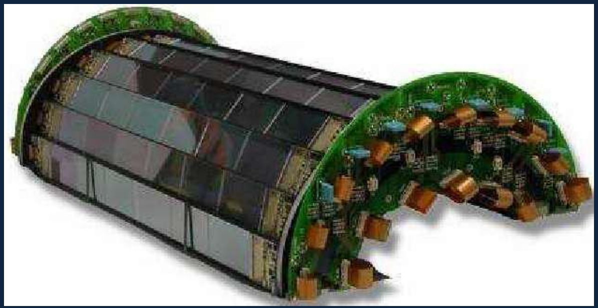

BST= 6 wheels (u/v) for tracking 84k channels
Plus 4 trigger wheels with pads
CST=**2 layers, 82k channels;**
Radiation hard electronics

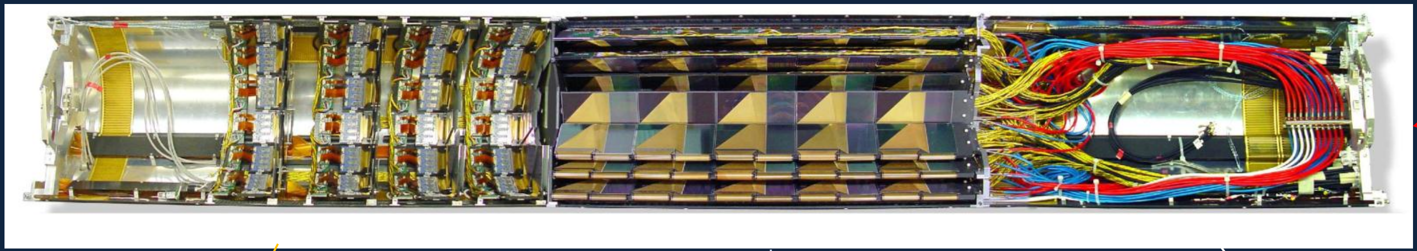

ZEUS Micro-Vertex

The **forward** section:
- 4 wheels;
- each one composed by 2 layers of 14 Si detectors
- Total of 112 hybrids, >50k channels

The **barrel** section:
- 30 ladders;
- each one composed of 5 modules of 4 Si detectors
- Total of 300 hybrids, >150k channels

The rear section:
- Cooling pipes and manifolds;
- Distribution of FE, slow control and alignment cables

The LHC Detectors

ATLAS and CMS use alone more that 250m^2 of Silicon Strips to “image” charged particles

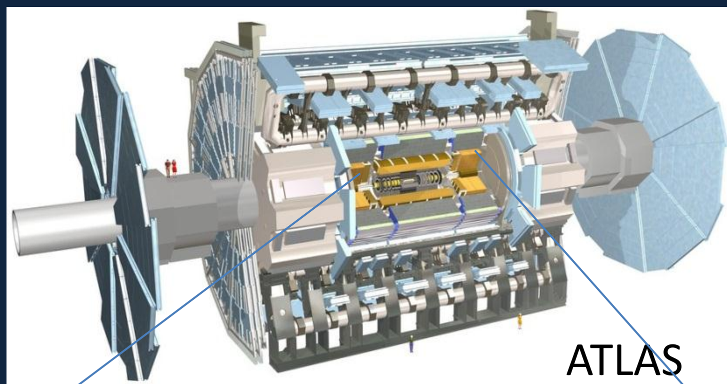

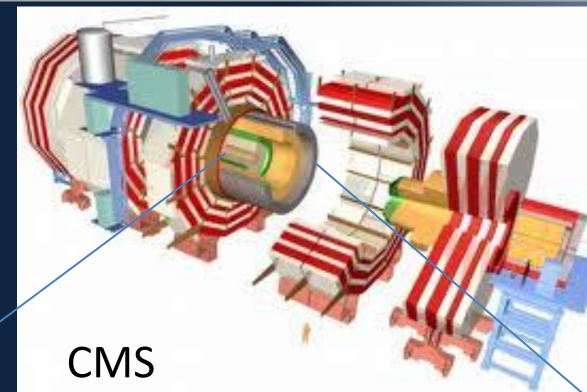

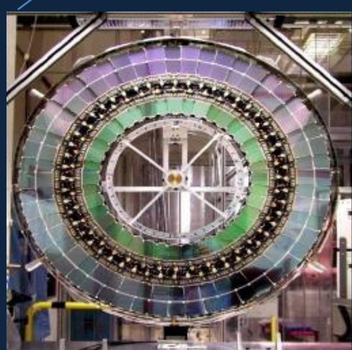

Strips
61m^2 of silicon.
6.2million channels 4 barrel layers + 9 disks per endcap
30cm < R < 52cm

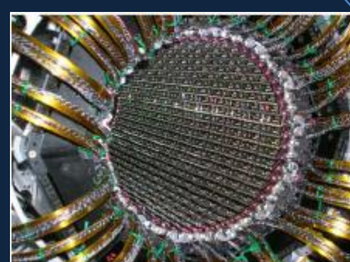

Pixels
3 Barrel layers
(r=5,9,12 cm)
2 end caps each with 3 disks
80Mpixels
50x400um2
Digital I/O

Pixels
3 barrel layers
2 end caps each with 2 disks
66 Mpixels 150 x 100um2
Analog I/O

Strips
198 m^2 of silicon,
9.3 million channels
Inner : 4 barrel layers, 3 end-cap disks
Outer: 6 barrel layers, 9 weels
22cm < R < 120cm

MANCHESTER
1824

LHCb VErtex LOcator (VELO)

Search for physics beyond the Standard Model: CP-violation and rare decays of heavy hadrons

C. Farinelli

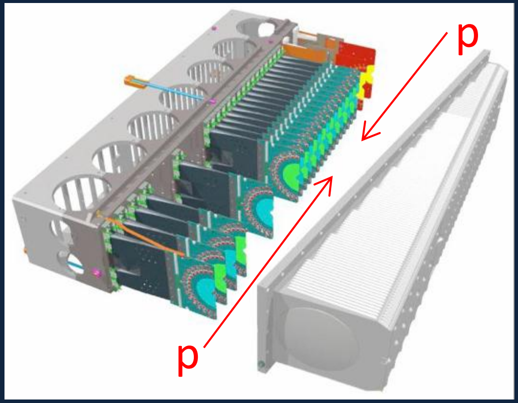

VELO characteristics:

- silicon sensors in secondary vacuum
- shielded by 300 µm RF foil
- 172,032 channels in total
- operating temperature of cooling system = -8°C

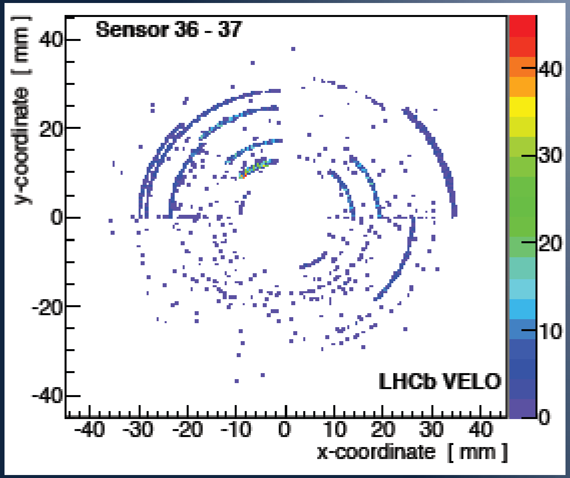

beam

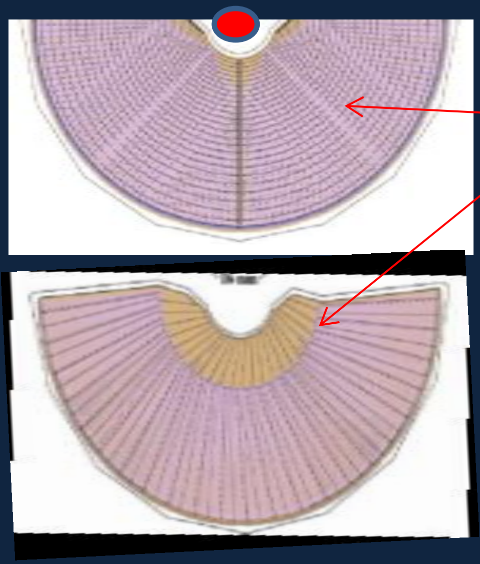

Silicon sensors with R-strips and ϕ-strips (2048 strips per sensor)

Sensor characteristics:

- 300 µm thick
- 8mm < radius < 42.2mm
- 40 µm < pitch < 101.6 µm
- radiation hard design:
- oxygenated silicon
- n-on-n type

TOTEM Roman Pots

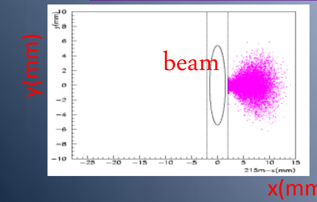

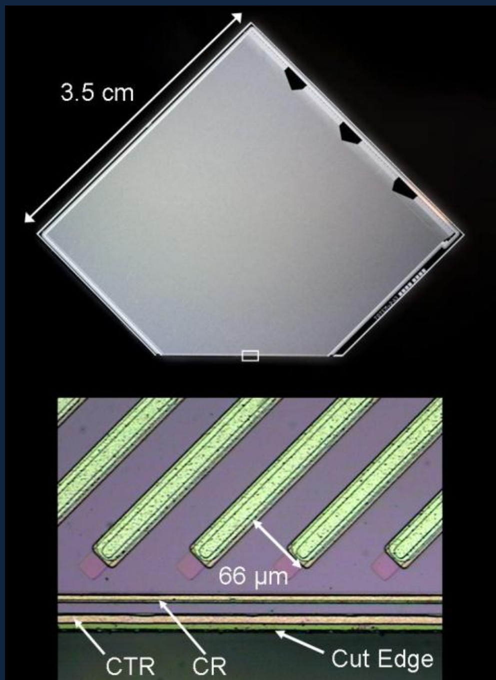

Totem measures the elastic scattering and the Total Cross Section at the LHC.

- Roman Pots are inserted in the beam pipe at 140-170m from the CMS experiment on both sides

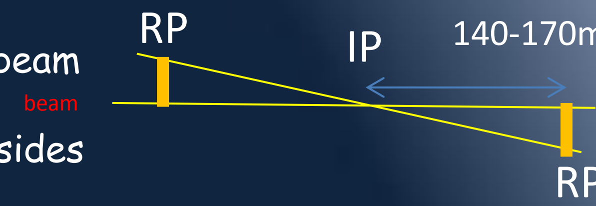

- Standard planar technology is placed in a secondary vacuum at few mm from the beam

- Edge width 50um at few mm from the beam

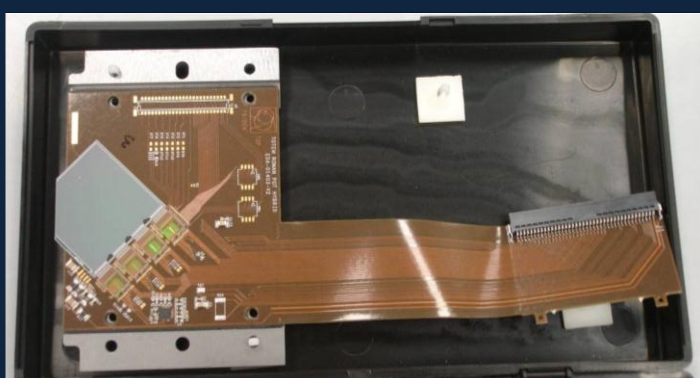

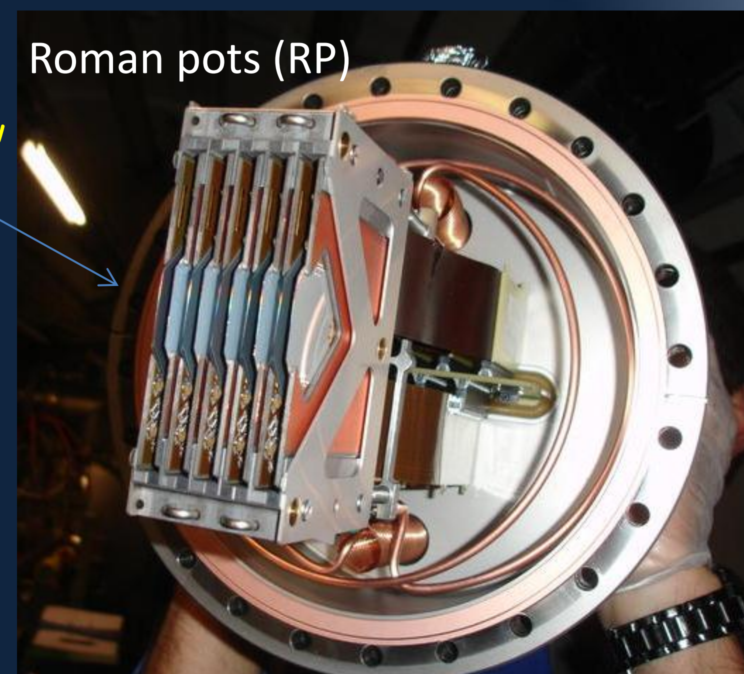

ALICE silicon drift detectors

study of heavy-ion collisions at the LHC

G. Batigne IFAE

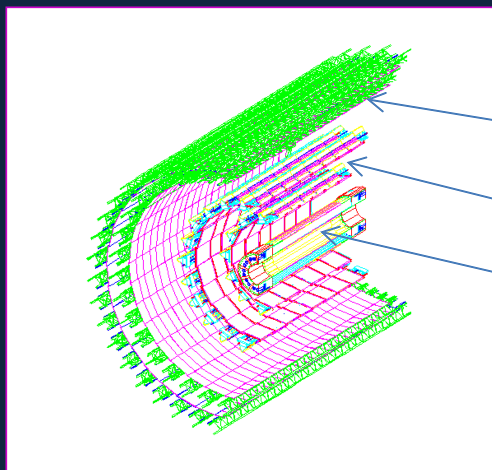

strips

SD

pixels

Position reconstruction : Centroid calculation
Position X : anods n+
Position Y : drift time (calibration of Vdrift)
dE/dx : Integral of the signal

Very low C and therefore very low noise!

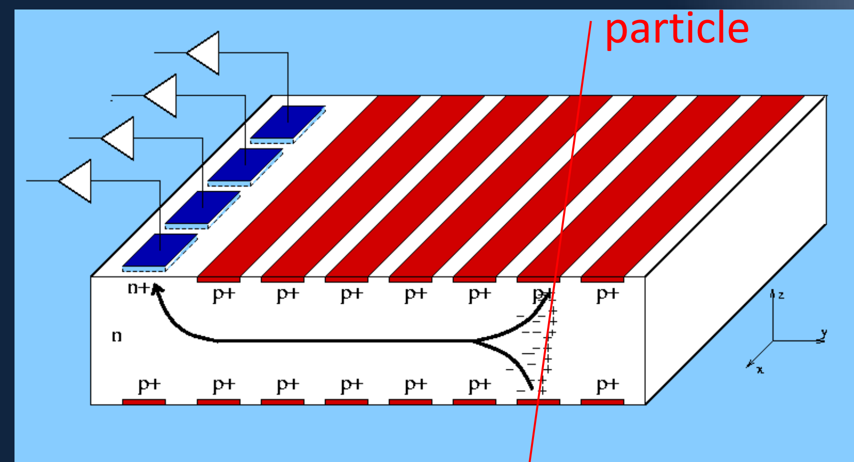

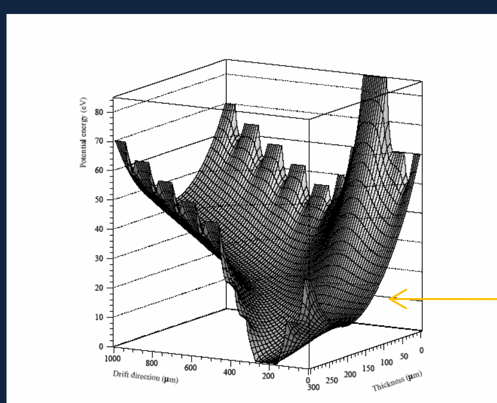

p+ cathods on both side of the wafer :
- Depletion of the Silicon
- HV decreases toward the n+ anods

Drift field (Toboggan effect)

Last cathods below anods :
- kick-up voltage

.. But also .. space applications..

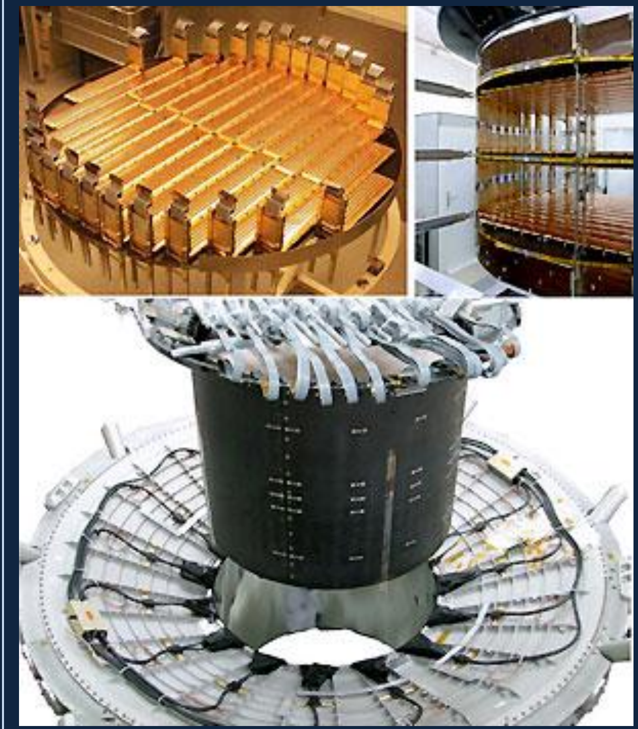

AMS

6 detector planes
<u>each plane</u>: composed by 3 "ladders"

<u>the "ladder"</u>: 2 microstrip silicon sensors + 1 hybrid circuit with front-end electronics (VA1 chip)

<u>silicon sensors</u>: double sided; double metalization; integrated decoupling capacitance

Geometrical Dimensions	70.0 x 53.3 mm^2
Thickness	300 μm
Leakage Current	< 3 μA

PAMELA

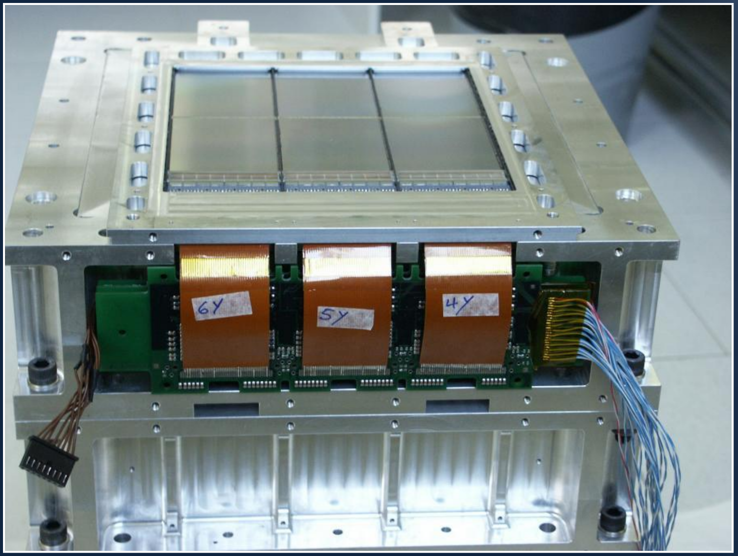

6 planes, $6m^2$ double sided strips
180.000 readout channels
400W power
10um mechanics
X/Xo<3.2%

Few brief words on strips and pixels (mainly) in medical applications

Detailed presentations in this school

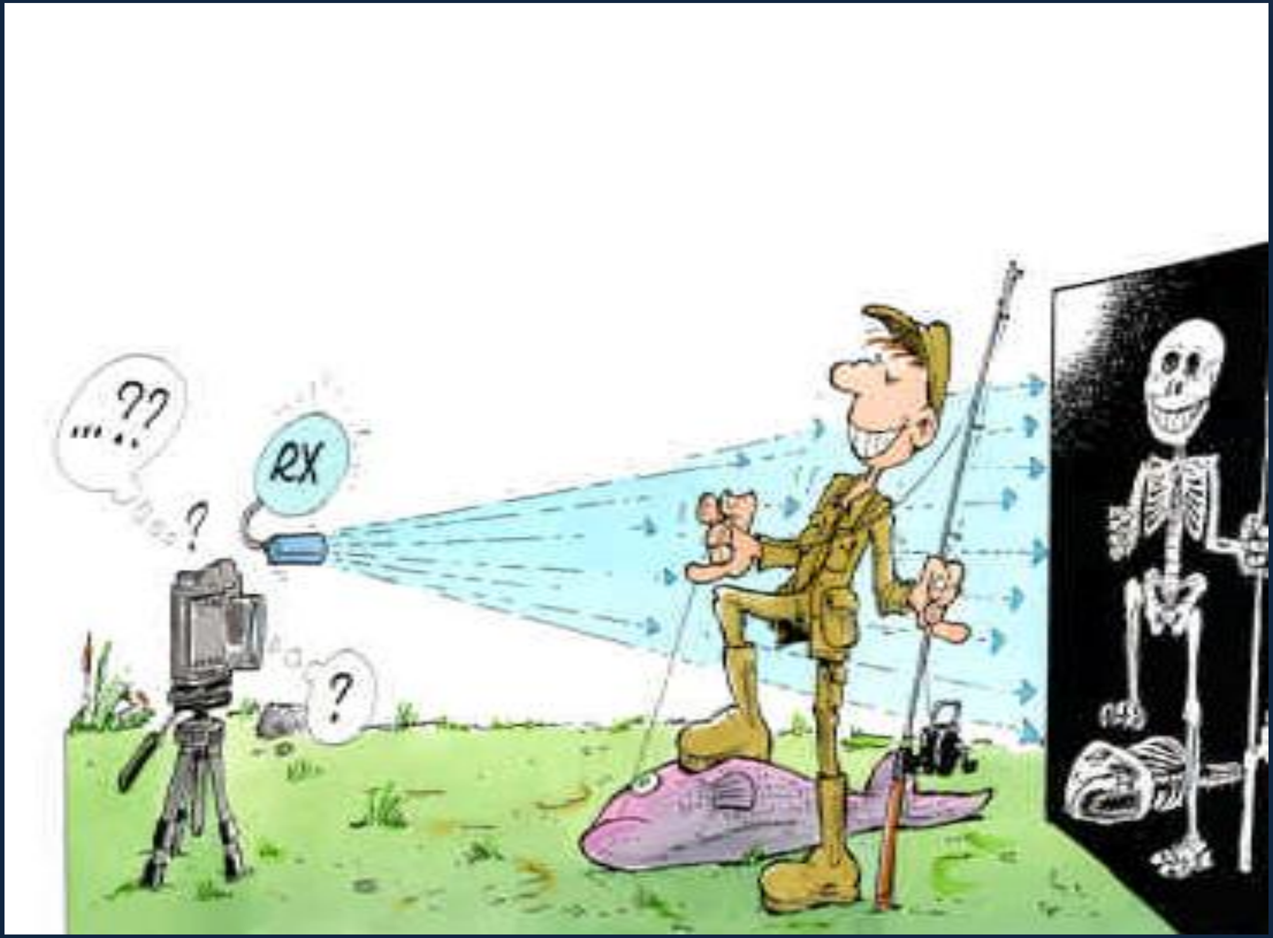

X-ray energy of the most common medical and biological applications

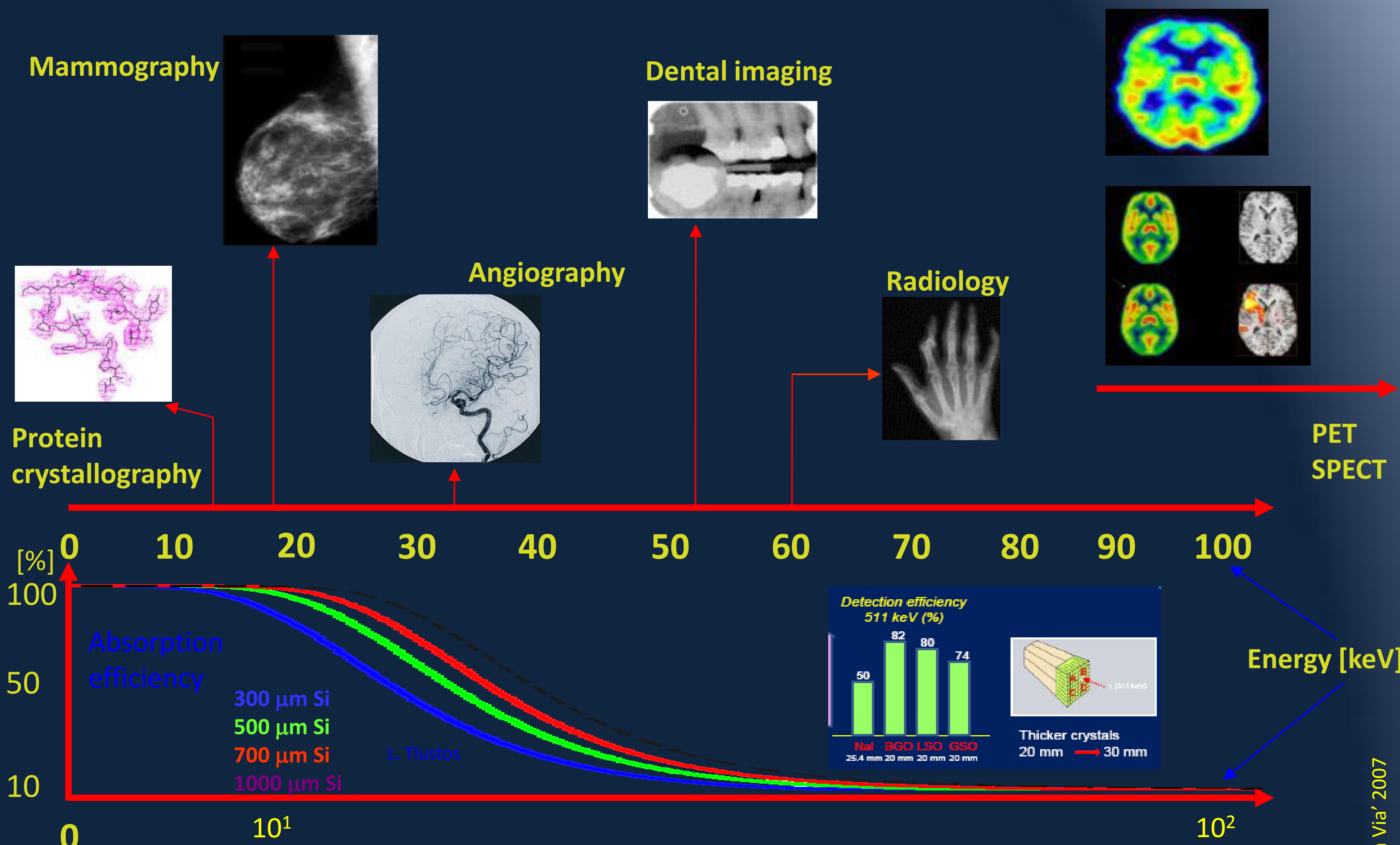

Cinzia Da Via, Uni. Manchester INFIERI 2013 , Oxford July 2013

X-ray detection strategy

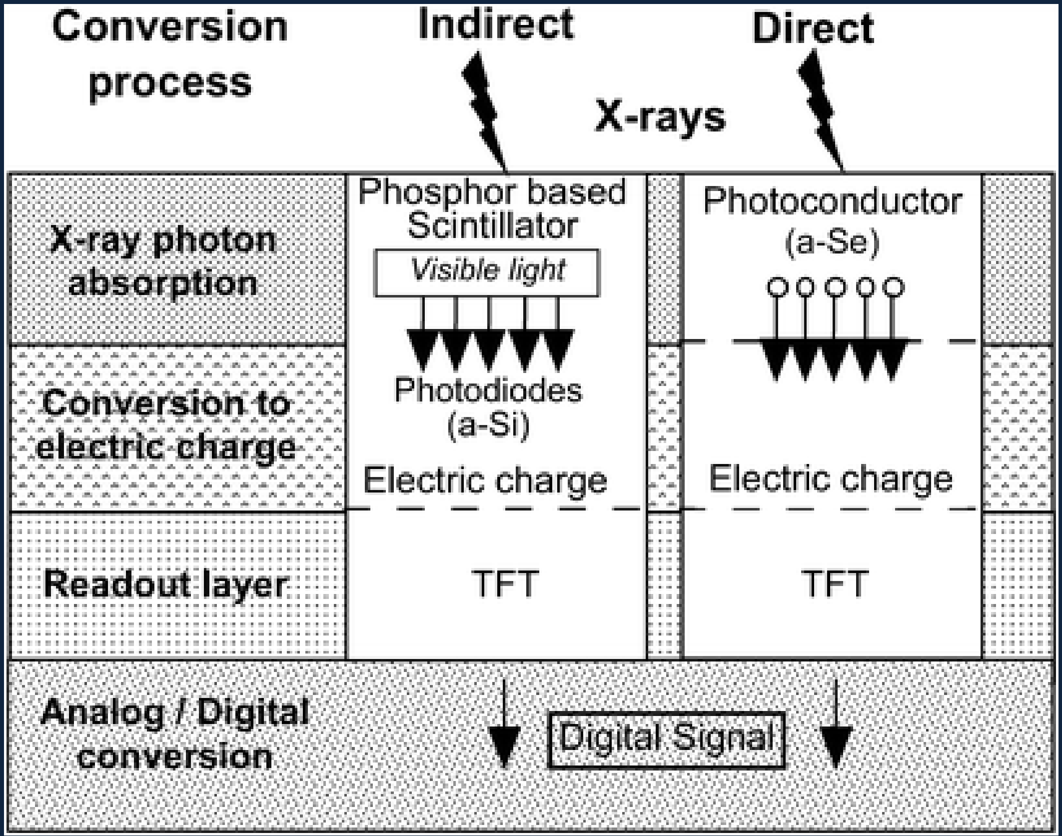

- Photon-counting electronics measure each individual x-ray photon separately
- They use one (one more thresholds and a counter
- are normally more sensitive since they do not suffer from thermal and readout
- they can be set to count only photons in a certain energy range, or even messure the energy of each absorbed photon noise

- integrating electronics measure the total amount of energy deposited in the active region of the detector.
- The charge is integrated in capacitors
- are normally simpler and can handle much higher photon fluxes.

Some of the existing electronics chips

Single photon Counting

Charge Integration

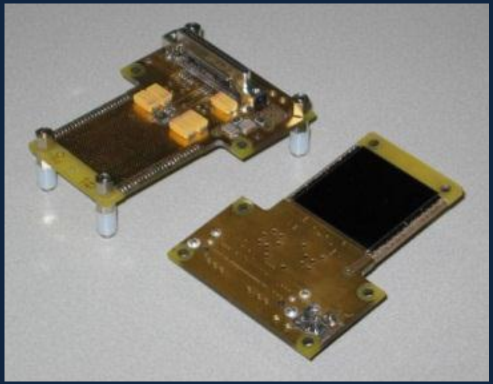

Medipix2 Quad
Pixels: 512 x 512
Pixel size: 55 x 55 μm^2
Area: 3 x 3 cm^2

Medipix

pixellated detector (Si, GaAs, CdTe, 3D thickness: 300/700/1000μm

Gotthard

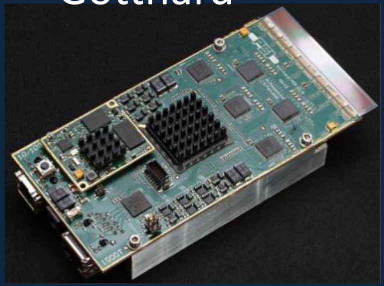

AGIPD

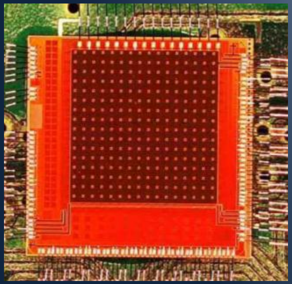

Mithen II

Eiger

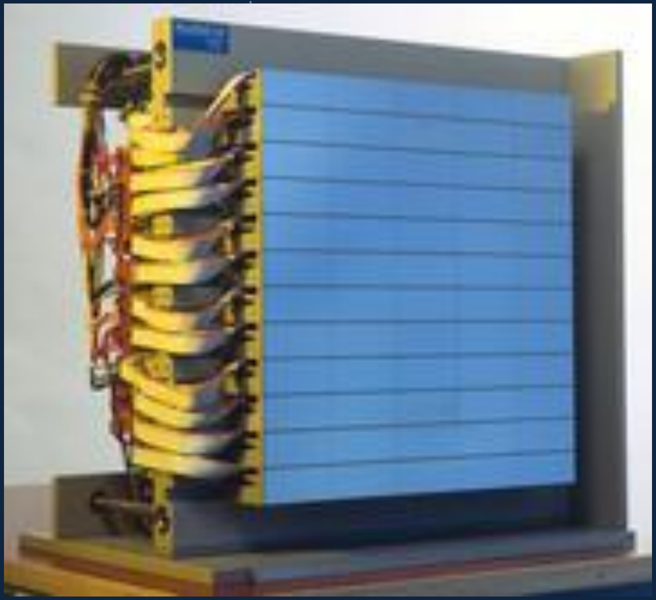

The PILATUS 6M,

424 x 435 mm2 with 170 × 170 μm^2 (2463 x 2527) 6 million pixels, has been developed at PSI and commercialized by the company Dectris for synchrotron imaging

High Z semiconductors: CdTe and CdZnTe

Taka Tanaka (SLAC/KIPAC)

- High detection efficiency
- Poly-crystalline material
- Poor uniformity
- Very high resistivity (semi-insulating)
- Low leakage current

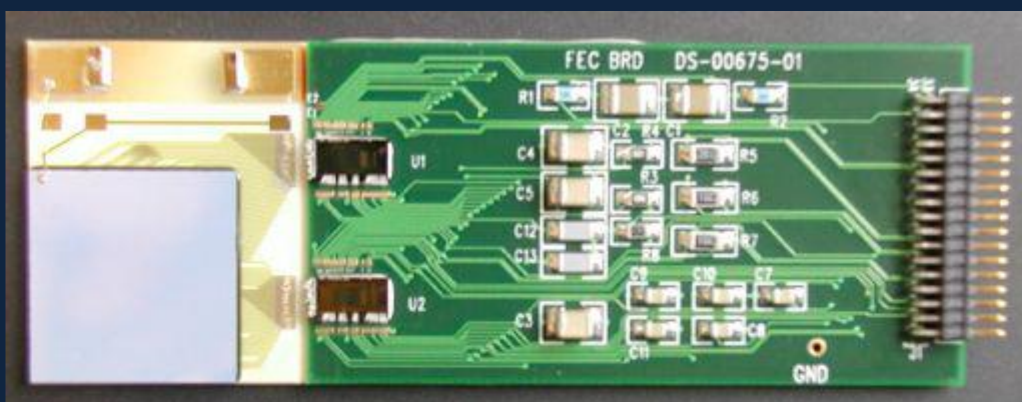

area: 18 " 18 mm2
thickness: 0.5 mm
pixel size: 2 " 2 mm2,
64 ch, cathode side
guard ring: 1 mm width

Fabricated at IDEAS Norway

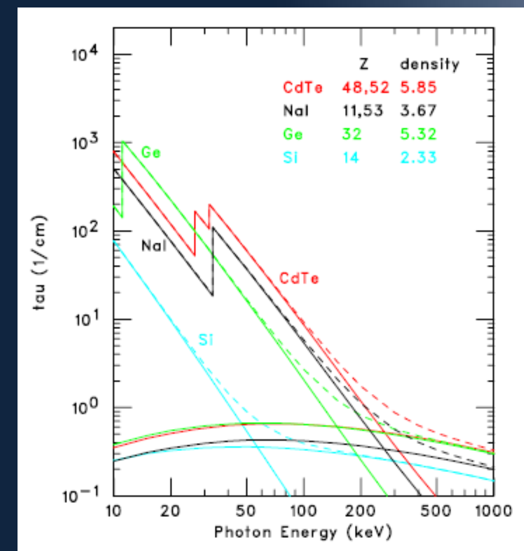

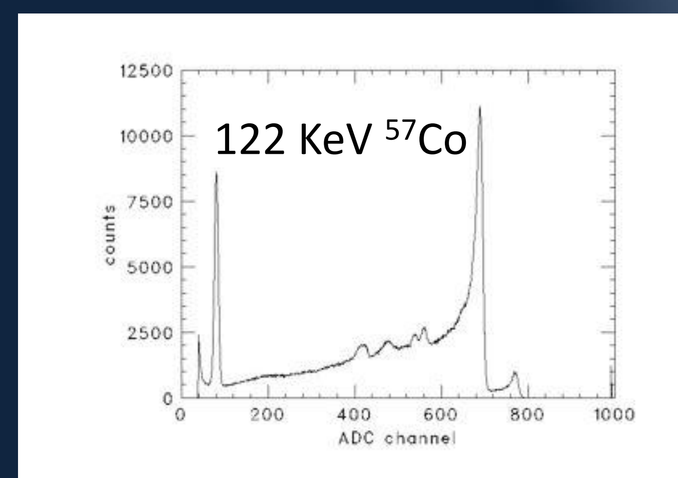

Indirect Conversion: Scintillators and Silicon Photomultipliers (SiPm, GM-APD, MPPC…)

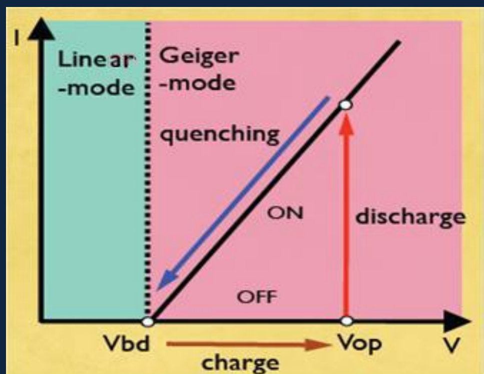

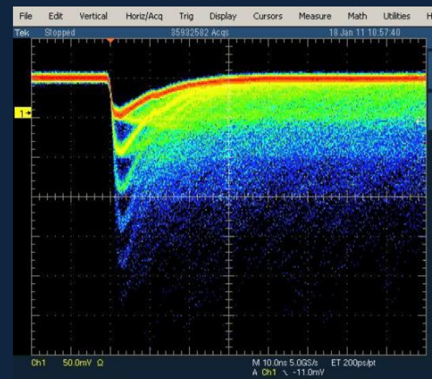

1 pixel
2 pixels
3 pixels

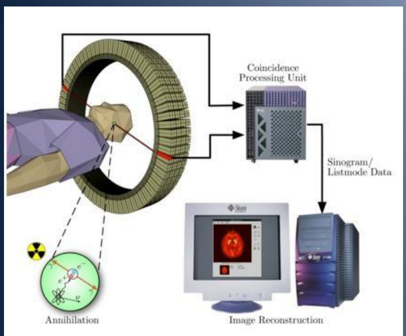

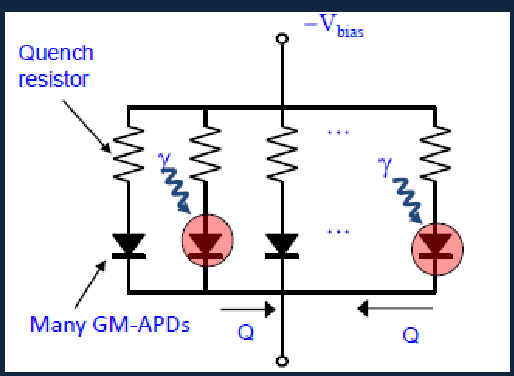

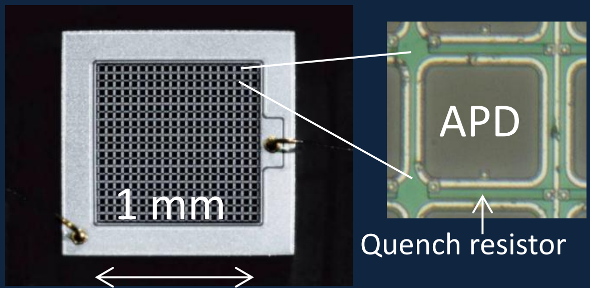

- SiPm requires a special doping profile to allow a high internal field ($>10^5$ V/cm) which generates avalanche multiplication
- APD cell operates in Geiger mode (= full discharge), however with (passive/active) **quenching**.
- The avalanche formation is intrinsically very fast (100ps), because confined to a small space.
- High Gain $G \sim 10^5$ -10^6 at rel. low bias voltage (<100 V)
- G is Sensitive to temperature and voltage variations
- Fill factor still low due to quench resistor on the surface (but work in progress to solve this)

Applications in PET

coincidence of two 511 keV photons define a line of record.

•Take projections under all angles

•(2/3D) Tomographic reconstruct of data

Overview of commonly used scintillators

Scintillators for PET

	1962	1977	1995	1999	2001	2003	2007
	NaI	BGO	GSO:Ce	LSO:Ce	LuAP:Ce	$LaBr_3$:Ce	LuAG:Ce
Density (g/cm^3)	3.67	7.13	6.71	7.40	8.34	5.29	6.73
Atomic number	51	75	59	66	65	47	63
Photofraction	0.17	0.35	0.25	0.32	0.30	0.13	0.30
Decay time (ns)	230	300	30-60	35-45	17	18	60
Light output (hν/MeV)	43000	8200	12500	27000	11400	70000	>25000
Peak emission (nm)	415	480	430	420	365	356	535
Refraction index	1.85	2.15	1.85	1.82	1.97	1.88	1.84

SiPm Commercial Activity

From C. Joram CERN

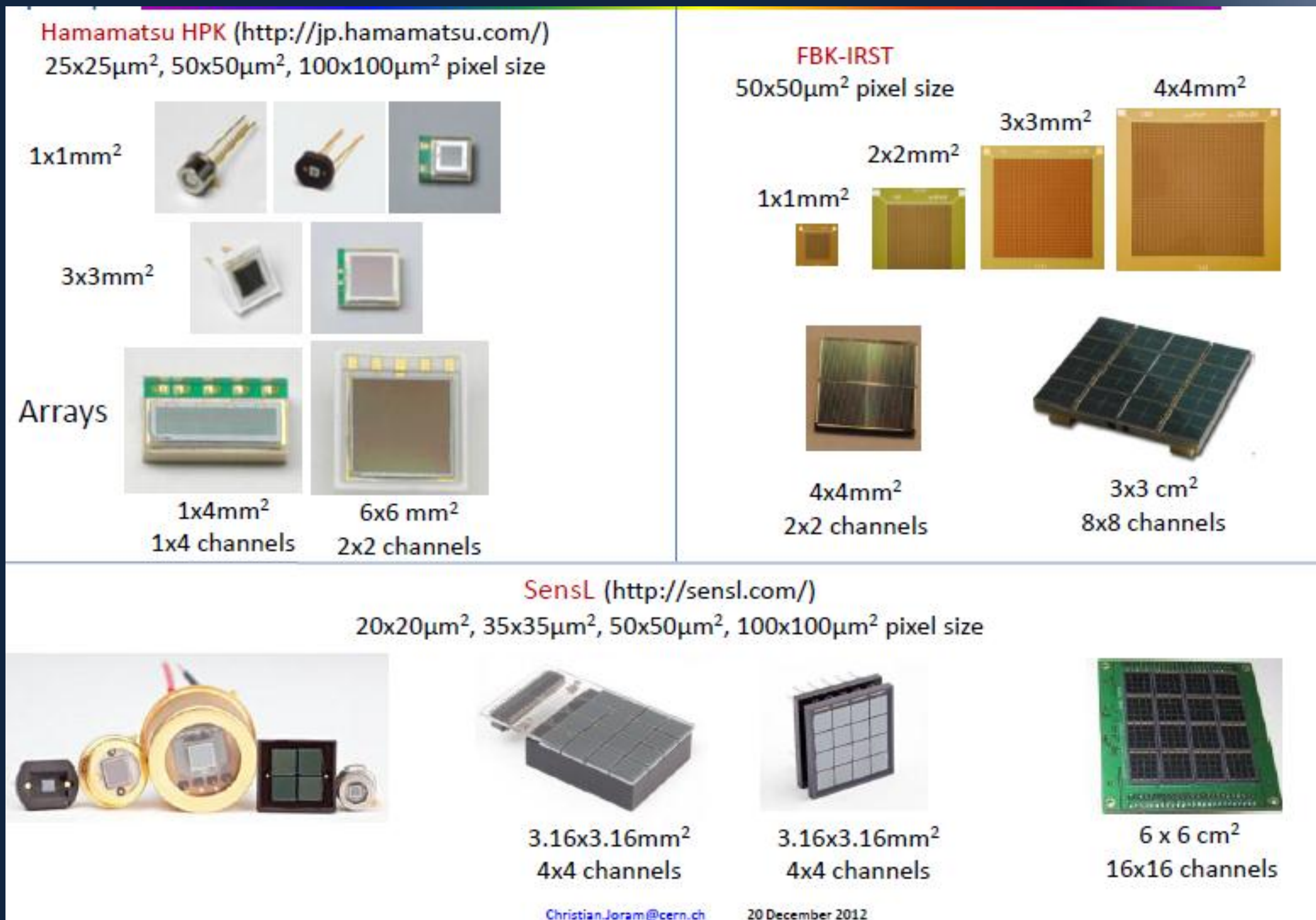

In HEP Technologies for pixels depend on the environment

A. Cattai @ CERN

Radiation hardness ⟷ High granularity

HL-LHC — Higgs Factory

today pitch
50 – 100s μm

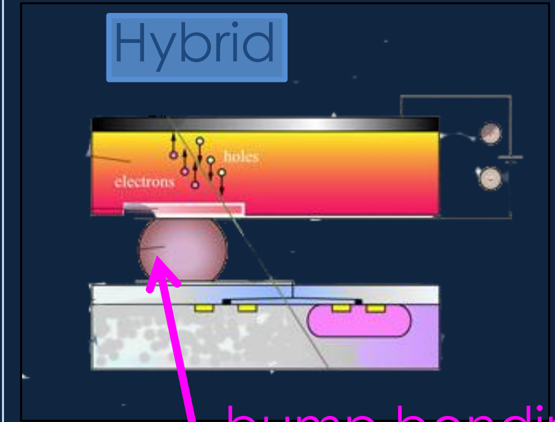

bump bonding

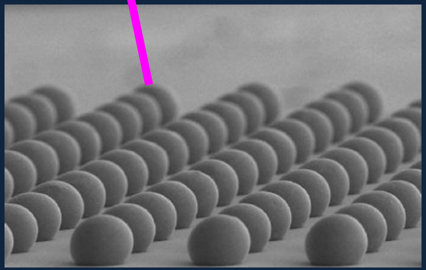

tomorrow 50 – 25 μm

→ R&D on connectivity
- bb facilities
- Through Silicon Vias
- micro bb

→ MONOLITHIC

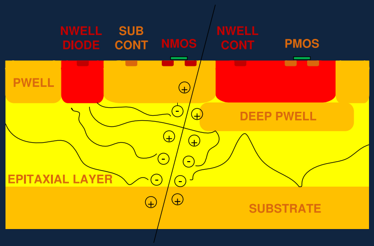

less X_0

day after tomorrow
25 μm and less

→ Invest on R&D on
- Monolithic
- 3D vertical integration

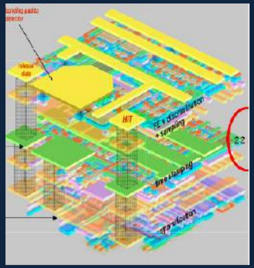

Pixels detectors ongoing development

Radiation Hardness ⟷ Granularity, low mass

3D sensors

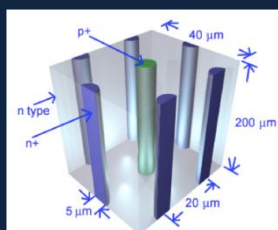

diamond

n-in-n, n-in-p-planar

CCD

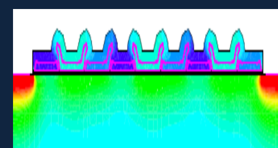

Mimosa

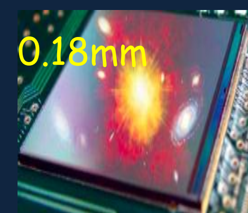

HV-MAPS

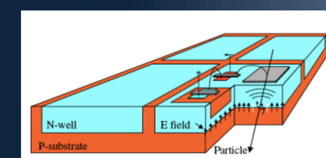

DEPFET

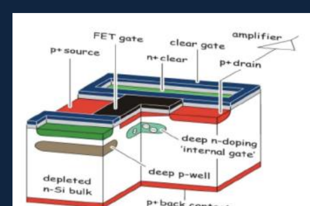

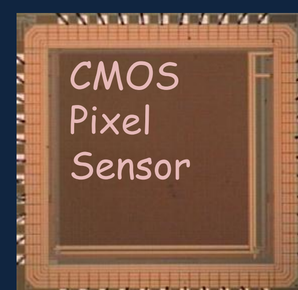

deepNwell

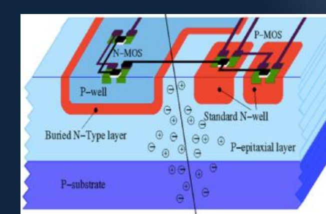

SOI

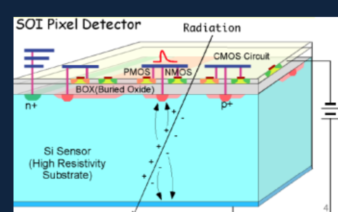

INMAPS

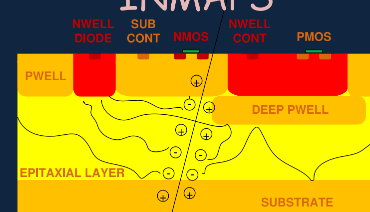

LePiX

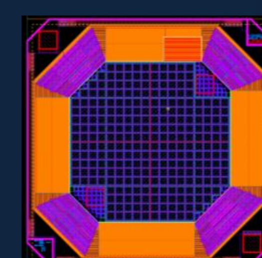

HEP Environment 1-The current LHC

- Pixels and Strips are immersed is a multiple-particle environment
- Radiation decrease radially from the beam
- Several vertices to identify

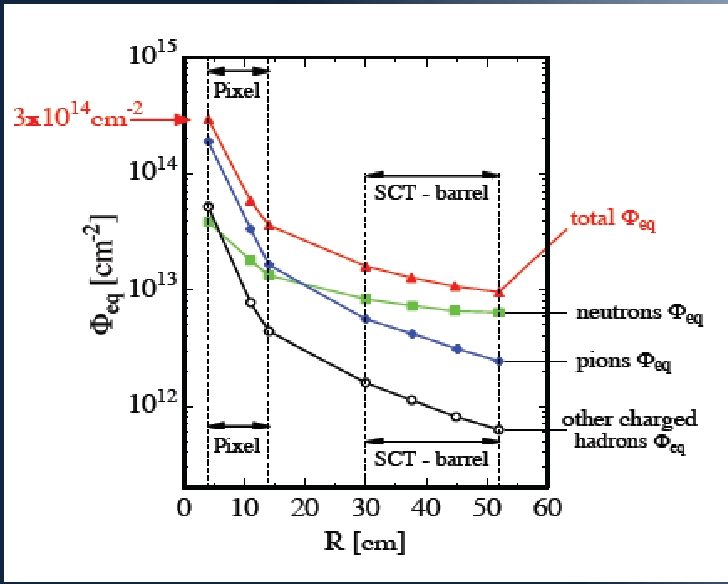

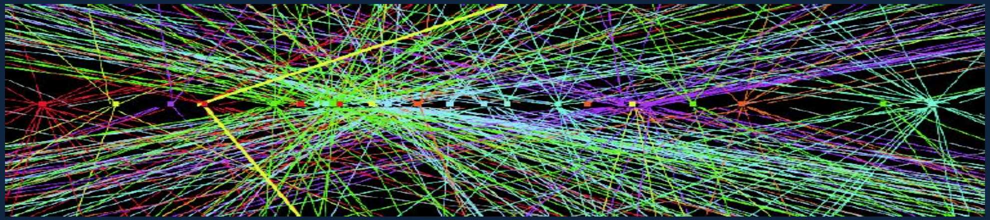

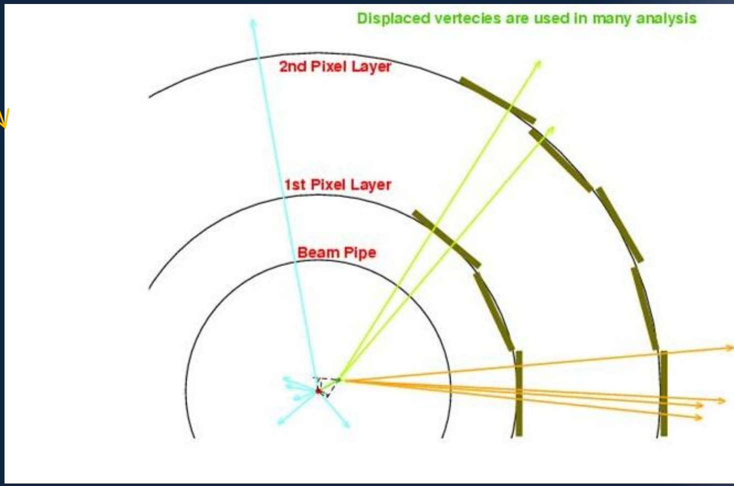

MANCHESTER 1824

Non Ionising Energy Loss

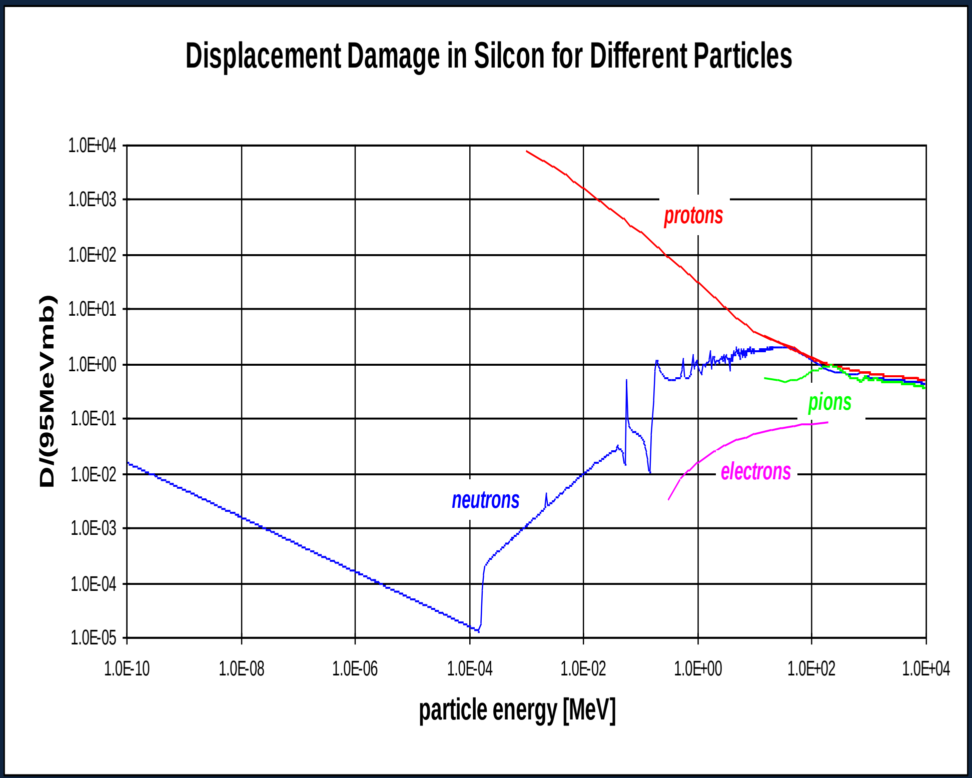

$$D_{\rm eff} = \int D(E)\Phi(E)\,\mathrm{d}E = D_{\rm neutron}\,(1\ \mathrm{MeV})\cdot\Phi_{\rm eq}$$

$$\Phi_{\rm eq} = \kappa\Phi_{\rm tot} = \kappa\int\Phi(E)\,\mathrm{d}E$$

In a multiple particle environment

Used to relate the fluence of a particle with energy E with the equivalent one produced by 1 MeV neutrons

D_{eff} = Damage efficiency
D(E)= damage displacement function
Φ(E)=fluence energy distribution
K= hardness factor

Neutrons in the MeV range an increasing number of nuclear reactions lead to an increase of D(E)

Protons D(E) is dominated by Coulomb interaction at low E and is larger

MANCHESTER 1824

What happens during irradiation to strips and pixels?
Defects formation in irradiated silicon

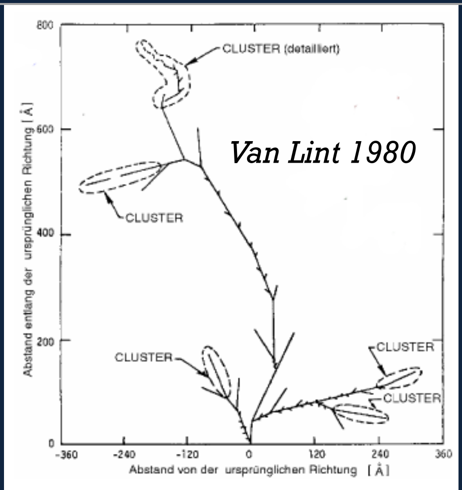

Primary Knock on Atom

Displacement thresholds in Si:
Frenkel pair E~25eV
Defect cluster E~5keV
For X-Rays E~250KeV

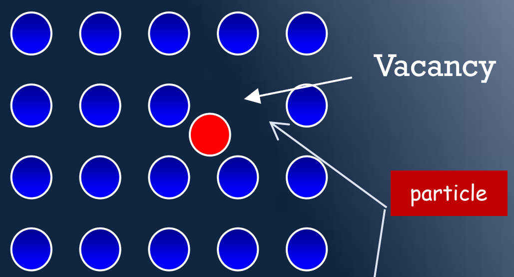

V,I MIGRATE UNTIL THEY MEET IMPURITIES AND DOPANTS TO FORM STABLE DEFECTS

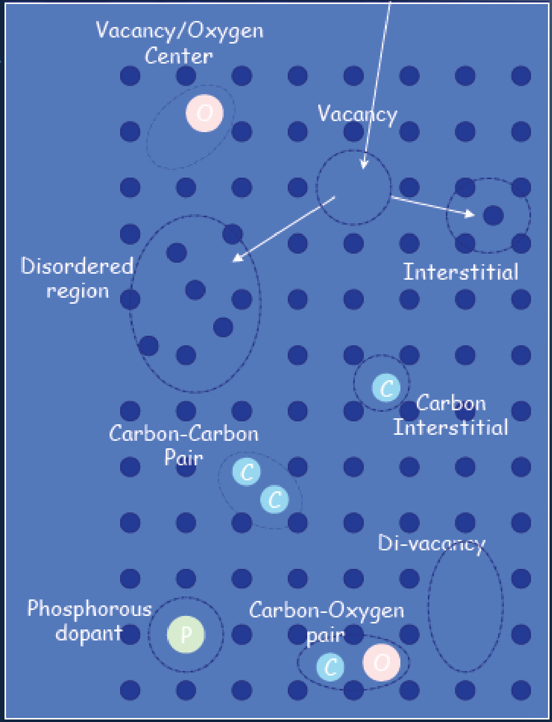

Table 3 Main reactions in defect kinetics modelling

I Reactions	V reactions	C_i Reactions
A) Diffusion reactions I + C_s -> C_i I + V_2 -> V I + VP -> P I + V_3O -> V_2O **I + B_s -> B_i**	 V + O -> VO V + P -> VP V + VO -> V_2O V + V_2O -> V_3O	 C_i + C_s -> CC C_i + O -> CO CO+I -> COI * CC+I -> CCI * **B_i + C_s -> BC** **B_i + O -> BO** **B_i + B_s -> BB** *Not thought to be electrically active
B) Reactions in PKA region I + V -> Si (annihilation) **I + I_N -> I_{N+1} (See text) +**	 V + V -> V_2 **V + V_N -> V_{N+1} (See text) +**	 **+ May occur for diffusing vacancies and interstitials - reactions A) - after heavy neutron irradiation.**

Radiation induced defects in the Si lattice and their annealing temperatures

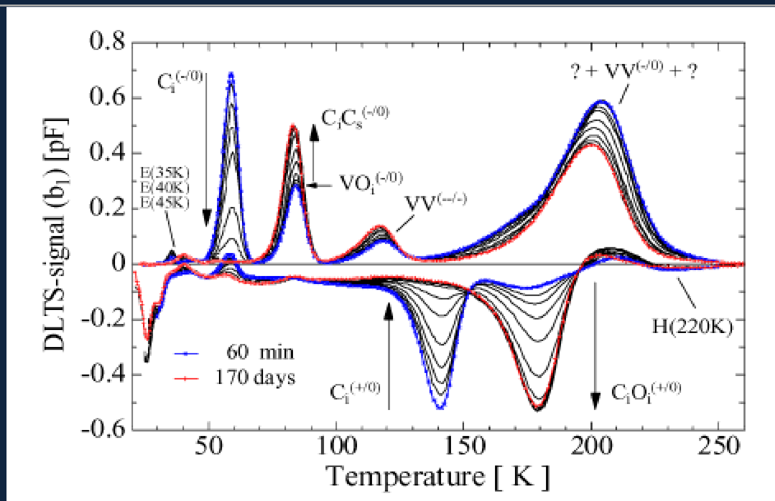

Measured defects with DLTS

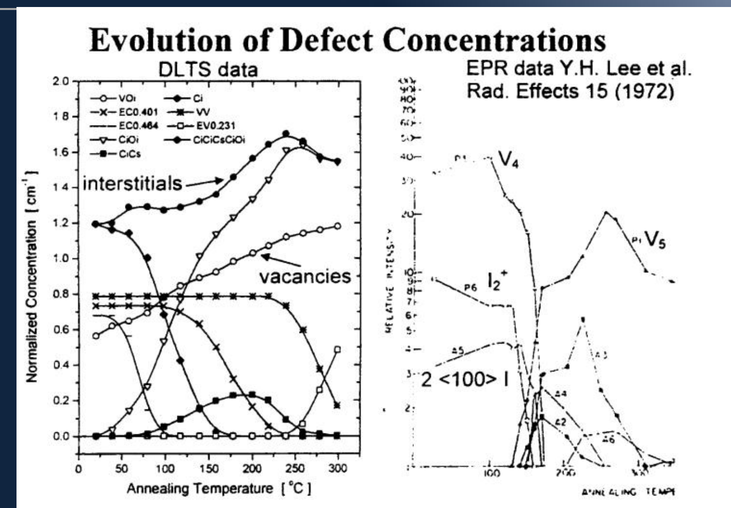

Evolution of defect concentration with temperature: annealing

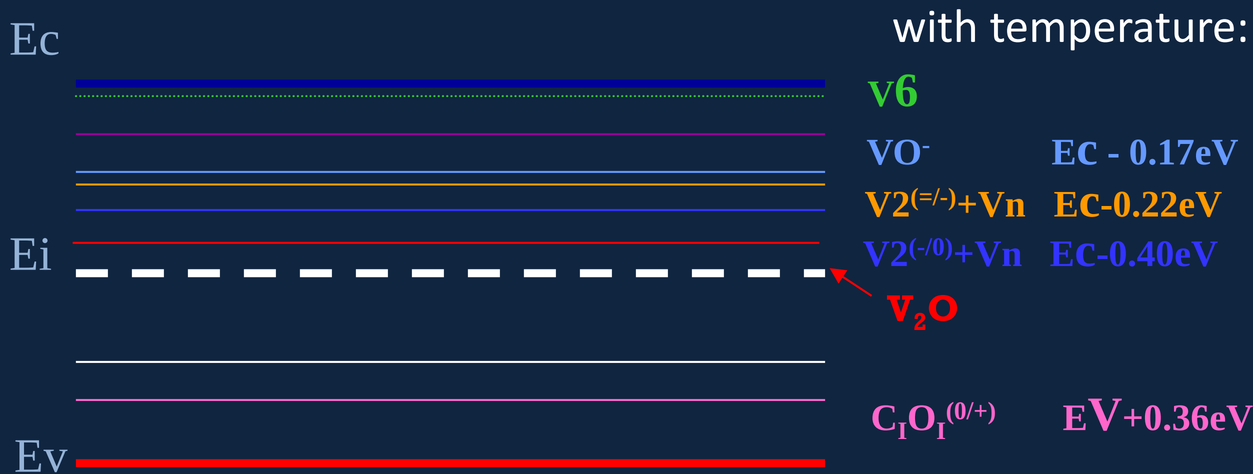

Defects position
In the bandgap

“Macroscopic” effects on the sensors

CHARGED DEFECTS ==> N_{EFF}, V_{BIAS}

DEEP TRAPS, RECOMBINATION CENTERS ==> CHARGE LOSS

DEEP TRAPS, GENERATION CENTERS ==> LEAKAGE CURRENT

SURFACE EFFECTS ==> Leakage current, BD voltage

Space Charge N_{eff} and Bias Voltage V_{bias}

depletion voltage

$$\boxed{V_{dep} = \frac{q_0}{\varepsilon\varepsilon_0} \cdot |N_{eff}| \cdot d^2}$$

effective space charge density

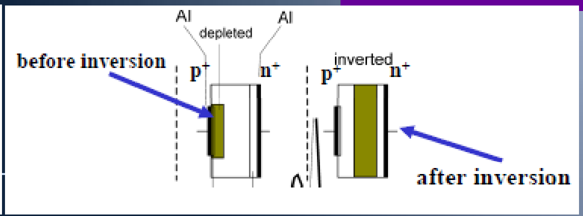

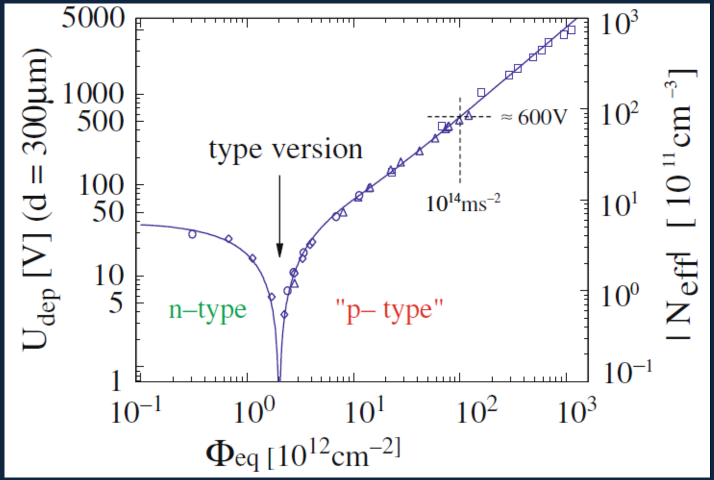

n-type bulk becomes 'effective' p-type (from positive to negative)

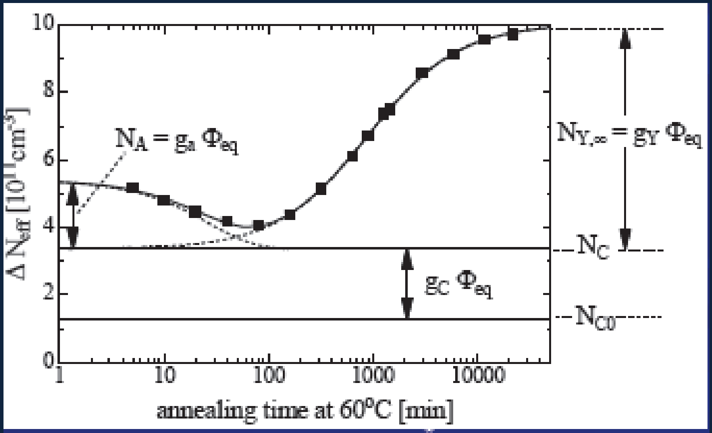

Space charge type-inversion in n-type silicon

Space charge ΔN_{eff} (T,t,Φ) due to 3 main components:

$\Delta N_{eff}(T,t,\Phi) = NA + NC + NY$

- **Short term annealing (NA)**

$NA = \Phi_{eq}\, \Sigma g_{a,i} \exp(-k_{a,I}(T)t)$

- Reduces N_Y (beneficial)
- Time constant is a few days at 20 C

- **Stable component (Nc)**

$Nc = N_{c0}(1-\exp(-c\Phi_{eq}))+g_c\Phi_{eq}$

- Does not anneal
- Partial donor removal (exponential)
- Creation of acceptor sites (linear)

- **Long term reverse annealing (N_Y)**

$N_Y = N_{Y,\infty}[1-1/(1+ N_{Y,\infty}k_Y(T)t)]$, $N_{Y,\infty}= g_Y\Phi_{eq}$

- Strong temperature dependence
- 1 year at T=20 C or ~100 years at T=-7 C (LHC)!!!

Solution: introducing oxygen in the bulk!

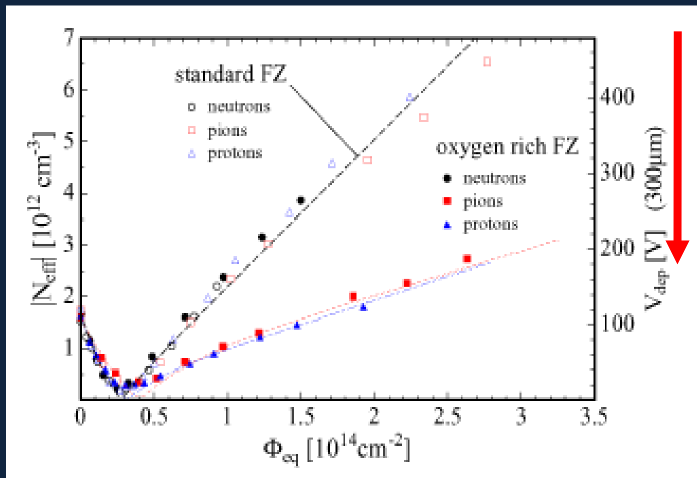

Nucl. Instr. Meth. A 466 (2001) 308

REDUCED
V_{FD}
3 times
With p and
pions but
Not neutrons!

Reduced
Reverse
Annealing
Saturation
(2 times)

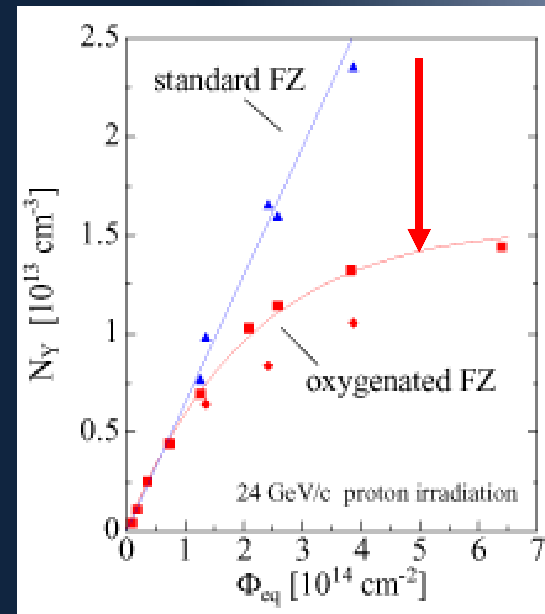

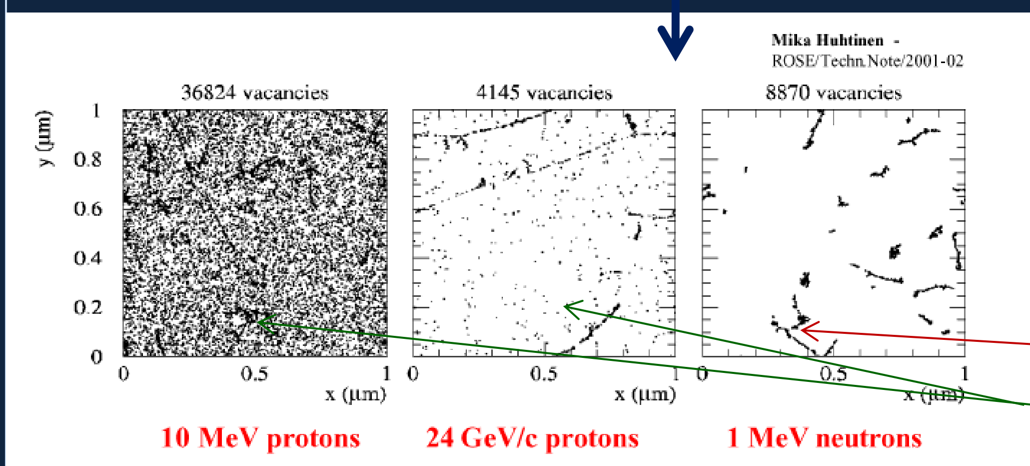

But.. Neutron proton puzzle
Competing mechanism due to Coulomb
Interaction: more point defects when
Irradiated with charged particles

$V2+O=V_2O$ contributes to Neff
$V+O=VO$ does not contribute to Neff

Oxygen rich materials: helps with pions and protons

Float Zone Silicon
Using a single Si crystal seed, melt the vertically oriented rod onto the seed using RF power and "pull" the monocrystalline ingot
Can be oxygenated by diffusion at high T

Czochralski silicon
Pull Si-crystal from a Si-melt contained in a silica crucible while rotating.
Silica crucible is dissolving oxygen into the melt
high concentration of O in CZ
Material used by IC industry (cheap), now available in high purity for use as particle detector (MCz)

Epitaxial silicon
Chemical-Vapor Deposition (CVD) of Silicon
CZ silicon substrate used for oxygen diffusion
Growth rate about 1µm/min
Excellent homogeneity of resistivity
150 µm thick layers produced (thicker is possible)
price depending on thickness of epi-layer but not extending ~ 3 x price of FZ wafer

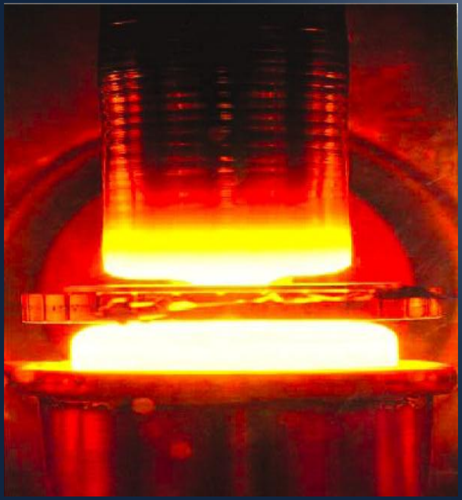

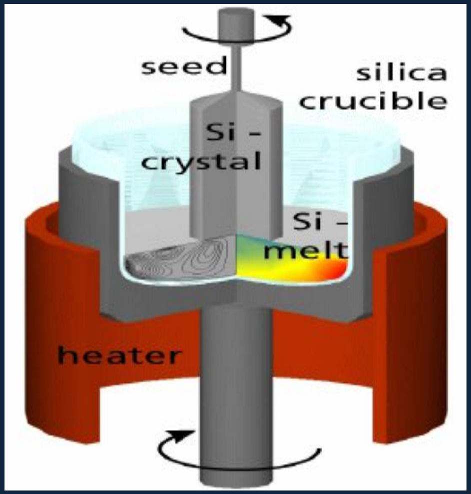

Oxygen Concentration and depth homogeneity

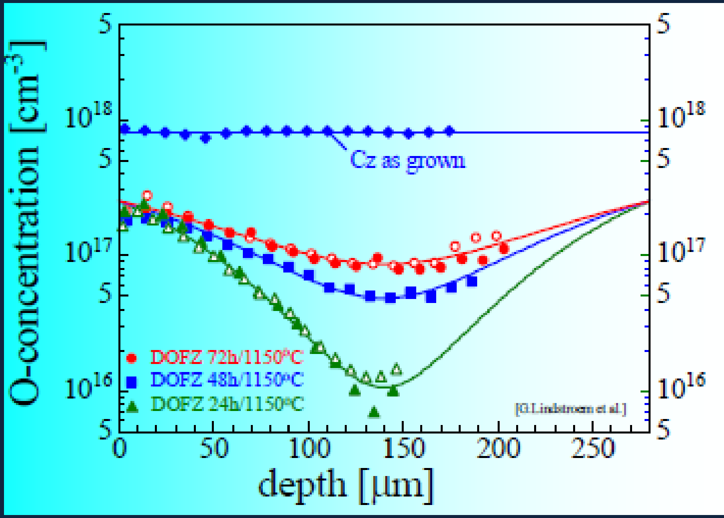

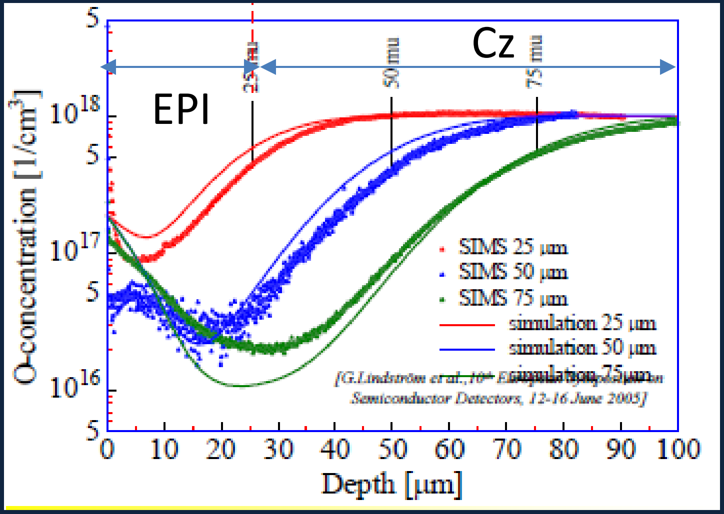

Cz has a has grown homogeneous high oxygen concentration –

Oxygen dimers and thermal donor Formation

DOFZ requires high T Oxygen diffusion to reach working homogeneity and high concentration

EPI oxygen diffusion from Cz Substrate. Dis-homogeneous

Magnetic Czochralski silicon

V. Cindro et al., 8th RD50 workshop
N. Manna for SMART, 8th RD50 workshop
G.Kramberger, RESMDD06, October 2006

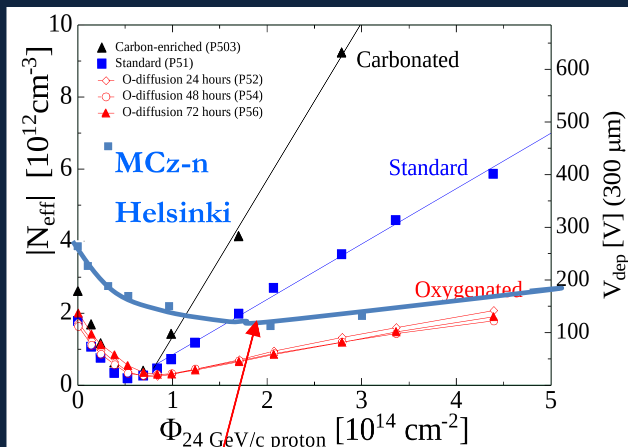

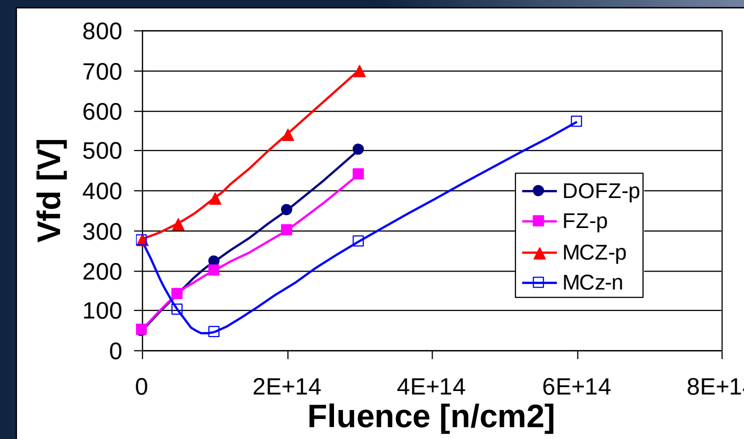

Control of the impurities concentration
So oxygen is high and carbon is low

High Oxygen content ~4.9 x $10^{17}cm^{-3}$
Low Carbon content ~$10^{15}cm^{-3}$

Low bias voltage so Lower power dissipation

Inhomogeneity of response in
Different regions of the wafer
observed

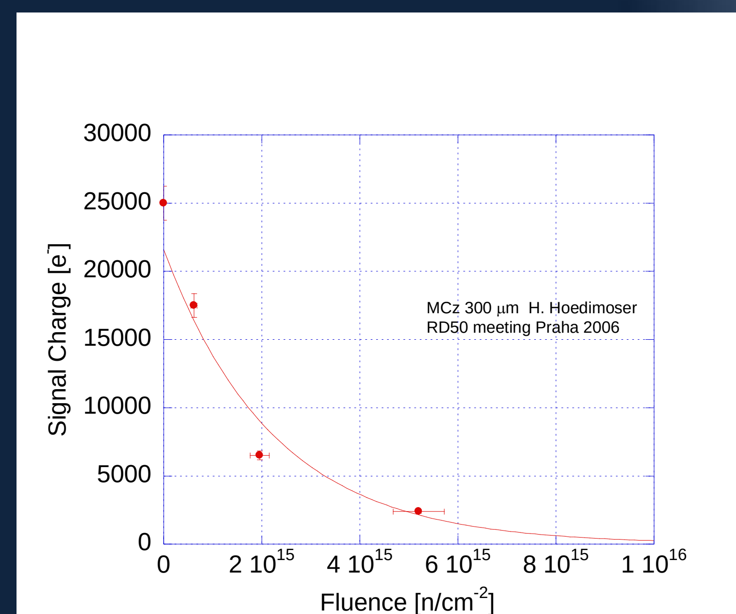

Oxygen rich materials: EPI silicon

G.Lindström et al.,10th European Symposium on Semiconductor Detectors, 12-16 June 2005
G.Kramberger et al., Hamburg RD50 Workshop, August 2006

- Epitaxial silicon
  - Layer thickness: 25, 50, 75 μm **(resistivity: ~ 50 Ωcm)**; 150 μm **(resistivity: ~ 400 Ωcm)**
  - Oxygen: [O] ≈ 9×10^{16}cm^{-3}; Oxygen dimers **(detected via IO_2-defect formation)**

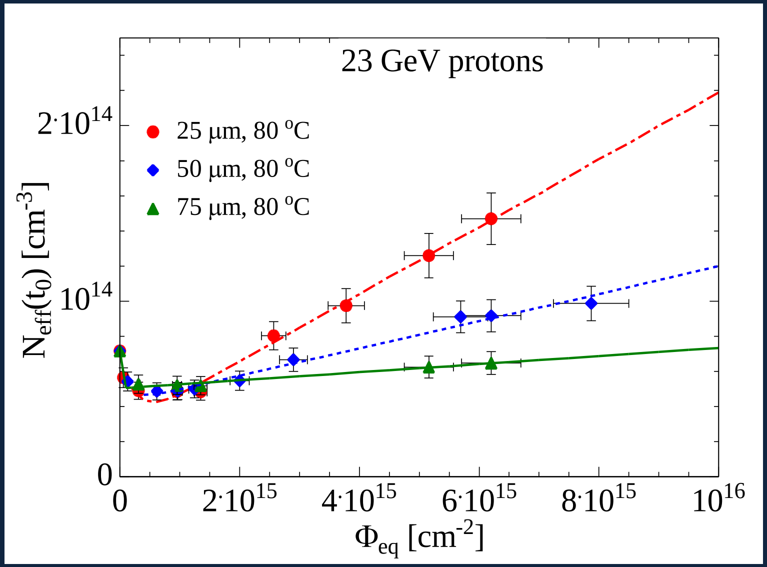

≈105V (25μm)

≈230V (50μm)

≈320V (75μm)

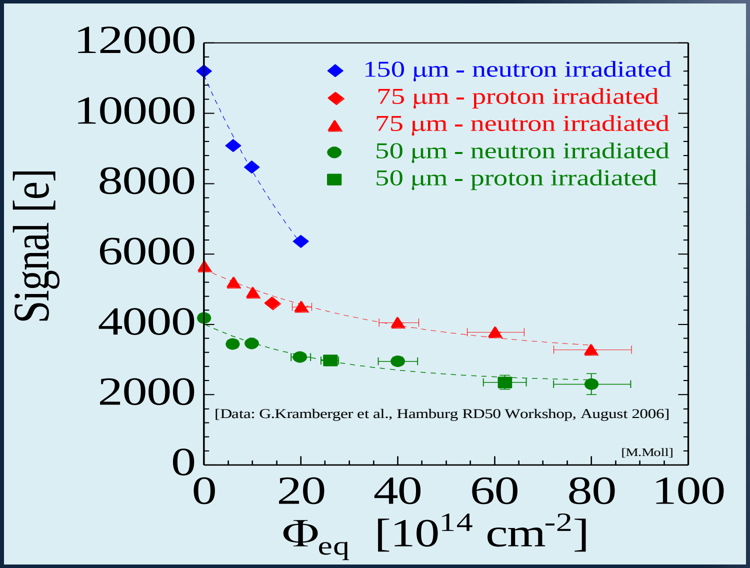

- Only little change in depletion voltage
- No type inversion up to ~ 10^{16} p/cm^2 and ~ 10^{16} n/cm^2
  ⇨high electric field will stay at front electrode!
  ⇨reverse annealing will decreases depletion voltage!
- Explanation: introduction of shallow donors is bigger than generation of deep acceptors

- CCE (Sr^{90} source, 25ns shaping):
  ⇨ 6400 e (150 μm; 2×10^{15} n/cm^{-2})
  ⇨ 3300 e (75μm; 8×10^{15} n/cm^{-2})
  ⇨ 2300 e (50μm; 8×10^{15} n/cm^{-2})

From M. Moll, January 07

Radiation induced leakage current (bulk)

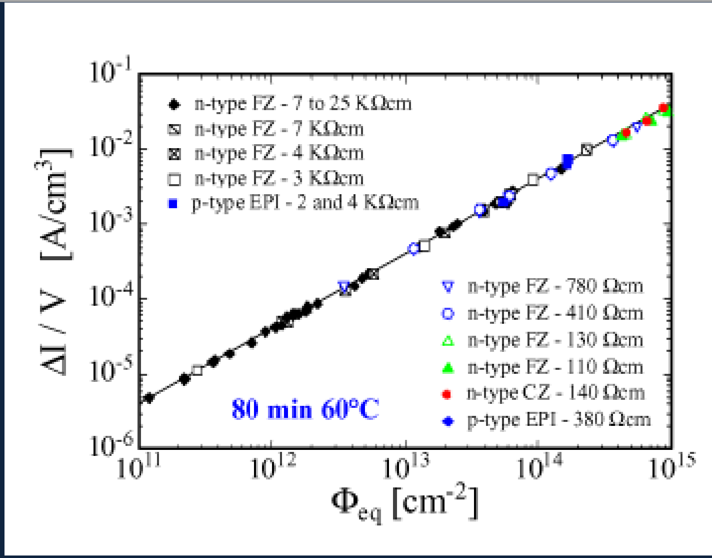

$\Delta I/V = \alpha\phi$ is linear!

❖ When measured at full depletion and 20°C after annealing for 80min at 60° C

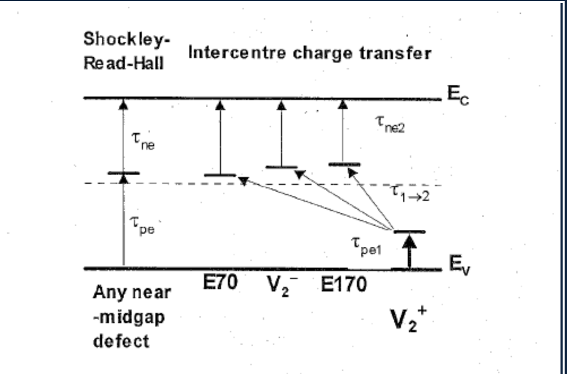

Figure 1. Schematic diagram of SRH and intercentre charge transfer generation processes. With intercentre charge transfer, the energy difference between the valence and conduction band is mediated by two steps instead of the single step in SRH generation.

Enhanced by "inter-center" charge transfer or charge 'hopping' to 'physically' close defects towards conduction band.

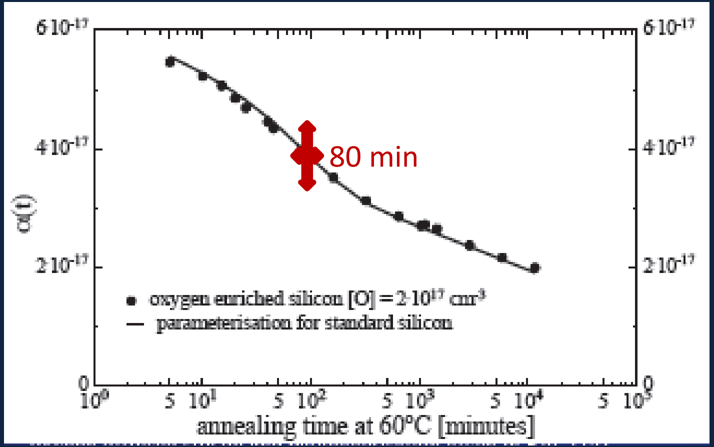

❖ Annealing at 60° C reduces $\Delta I/V$ with time

G. Lindstroem et the ROSE Coll. NIMA 466 (2001) 308–326

S. Watts et al, IEEE TNS vol.43, No6, December 1996

All pixel detectors in LHC experiments use oxygenated "bulk"

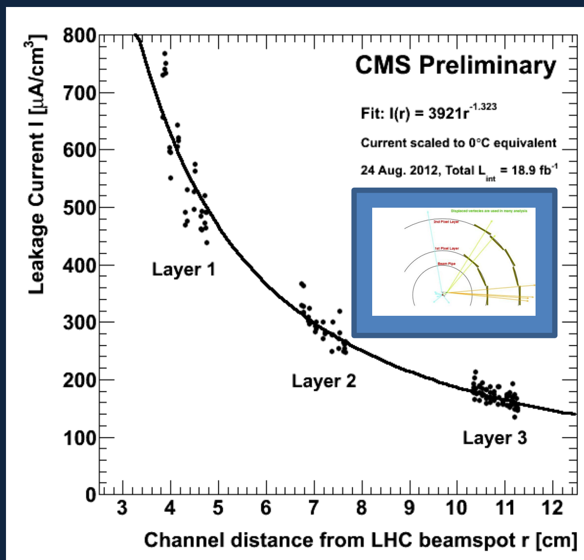

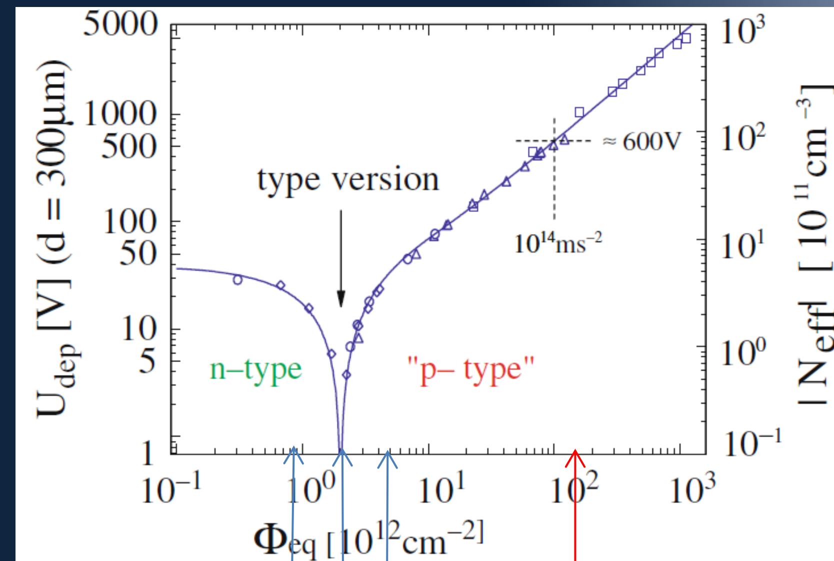

8.2mm VELO

At the time of these measurements ,the LHC delivered 20 fb^{-1} to ATLAS and CMS corresponding to a fluence of over ~5×10^{13} 1 MeV n_{eq} cm^{-2} at the innermost Pixel l layers.

This is now more than double the threshold required for type inversion.

The LHCb VELO is subject to an even higher fluence of ~6×10^{13} 1 MeV n_eq cm^{-2} *per* fb^{-1} at the inner tips of sensors only 8.2 mm from the beam.

Measured parameters during experimental runs (2012 data)

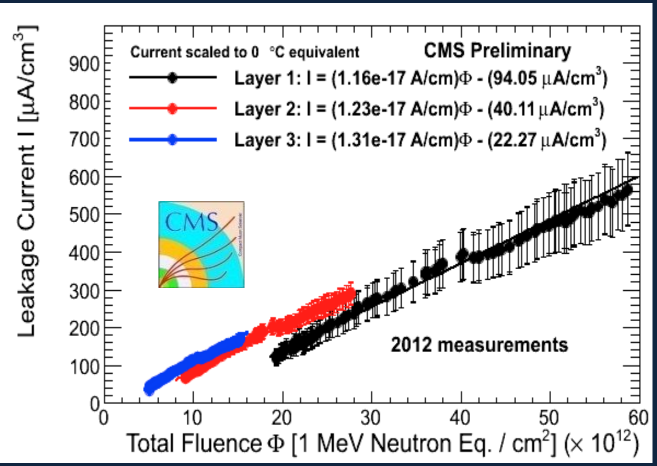

Radiation induced Leakage currents

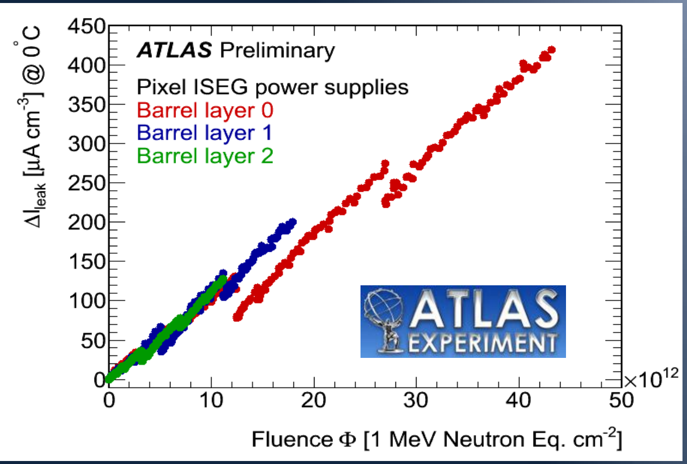

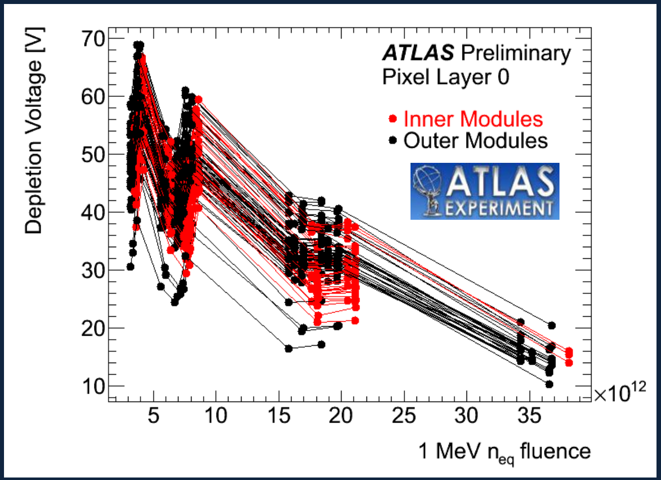

Bias Voltage
And variation
Of the effective
Doping concentration

$$V_{FD} = \frac{(W)^2 \times e \times |N_{eff}|}{2\varepsilon_0 \varepsilon_{Si}}$$

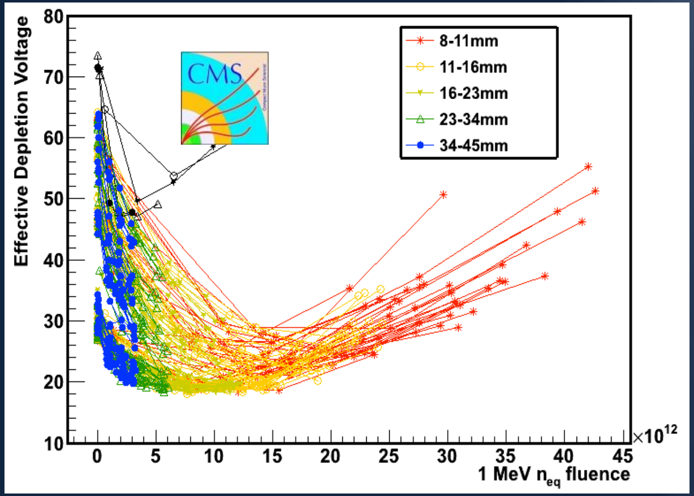

α ~ 1.1 e-^{17} A/cm

Stephen Gibson, Vertex 2012

n-on-n versus p-on-n after type inversion

- spatial precision loss due to un-depletion

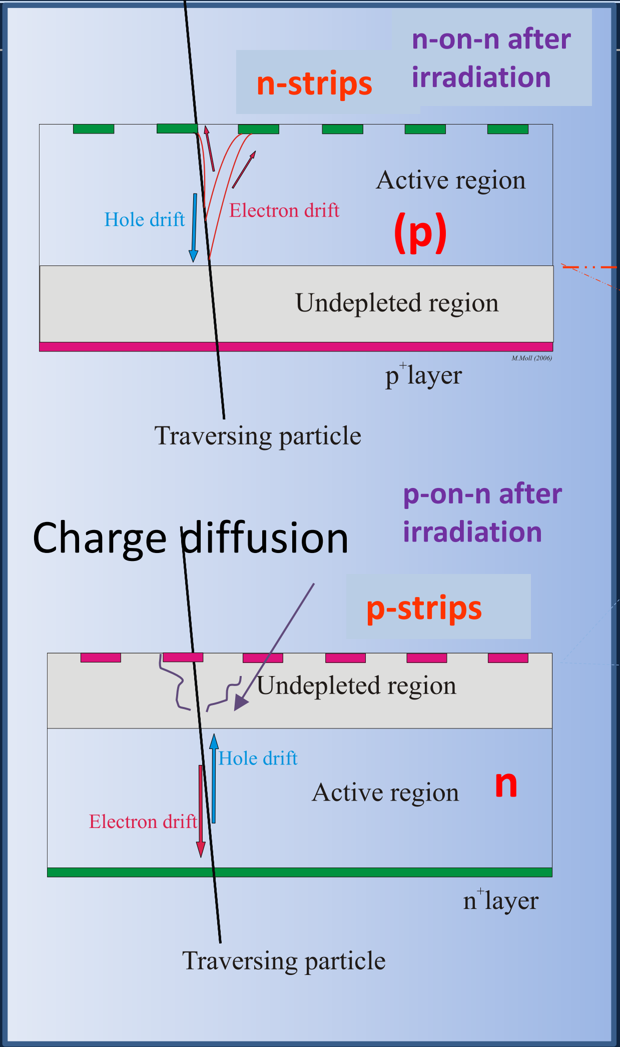

NIM A 440 (2000) 17

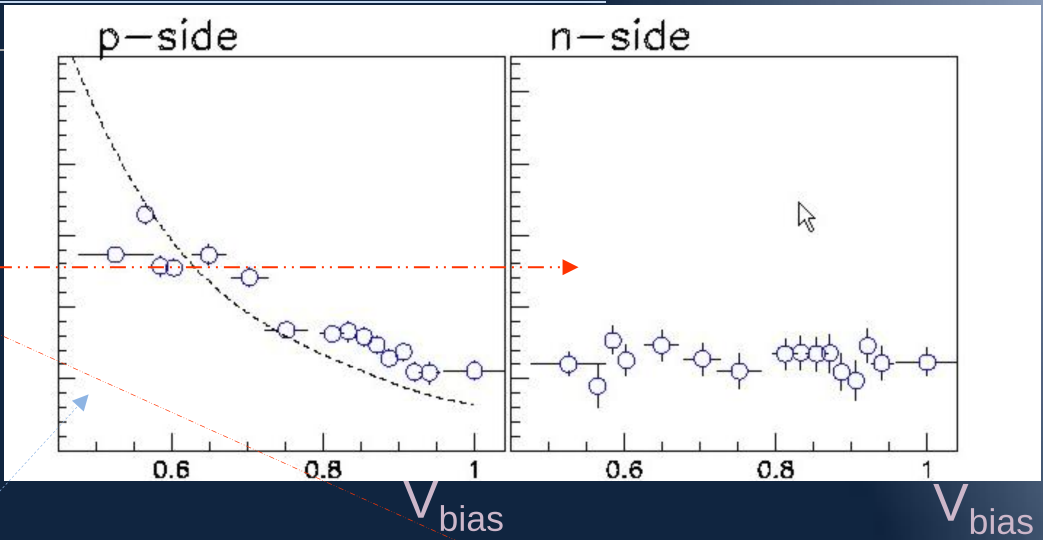

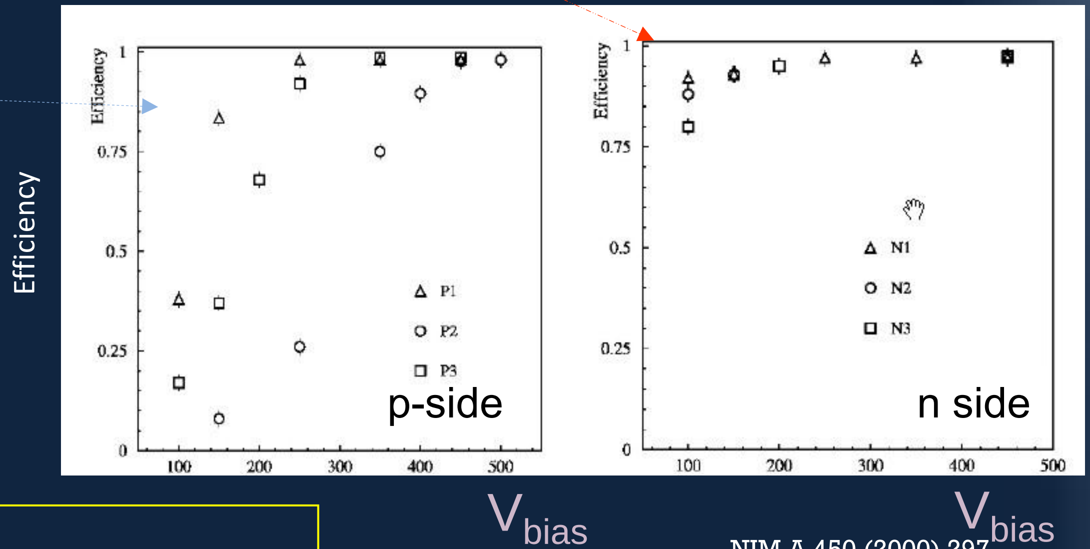

NIM A 450 (2000) 297

n-on-p solves the problem and is easier to process!!
However high bias in front of front-end in case of pixel readout

n-on-p silicon sensors

Miniature microstrip p-type detectors irradiated with 24GeV/c protons (black) and reactor neutrons (red)

- Collects electrons

- Does not type invert
→depletion always from the same electrode

- Good annealing stability

- However for pixels better n-on-n (guard rings on back side) since n-on-p have high field close to electronics input

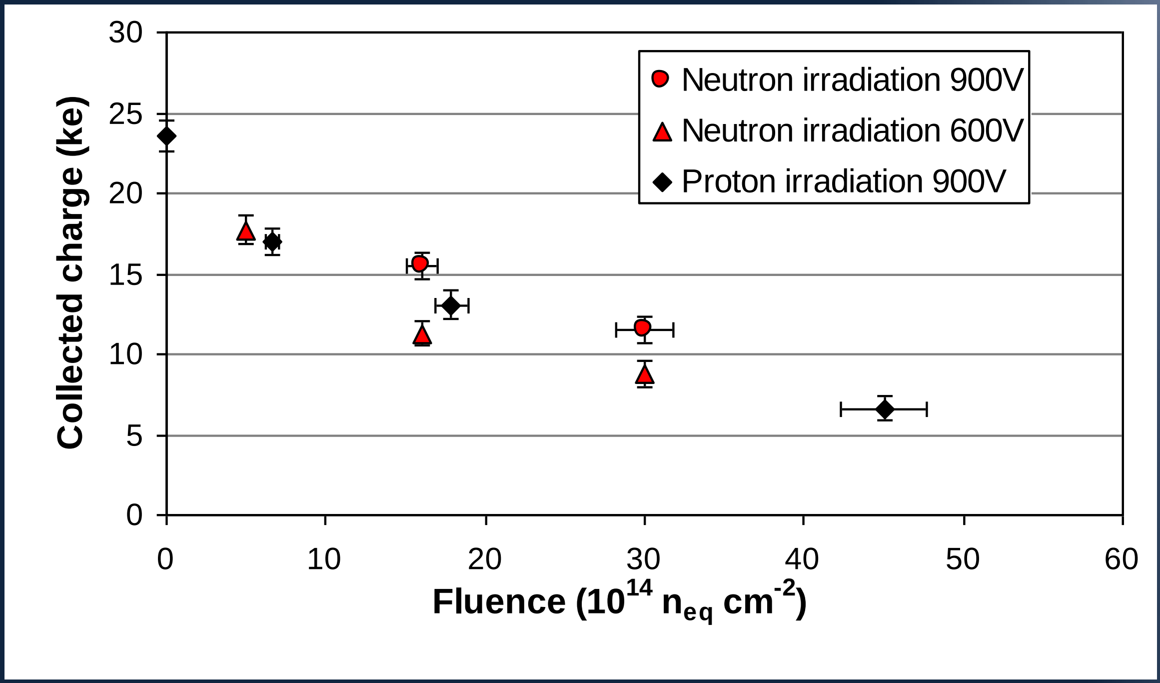

Micron and CNM sensors Measurements: Liverpool

LHC upgrades timeline

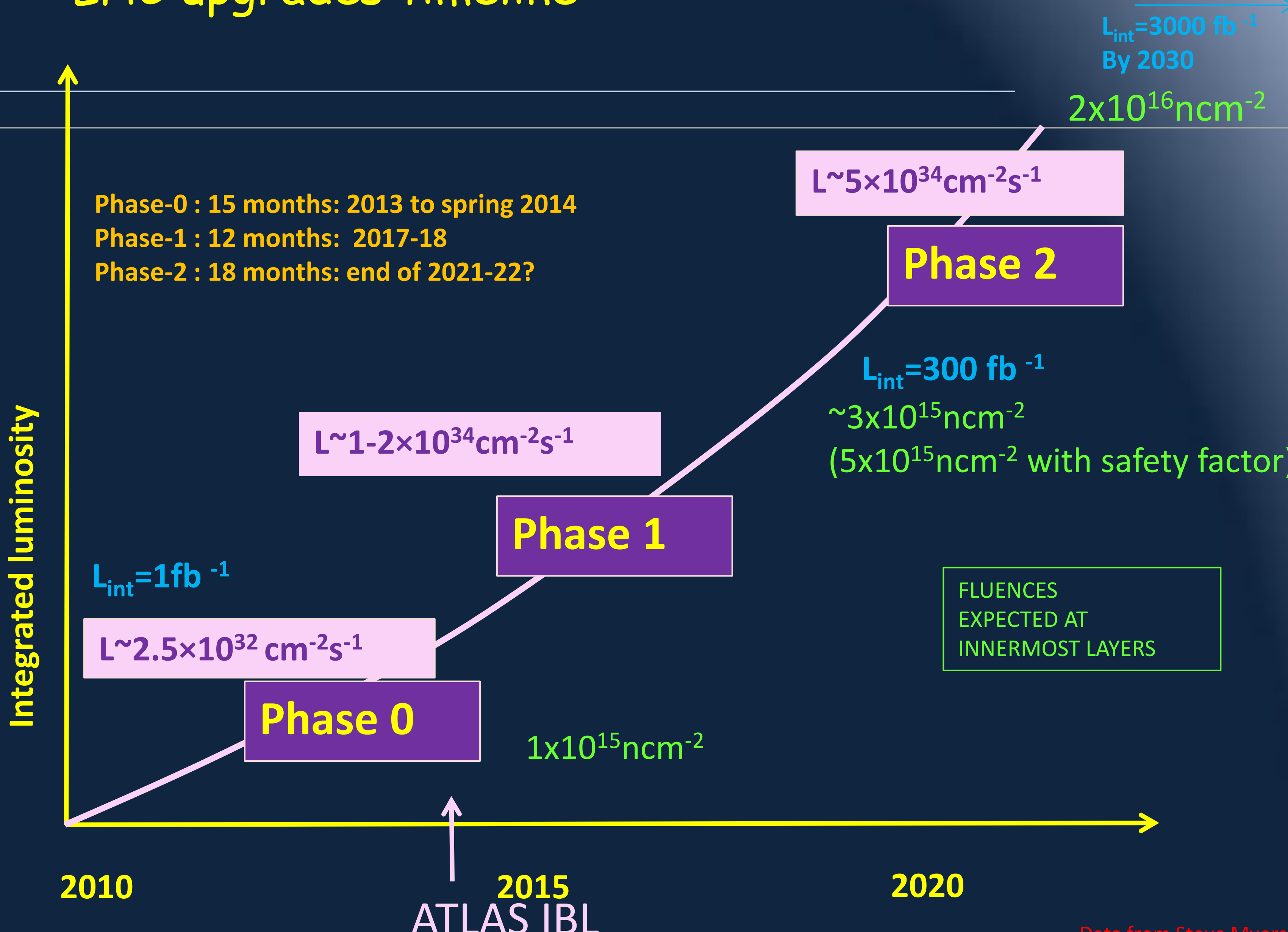

Data from Steve Myers CERN sLHC 23rd June 2010.

HEP Environment 2: the HL LHC (PH2)

Precise vertex determination →

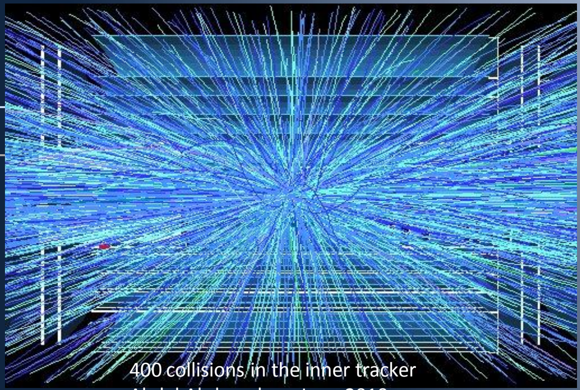

Important role in pattern recognition/ track reconstruction

200 pileup events/bc at $5x10^{34}cm^{-2}s^{-1}$!!!!!

Key Issues:

- Material budget –less multiple scattering, better primary vertex resolution
  - Thin/small beam-pipe
  - Ultra-light detectors
  - Many channels to reduce occupancy
  - High data rates –

IBL $1.5\%X_0$

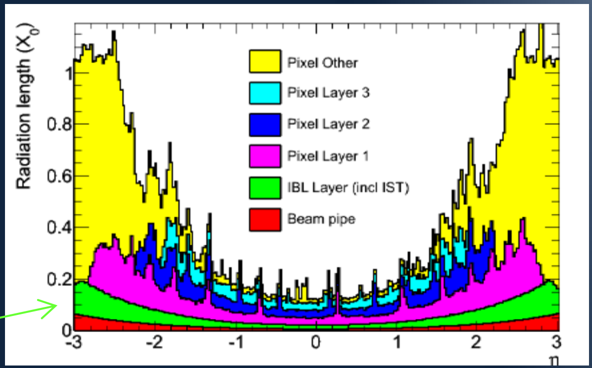

- **High-precision detectors very close to IP**
- **Ultra radiation hard detectors**

Radiation hardness up to

$2X10^{16}$ 1MeV neutron/cm^2 at innermost layers at 3000 fb^{-1} $5X10^{15}ncm^{-2}$ at 300 fb^{-1}

⇒ Signal/threshold

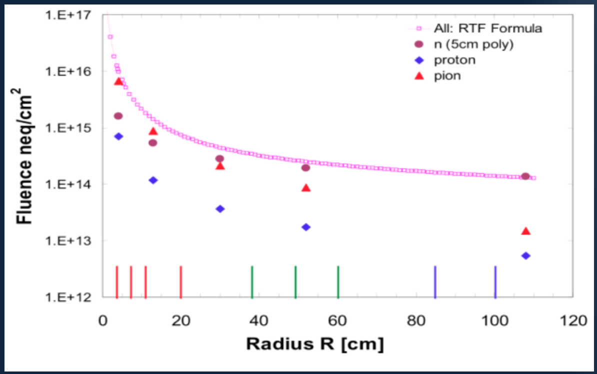

StripsATLAS Radiation Taskforce [ATL-GEN-2005-01]

A high fluences charge trapping is the dominant effect on the signal

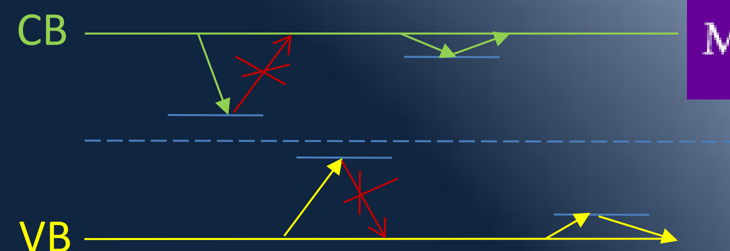

Trapping is characterized by an effective trapping time τ_{eff} for e^- and h:

$$Q_{e,h}(t) = Q_{0e,h} \exp\left(-\frac{1}{\tau_{eff\ e,h}} \cdot t \right)$$

where

$$\boxed{\frac{1}{\tau_{eff\ e,h}} \propto N_{defects} \propto fluence}$$

Increase of $1/\tau$ with fluence | **$1/\tau$ changes with annealing**

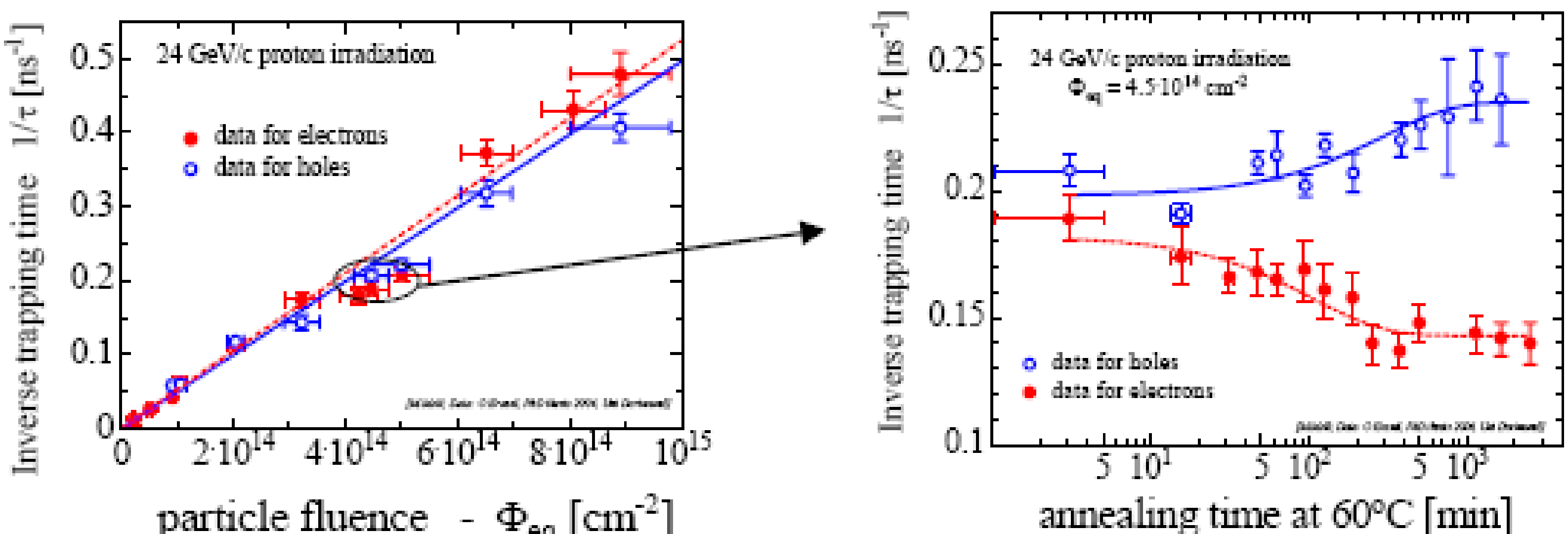

Trapping was measured for electrons and holes by G. Kramberger (Ljiubliana) NIMA 481 (2002) 100

Signal after trapping

The carriers move for shorter distances
→ less signal since the signal is only induced when charges move

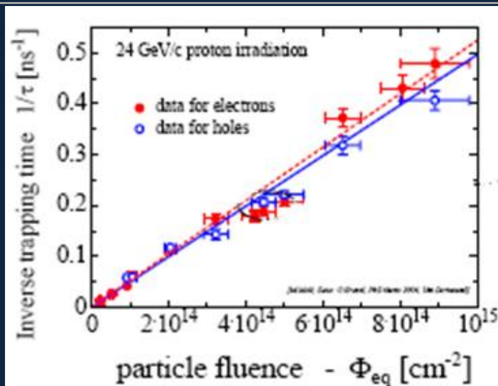

τ_{tr}

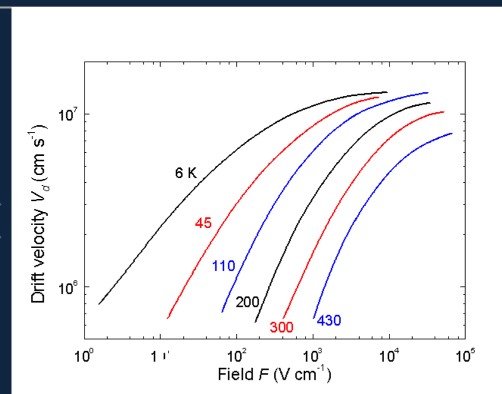

V_{drift}

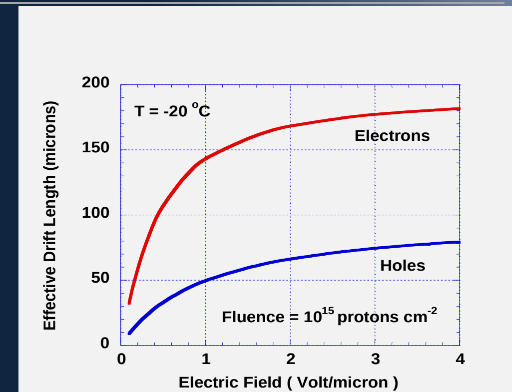

λ (trapping distance)

$$\frac{dS}{dt} = q\frac{dV_W}{dx}\frac{dx}{dt}\exp\left(-\frac{x}{\lambda}\right)$$

$$S = \frac{\lambda}{L}\left[1 - \exp\left(-\frac{x}{\lambda}\right)\right]$$

Expected signal after irradiation depends on λ/L (This is also true for Diamond)

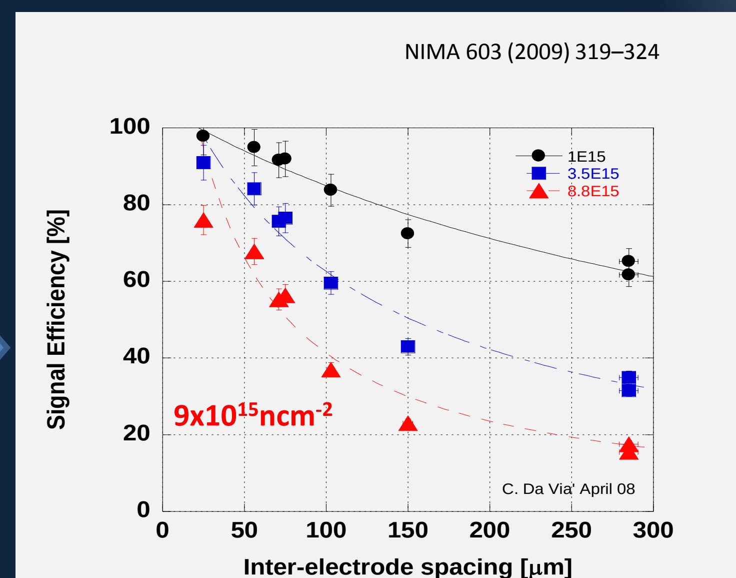

Trapping times from Kramberger et al.
NIMA 481 (2002) 100

Smaller IED: 3D Silicon sensors ..

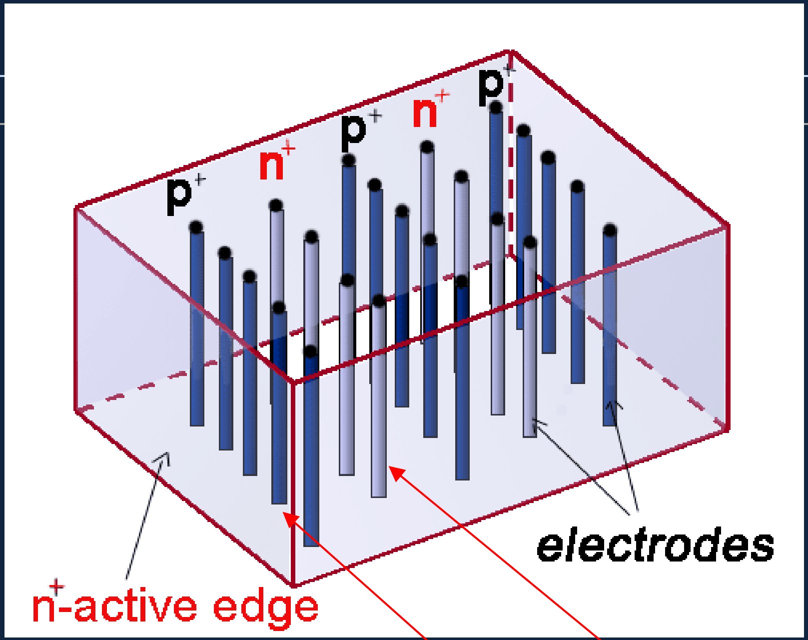

Stanford Nanofabrication Facility

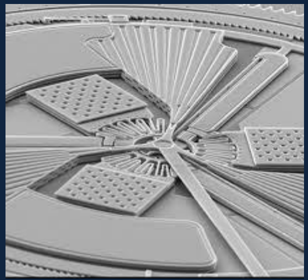

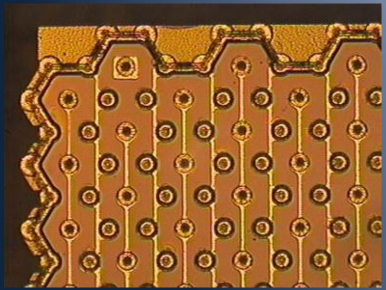

1. NIMA 395 (1997) 328
2. IEEE Trans Nucl Sci 46 (1999) 1224
3. IEEE Trans Nucl Sci 48 (2001) 189
4. IEEE Trans Nucl Sci 48 (2001) 1629
5. IEEE Trans Nucl Sci 48 (2001) 2405
6. Proc. SPIE 4784 (2002)365
7. CERN Courier, Vol 43, Jan 2003, pp 23-26
8. NIM A 509 (2003) 86-91
9. NIMA 524 (2004) 236-244
10. NIM A 549 (2005) 122
11. NIM A 560 (2006) 127
12. NIM A 565 (2006) 272
13. IEEE TNS 53 (2006) 1676

3D silicon detectors were proposed in 1995 by S. Parker, and active edges in 1997 by C. Kenney.

Combine traditional VLSI processing and MEMS (Micro Electro Mechanical Systems) technology.

Electrodes are processed inside the detector bulk instead of being implanted on the Wafer's surface.

The edge is an electrode! Dead volume at the Edge < 5 microns! Essential for

3D versus planar detectors (not to scale)

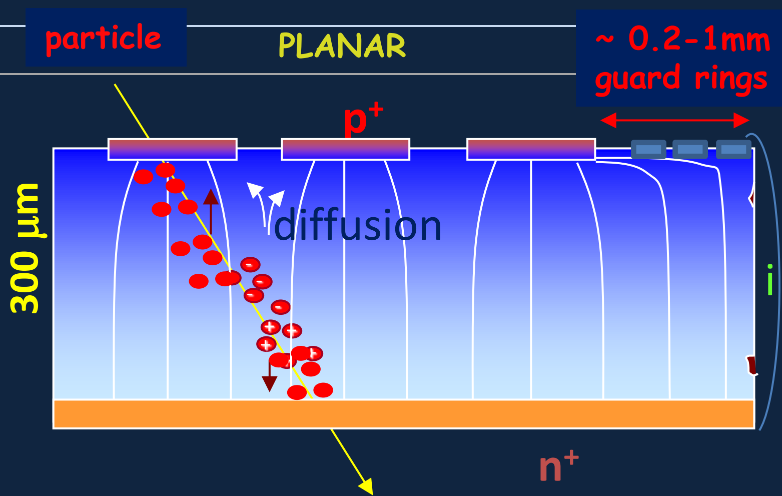

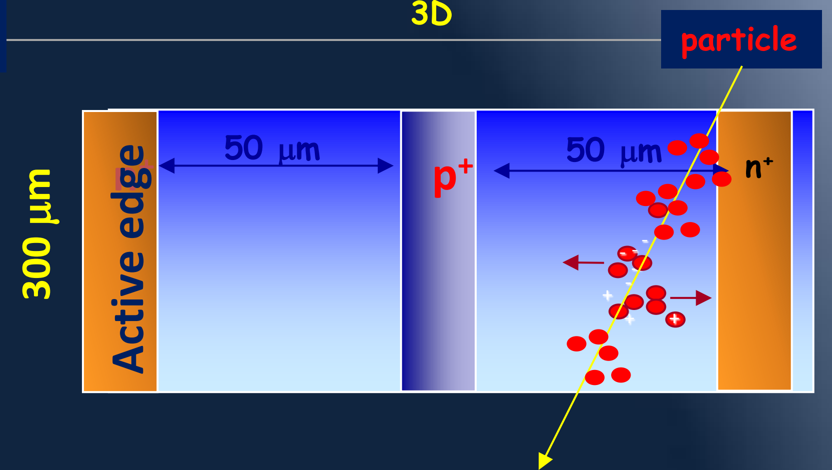

	3D	planar
❖DEPLETION VOLTAGES	< 10 V	70 V
❖After irradiation	180 V	1000V
❖Power dissipation	goes with V	goes with V
❖EDGE SENSITIVITY	< 5 mm	200 mm
❖CHARGE 1 MIP (300 mm)	24000e-	24000e-
❖CAPA CITANCE	30-50f	~20fF
❖COLLECTION DISTANCE	~50 mm	200 mm
❖SPEED	1-2 ns	10-20 ns

3D has Lower charge sharing probability

MEDICI simulation of a 3D structure

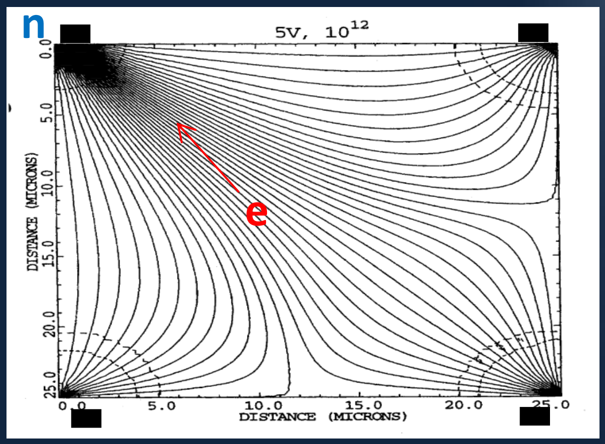

Drift lines parallel to the surface

Cinzia Da Via, Uni. Manchester INFIERI 2013 , Oxford July 2013

The key to fabrication: plasma etching

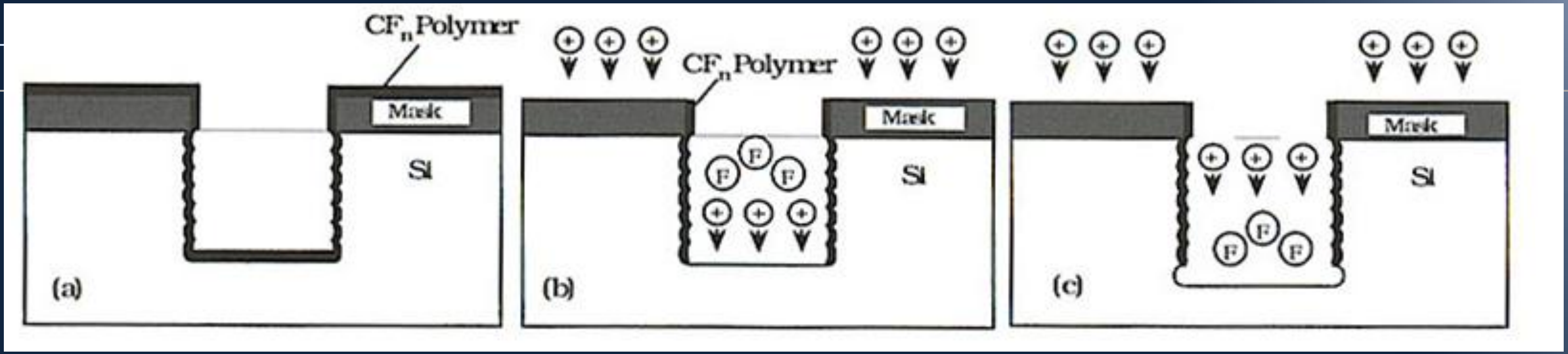

BOSCH PROCESS: alternating passivation (C_4F_8) and etch cycles (SF_6):

- Within the plasma an electric field is applied perpendicular to the silicon surface.
- The etch cycle consists of fluorine based etchants which react with silicon surface, removing silicon. The etch rates are ~1-5μm/minute.
- To minimize side wall etching, etch cycle is stopped and replaced with a passivation gas which creates a Teflon-like coating homogenously around the cavity. Energetic fluorine ions, accelerated by the e-field, remove the coating from the cavity bottom but NOT the side walls.

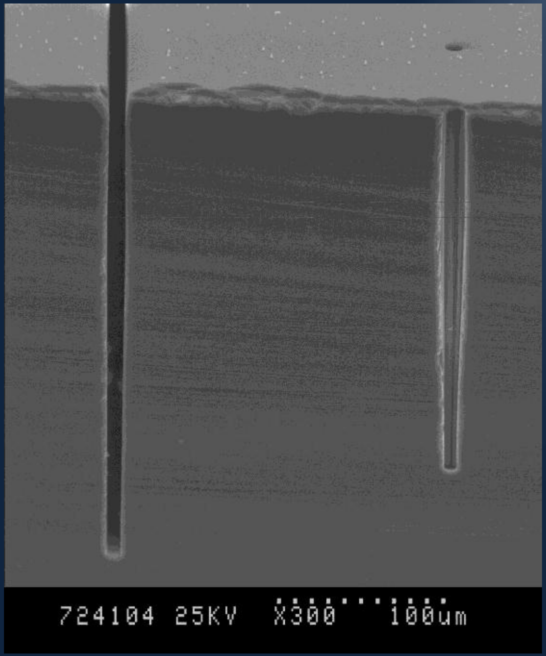

Slide from J. Hasi

Further micro-fabrication steps

1- etching the electrodes   2-filling them with dopants

Aspect ratio: D:d = 11:1

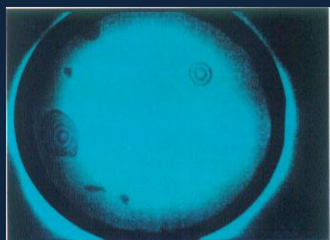

WAFER BONDING
(mechanical stability)
Si-OH + HO-Si -> Si-O-Si + H_2O

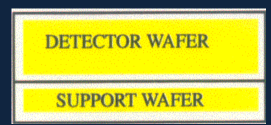

Step 1-3 oxidize and fusion bond wafer

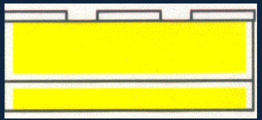

Step 4-6 pattern and etch p^+ window contacts

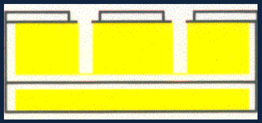

Step 7-8 etch p^+ electrodes

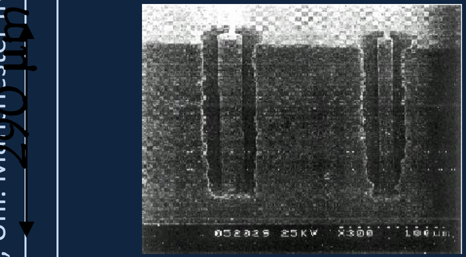

DEEP REACTIVE
ION ETCHING (STS)
(electrodes definition)
Bosh process
SiF_4 (gas) +C_4F_8 (teflon)

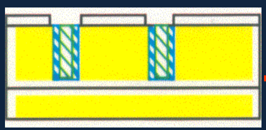

Step 9-13 dope and fill p^+ electrodes

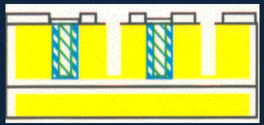

Step 14-17 etch n^+ window contacts and electrodes

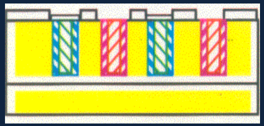

Step 18-23 dope and fill n^+ electrodes

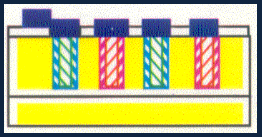

Step 24-25 deposit and pattern Aluminum

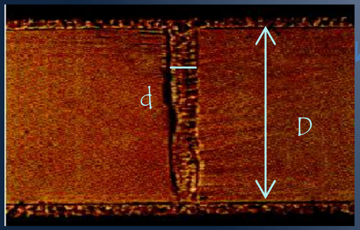

LOW PRESSURE
CHEMICAL VAPOR
DEPOSITION
(Electrodes filling with
conformal doped polysilicon
SiH4 at ~620C)
$2P_2O_5$ +5 Si-> 4P + 5 SiO_2
$2B_2O_3$ +3Si -> 4 B +3 SiO_2

Both electrodes appear on both surfaces

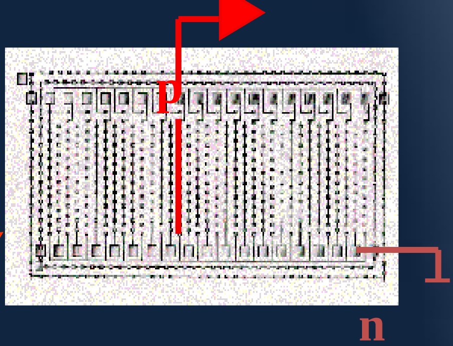

METAL DEPOSITION
Shorting electrodes of the same type
with Al for strip electronics readout
or deposit metal for bump-bonding

Existing 3D designs

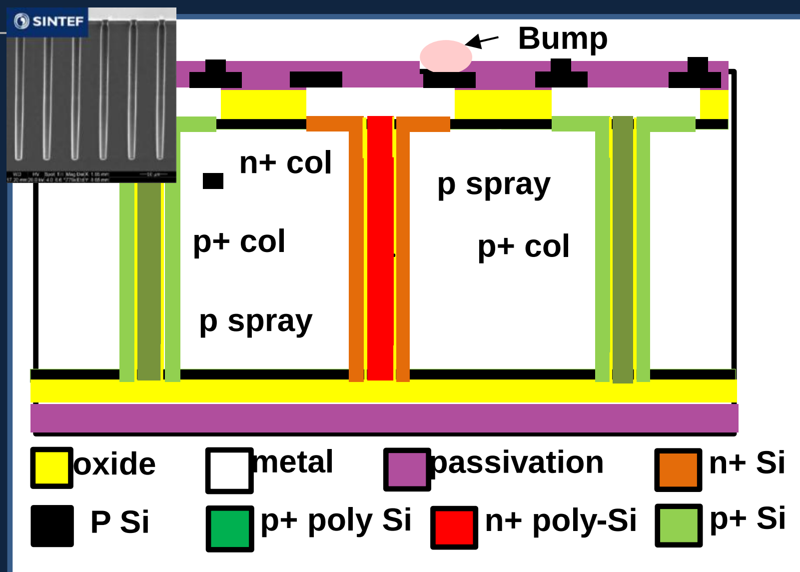

Single side, full 3D with active edges requires a support wafer which is removed later

Double sided full or partially through3D with slim-fences (~200um)

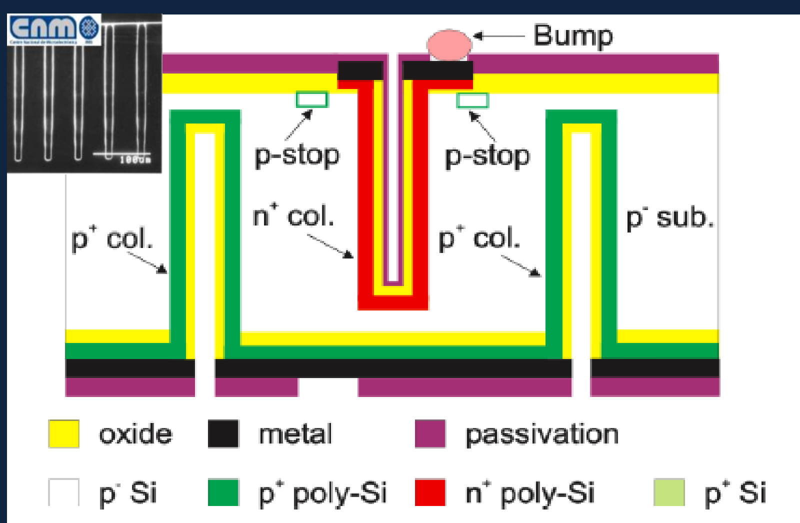

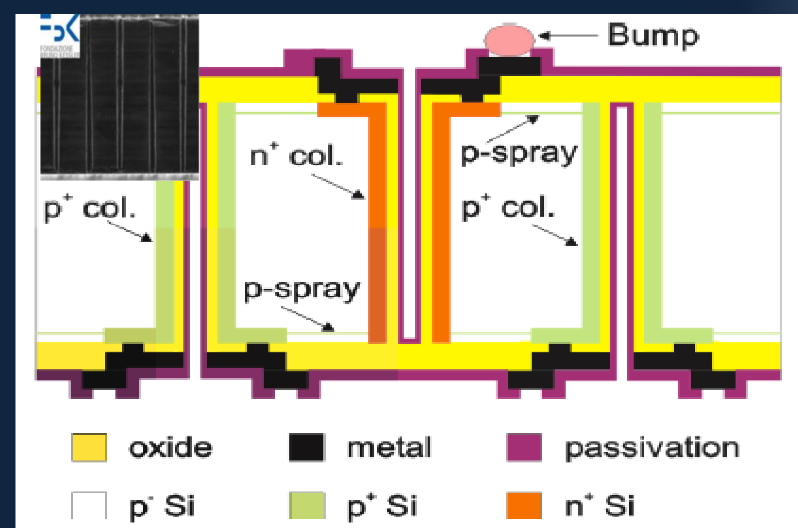

3D sensors will be used in the first LHC detector Upgrade in the ATLAS –Insertable B-Layer (IBL)
>300 sensors fabricated and now being loaded to cover 25% IBL

NIMA 694 (2012) 321–330

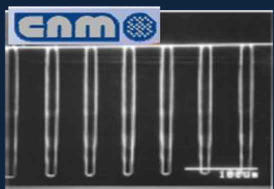

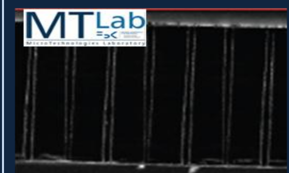

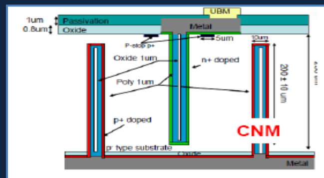

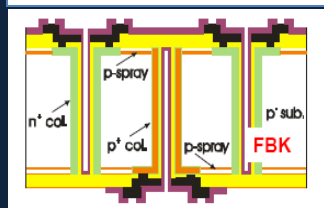

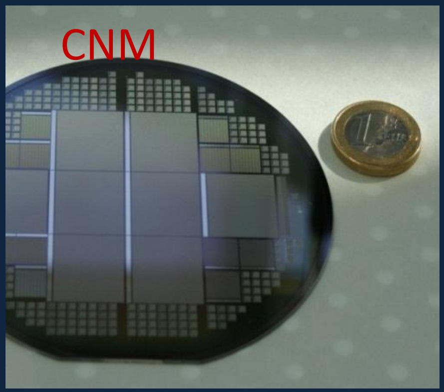

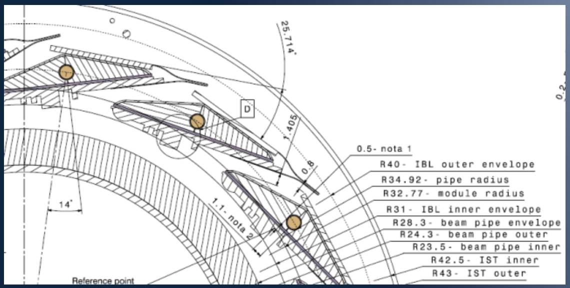

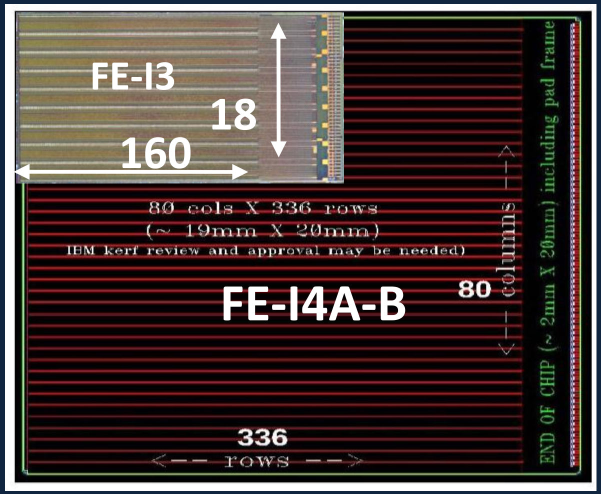

2x2cm2
250x50um2, 26880 pixels

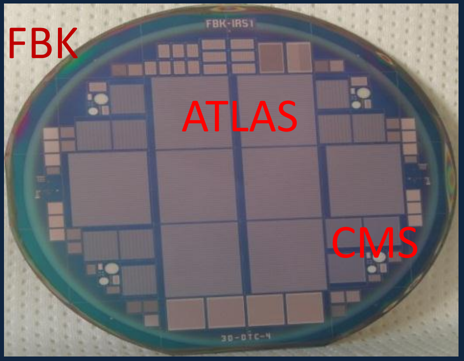

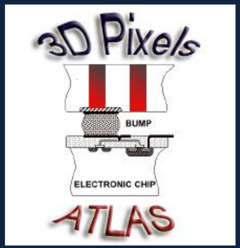

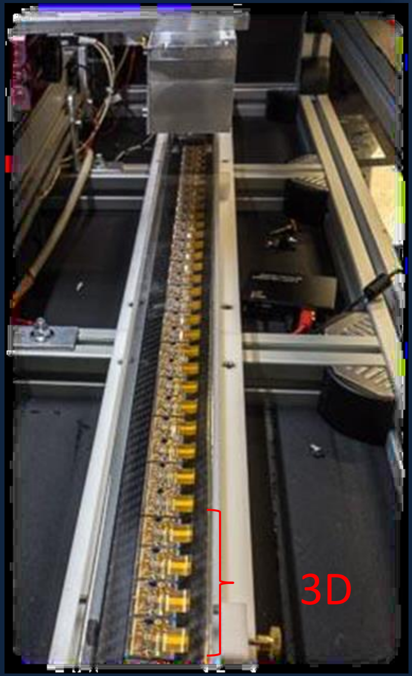

Different shapes depending on applications

Test with -.130nm fast amplifier designed at CERN by G.(Anelli)

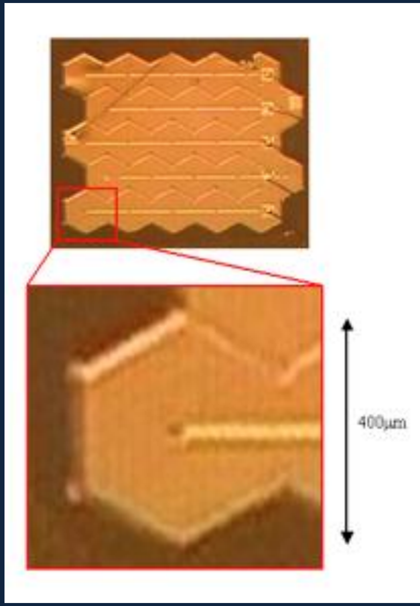

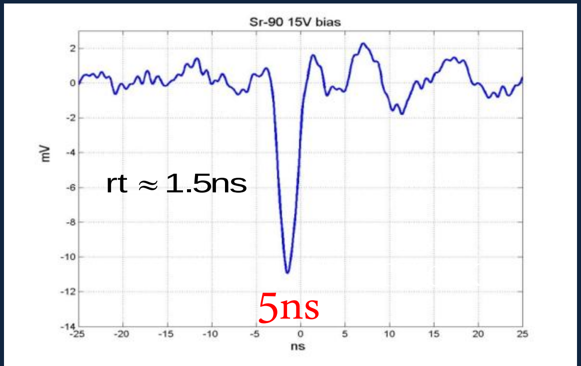

Hexagonal or parallel trench shapes:
Enhanced speed

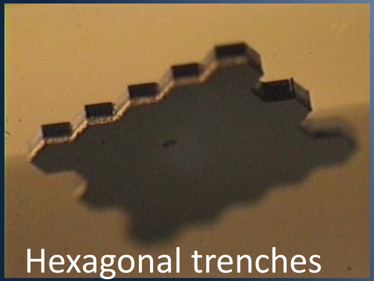

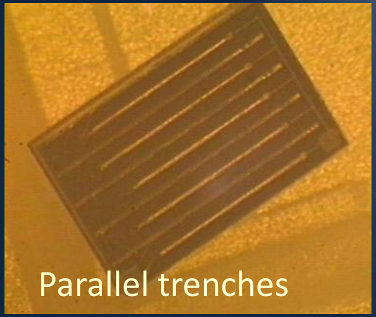

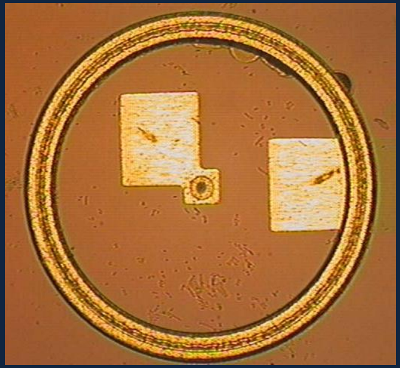

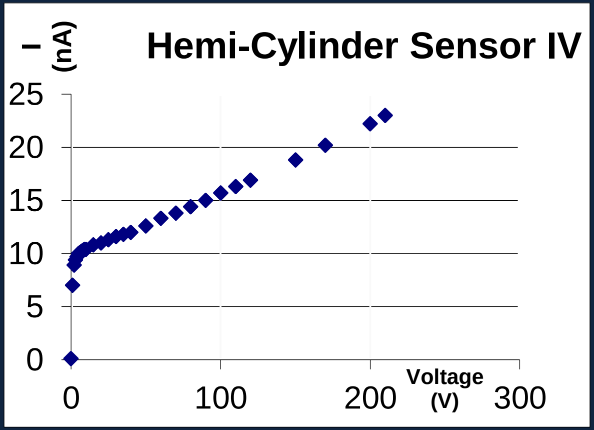

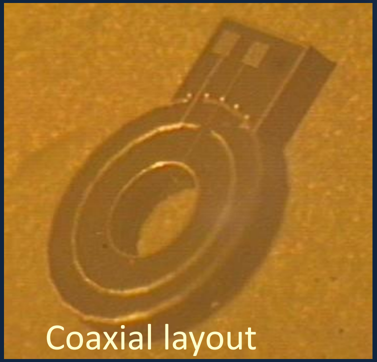

Fabrication J. Hasi and C. Kenney, SLAC/Stanford

Radiation Tolerance of 3D sensors

MANCHESTER 1824

L= Inter-Electrode Spacing

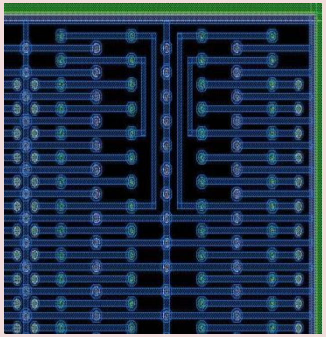

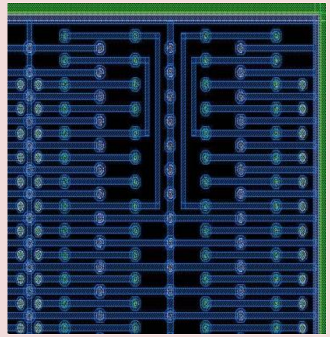

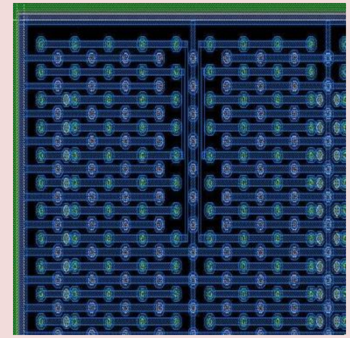

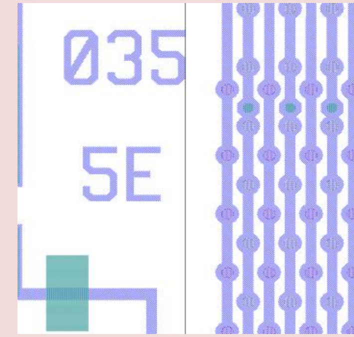

2E = 103um

3E= 71um (IBL DESIGN)

4E= 56um

5E= 47um

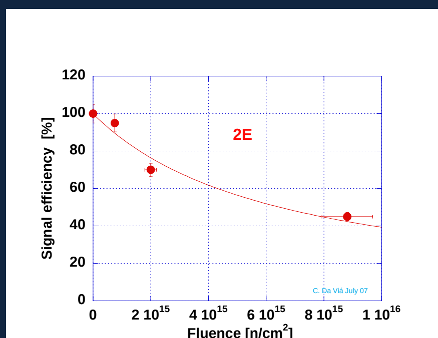

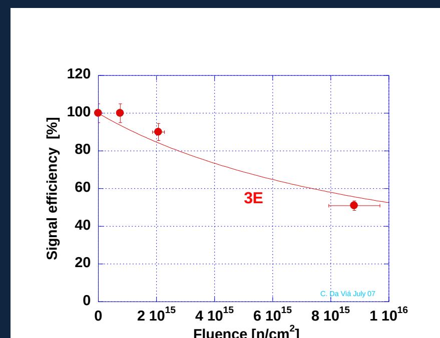

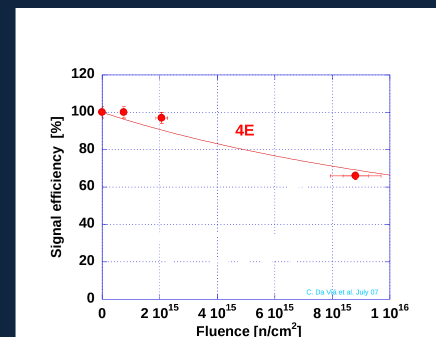

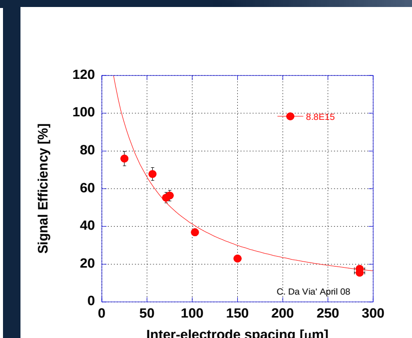

At 9×10^{15} ncm $^{-2}$ And biases below 200V

L=IES [um]	105	71	56	47
Signal Efficiency [%]	45	51	66	68
Charge 50um [e-]	1800	2040	2640	2720
Charge 100um [e-]	3200	4080	5280	5440

Nucl. Instrum. Meth. A 603 (2009) 319-324

3D is "geometrically" radiation hard at low V_{bias} (hence low power)

Ramo's theorem

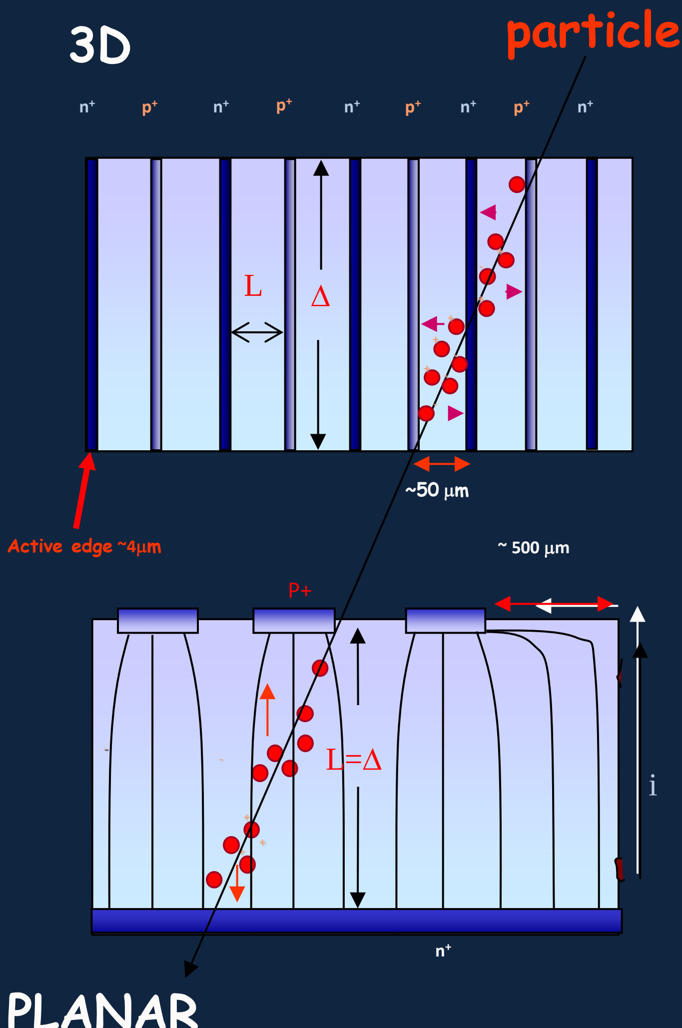

$$\lambda = v_D \cdot \tau$$

$$S = \frac{\lambda}{L}\left[1 - \exp\left(-\frac{x}{\lambda}\right)\right]$$

3D 4E
3D 3E
3D 2E
Diamond
Thick Si
Thin Si

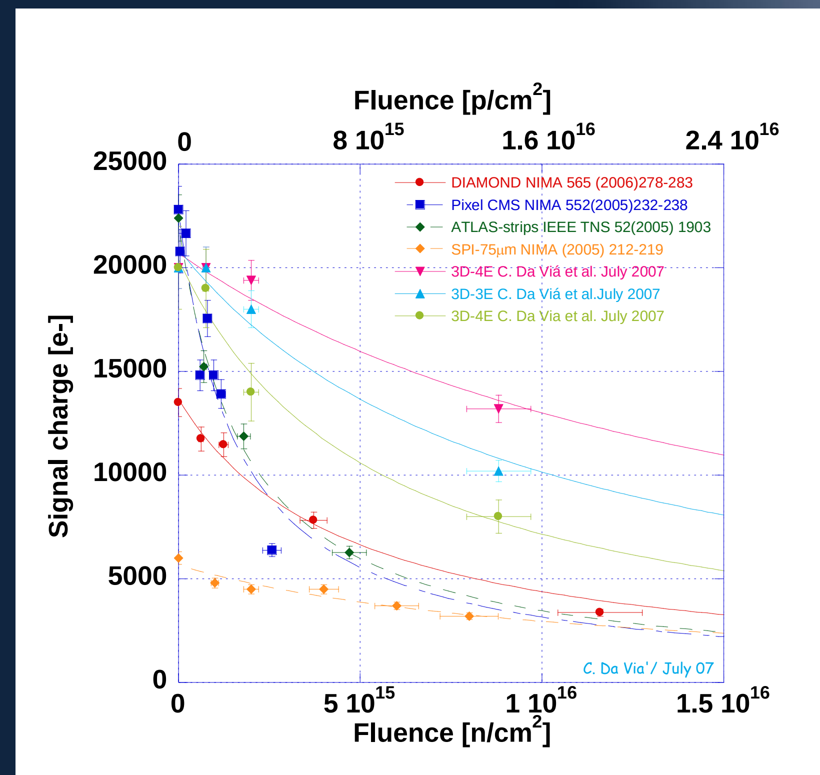

NIM A 603 (2009) 319–324

Best Bias and efficiency Conditions after irradiation

- CNM34, p-irrad 5e15 n_{eq} cm^{-2}
- Threshold at 1500 e-
- Efficiency and charge collection increase with voltage
- At 160V inefficiency regions due to n^+ columns disappear

T=-20C air

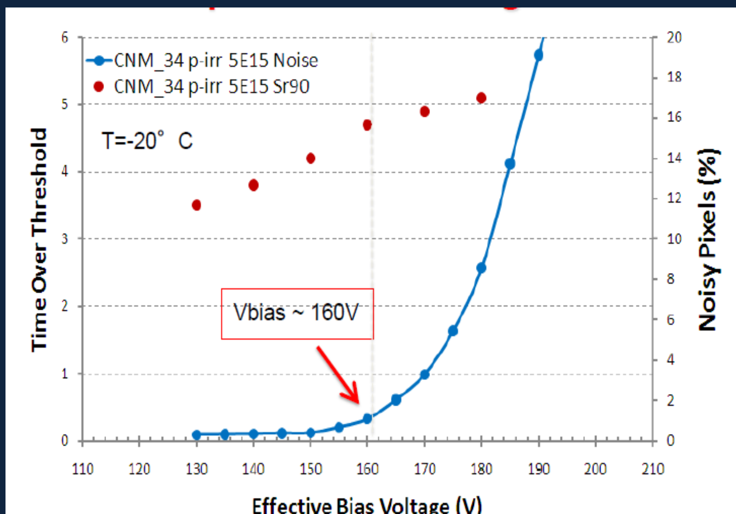

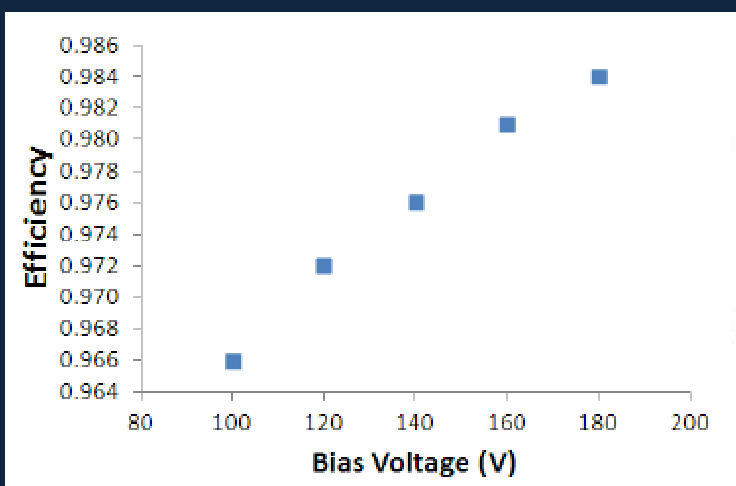

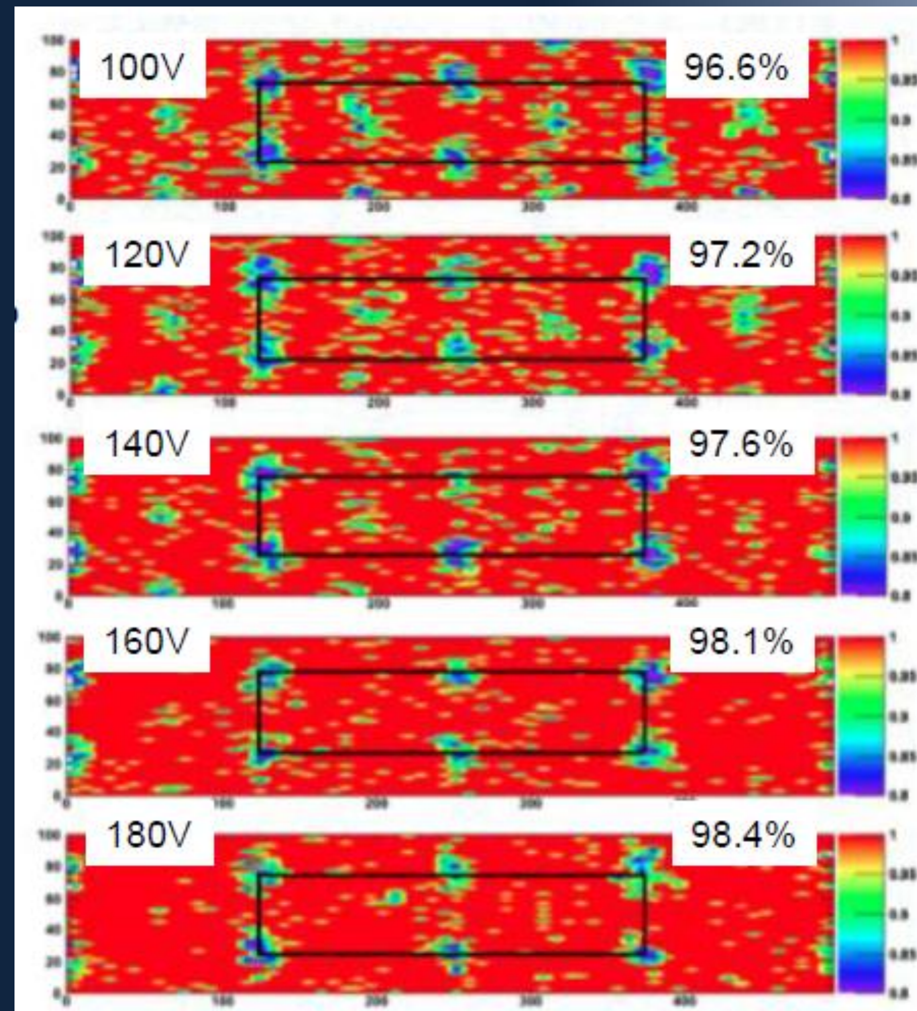

S. Grinstein, Sh. Tsiskaridze, A. Micelli

Edge efficiency after irradiation

- Evidence of field penetration in the fence region
- Test have shown that 150 micron edge is still reliable

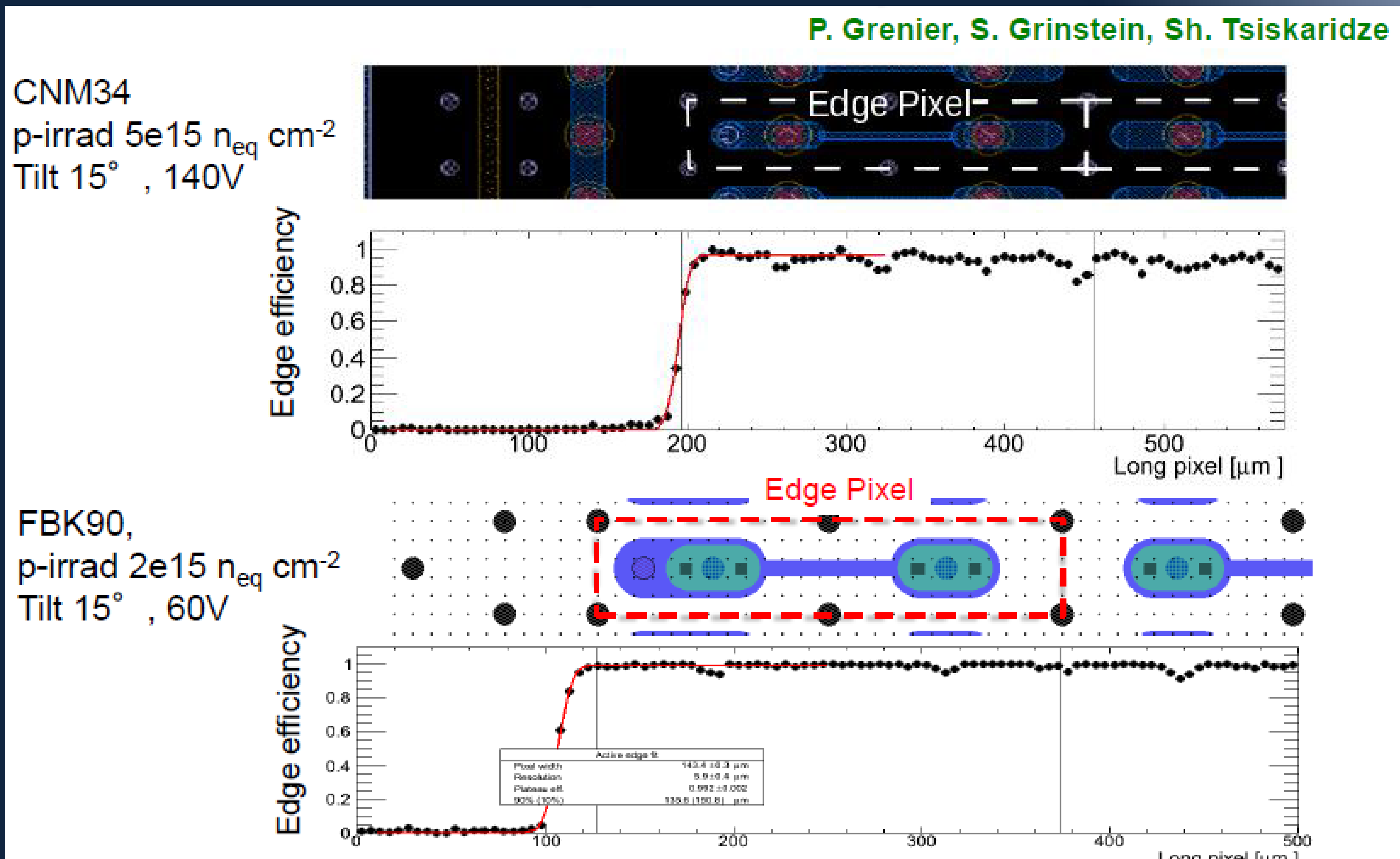

Effect of Operational Conditions

- Temperature
- Extreme high Voltage and charge multiplication
- Forward bias operations

Sensor Power Dissipation after irradiation

Example 3D detectors

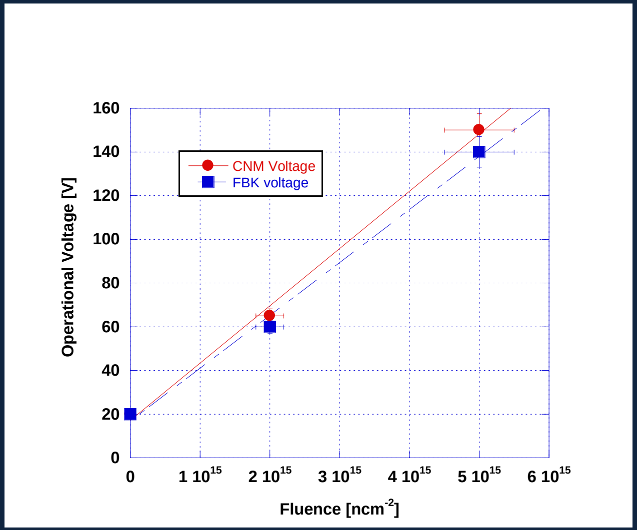

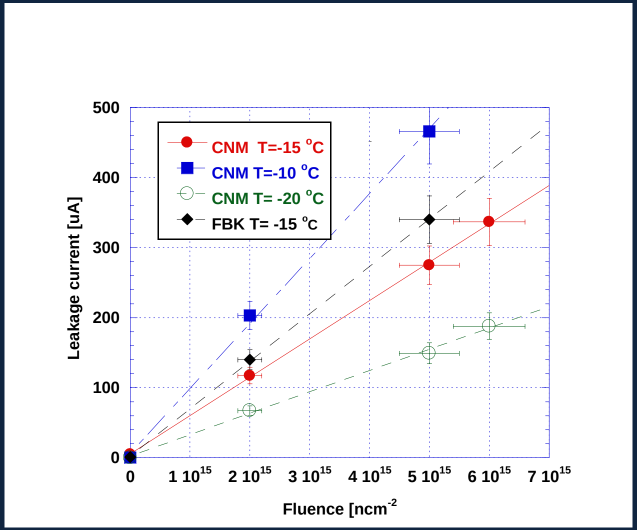

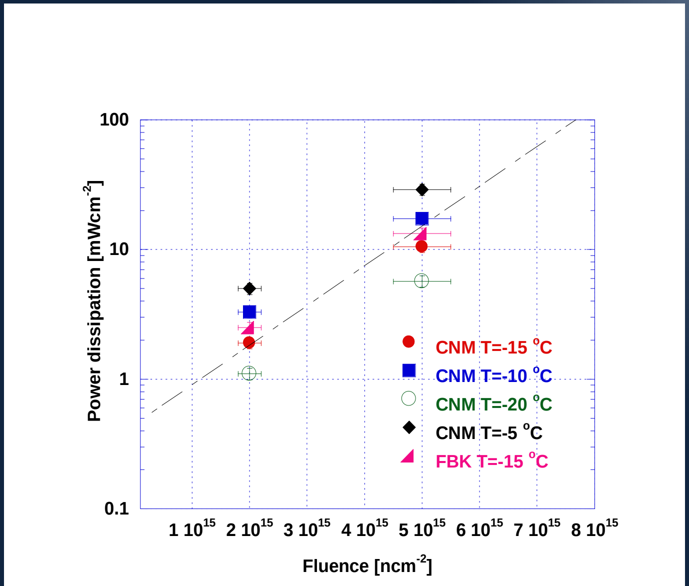

- P=IV

- Sensors can contribute as Much as chips after irradiation And need to be cooled to control Noise and electronics thermal runaway

Electronics thermal runaway

Thermal runaway refers to a situation where an increase in temperature changes the conditions in a way that causes a further increase in temperature, often leading to a destructive result. It is a kind of uncontrolled positive feedback

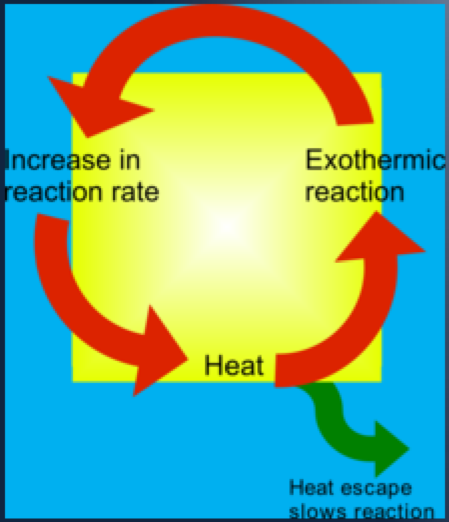

For trackers electronics this means that the power dissipation generates an increase of current

$$I_{leak} = T^2 e^{-\frac{1.2eV}{2kT}}$$

which increases the power and so on..

The detector cannot be used if the heat is not removed.

Case of ATLAS IBL for three different stave Design [from H. Pernegger]

IBL requirement on sensor Power dissipation < 200 mW/cm^2 at 5 x 10^{15} n_{eq}/cm^2 and -15 $^\circ$C (after annealing)

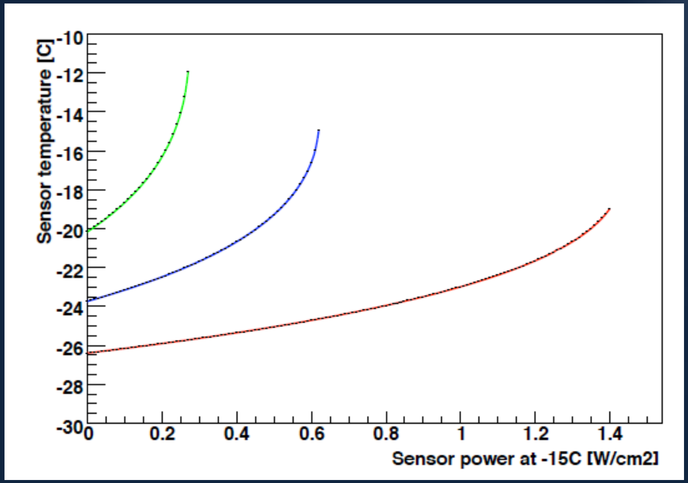

Cooling example: CO_2 bi-phase

MARCO cooling plant
1kW at -40C

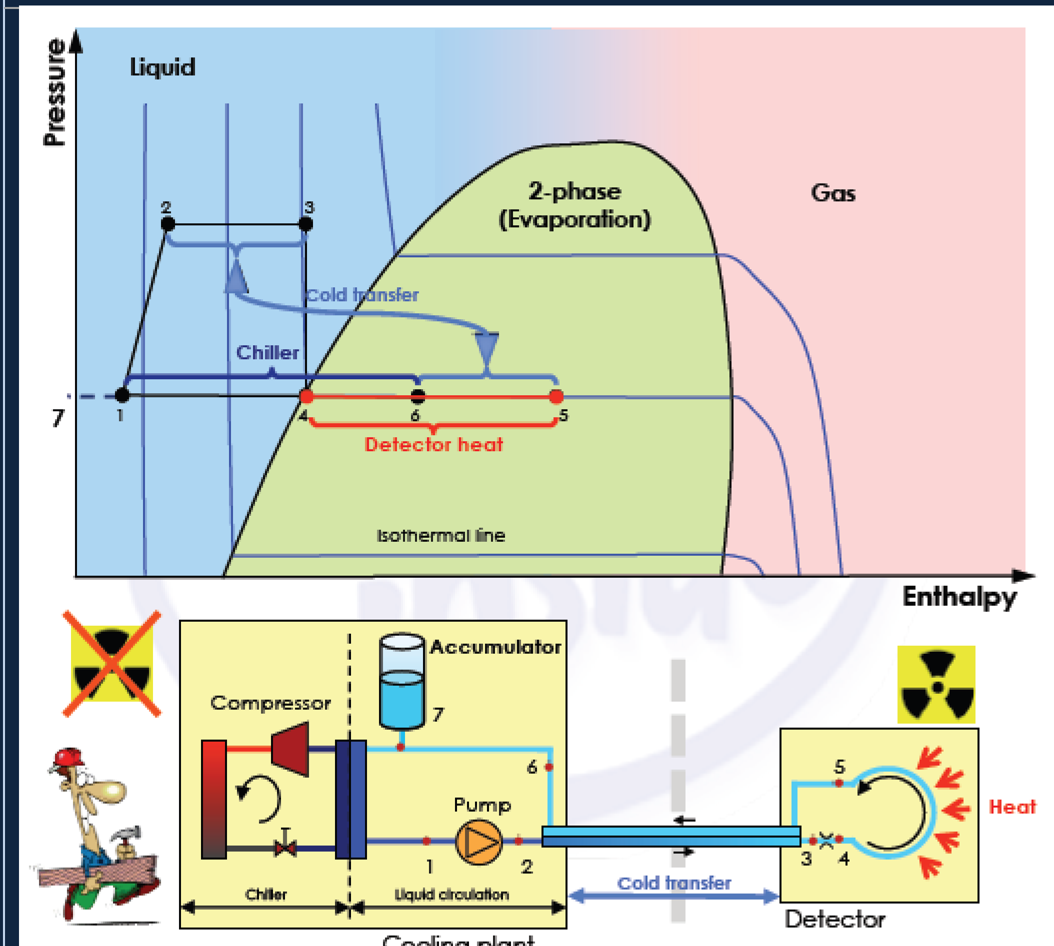

Jerome Daguin - CERN

The ATLAS IBL dissipates ~980W at -40C

CMS pixels upgrade will Dissipate ~9kW at -5C

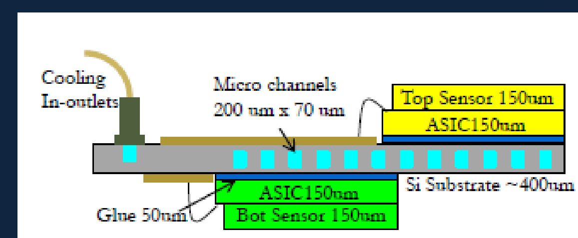

LHCb

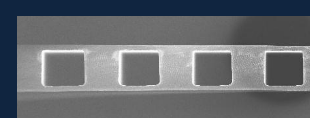

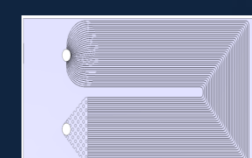

Also micro-fabricated
Channels for CO2 cooling
Will be used for NA62, ALICE and LHCb

T=130K The "Lazarus effect"

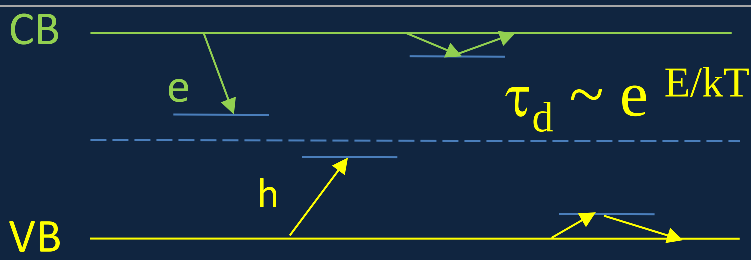

$\tau_d \sim e^{\,E/kT}$

- CCE INCREASES!
- Low leakage current
- No reverse annealing
- Higher carriers mobility

LAZARUS effect!!!

De-trapping time is longer at 130K for deep traps
So deep traps are filled by generated carriers
→ Neff compensation

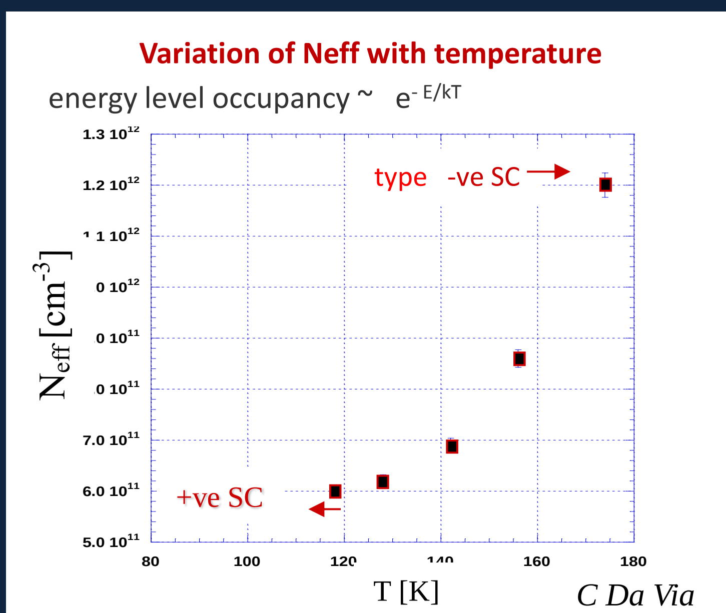

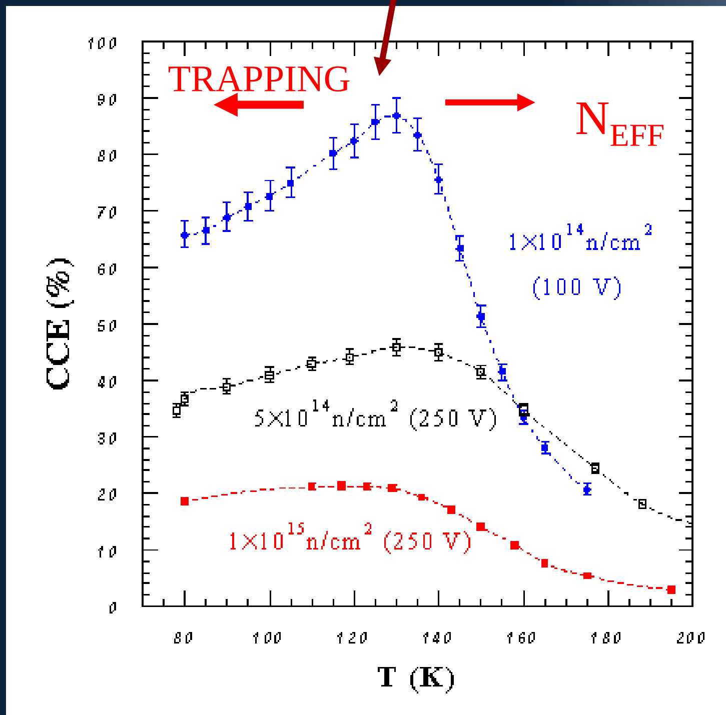

Nucl Inst Meth A 413 (1998) 475
Nucl Inst Meth A 440 (2000) 5

Forward bias operation at low T: needed because of polarization effect! Emission of deep traps with time

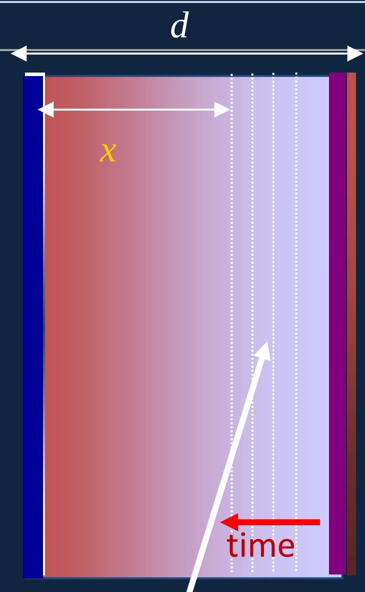

undepleted

NIM A 440 (2000) 5

$\phi = 10^{15}$ n/cm^2
T=130K

$\tau_d \sim e^{E/kT}$

CCE %

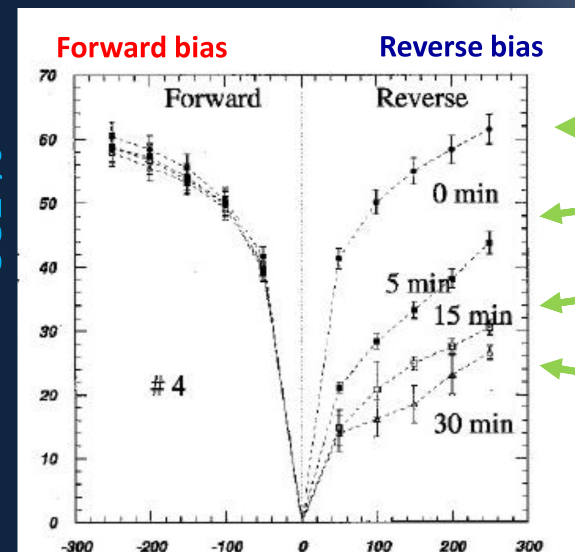

V bias

0 min
5 min
15 min
30 min

"polarization effect"

NIM A 439 (2000) 293

Forward bias also works at higher T
T=249K (-24C)
$\phi = 10^{15}$ n/cm^2

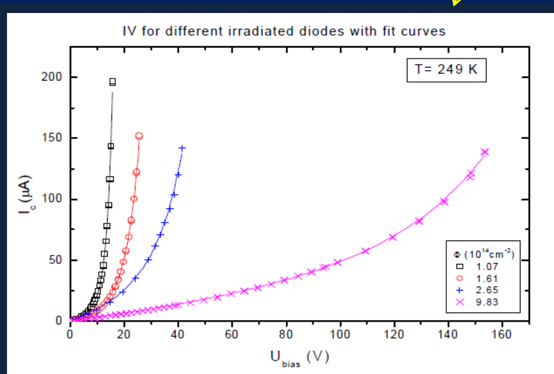

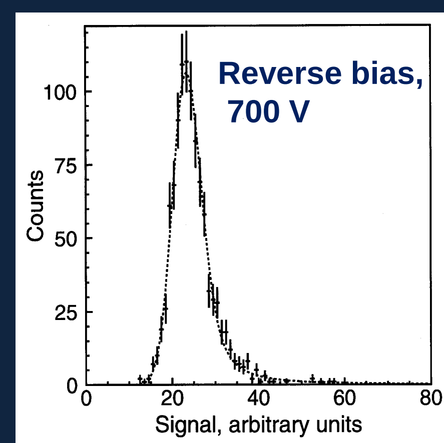

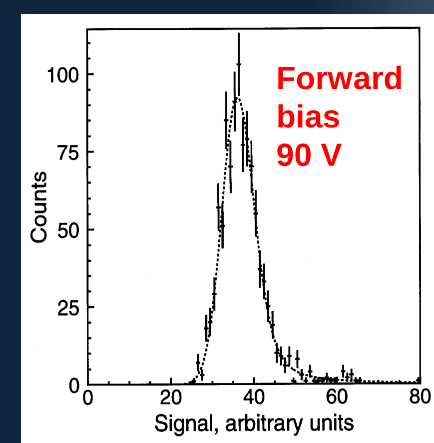

MANCHESTER 1824

Charge Multiplication by impact ionization

Nuclear Instruments and Methods in Physics Research A 636 (2011) S50–S55

Pair creation is a stochastic process described by the equation

$dN = \alpha N dx$

with $\alpha = \alpha_{e,h}$ the *impact ionization coefficient* for electrons and holes, respectively.

The coefficients were measured [13] to scale with the electric field E as

$\alpha_{e,h}(E) = A_{e,h} \exp(-b_{e,h}/E)$

for the electric fields of interest, with the resulting $\alpha_{e,h}(E)$ depicted in the Figure

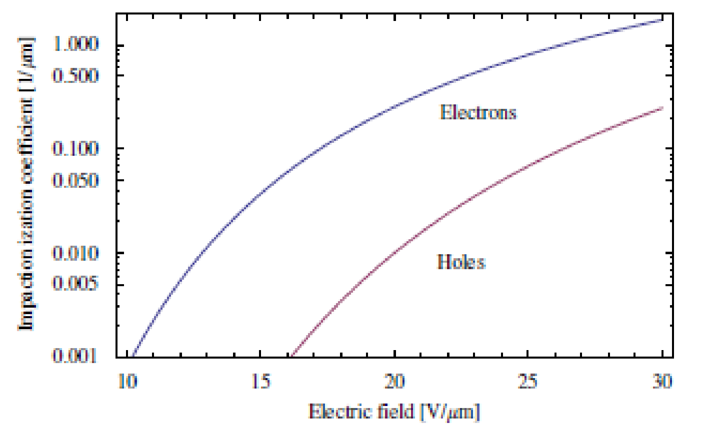

Fig. 2. Impact ionization coefficients as a function of electric field in silicon. Parameterization based on data from Ref. [13].

[13] W. Maes, K. De Meyer, R. Van Overstraeten, Solid State Electron. 33 (6) (1990) 705;
W.N. Grant, Solid State Electron. 16 (10) (1973) 1189.

Impact ionization dependence on electric field is a very steep function. Fields in excess of 10V/μm are needed to obtain single ion pair from an electron in 1mm of silicon. Holes are much less effective than electrons in producing impact ionization, although the relative difference decreases with increasing field.

For pair creation on the scale of 10 μm, so as to counter trapping at very high fluences, electrons need 17.5V/μm, holes 27V/μm. (the normal operational field before irradiation is 1V/μm)

Example of measured charge multiplication on planar sensors

I. Mandic, Ljubljana

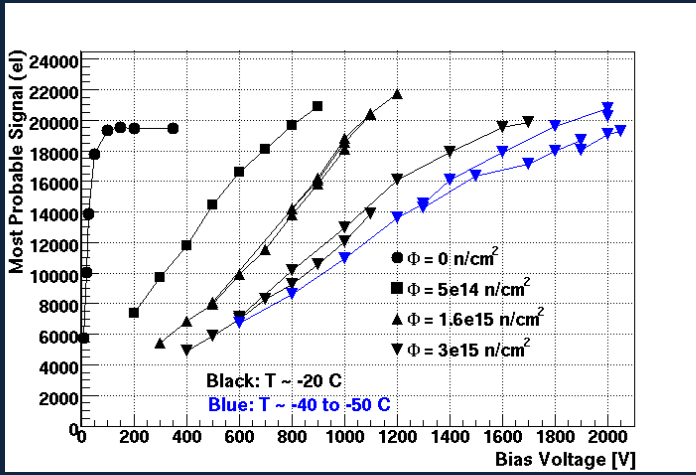

Casse, Liverpool

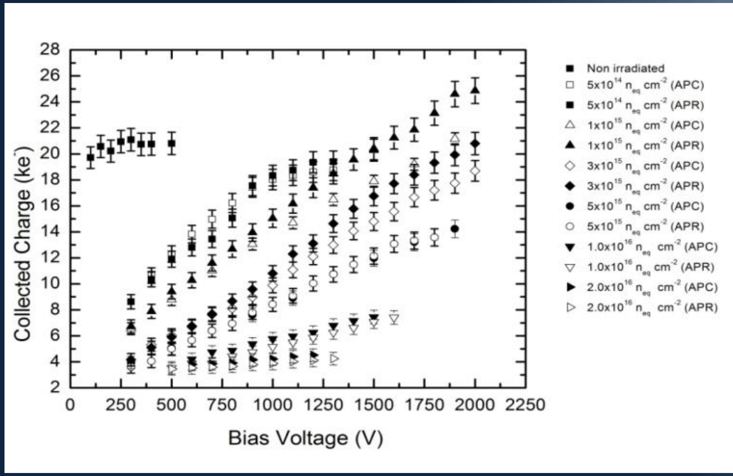

Excess charge is measured at high fluences and different thicknesses

- High bias voltages
- Noise?
- Long term stability?
- Cooling?

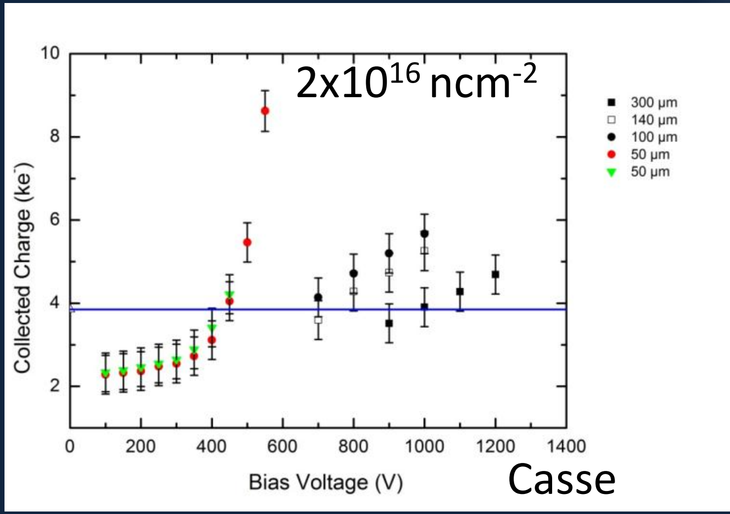

Charge multiplication also observed with 3D sensors

M. Kohler

Before irradiation total charge 22000e	$2x10^{15} ncm^{-2}$ 22000e^{-} at 100-150V	$2x10^{16} ncm^{-2}$ 15000e^{-} at 350-380V

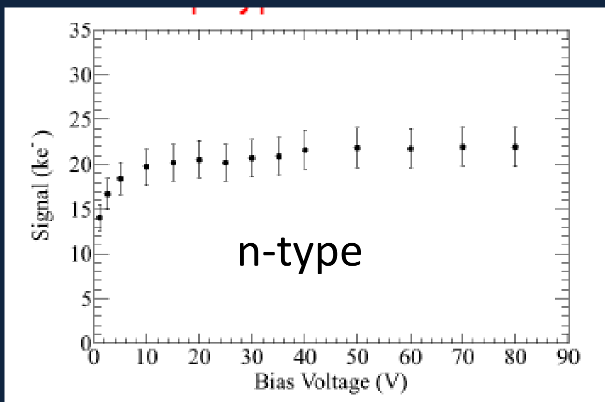

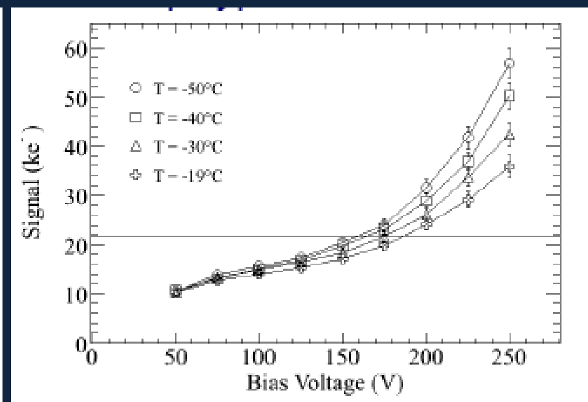

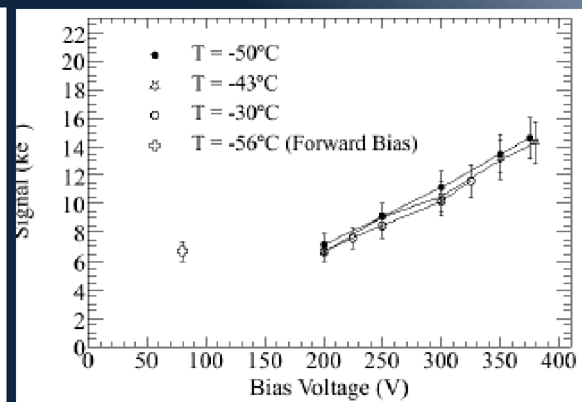

- 250 um column overlap, IES= 56 microns
- Detectors irradiated at the proton cyclotron Karlsruhe with 25 MeV protons
- Annealing state: ~ 5 days at RT (only p-type detector, $2x10^{16}$ neq/cm2: ~30 days)
- Noise at $2x10^{16}$is 1000e- at -45 °C -50 °C

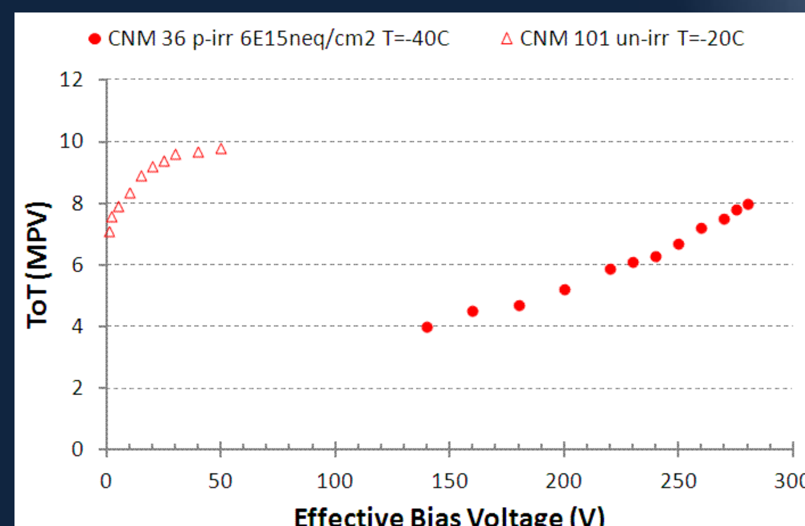

Full Size FE-I4 chip

Conclusions and Outlook

We had a look at some properties and parameters of strips and pixel detectors and their evolution since their first use in scientific applications (a lot is missing..)

I would encourage you to meditate on:

- How the signal is formed and detected
- How a detector design develops depending on applications and constraints
- On the past ideas looking towards the future challenges
- On the new ideas (including your own) which might look crazy now but might reveal a true innovation in few years time
- Don't be scared to be different!

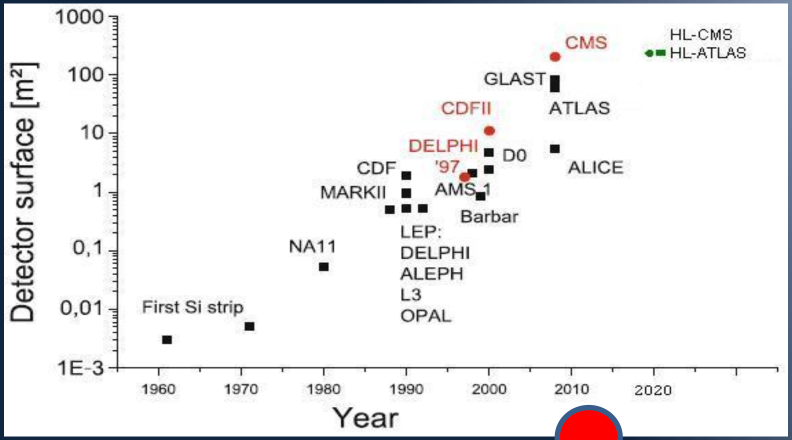

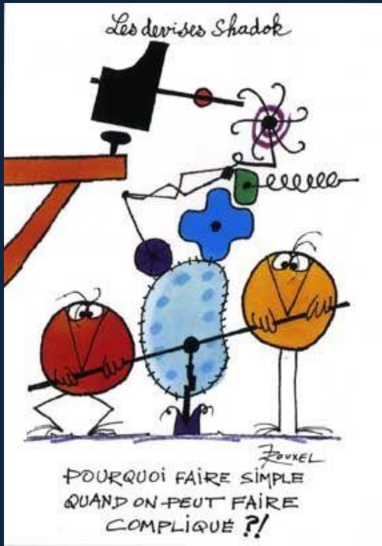

References

Daniela Bortoletto, CERN Summer Student Lectures 2012
Patrick Le Du, EDIT School 2013
Helmut Spieler, Lecture notes (IBL)
Hartmut Sadrozinski, GianLuigi Casse, Vienna Instrumentation Conference 2013
Michael Moll, PhD Thesis
Steve Watts, CERN Academic Training
Harris Kagan, TIPP 2009
Roland Horisberger, Silicon Detector WorkshopSplit, Croatia 2012
Marco Povoli, PhD thesis 2013
Gregor Kramberger
Andrea Castoldi, course given at the Advanced School and Workshop on nuclear signal processing, Acireale Italy, November 2011

Chris Damerell, Sherwood Parker, Erik Heijne, Ariella Cattai